Microfluidic Devices for Capturing, Imaging and Counting White Blood Cells

Anas Bin MOHD NOOR

Microfluidic Devices for Capturing, Imaging and Counting White Blood cells

Anas Mohd Noor

A thesis submitted in fulfilment of the requirement for the award of the

Doctor of Philosophy

Department of Micro-Nano Mechanical Science and Engineering

Graduate School of Engineering

Nagoya University

2020

ACKNOWLEDGMENT

In the name of Allah s.w.t. the Most Gracious and Most Merciful. It is my great pleasure to acknowledge all the people who are directly or indirectly connected in this research.

First of all, I would like to express my sincere gratitude to Professor Fumihito Arai from the Department of Micro-Nano Mechanical Science and Engineering, Nagoya University for guiding me with great patience, support, advice, comment and encouragement throughout the study.

Special thanks to Professor Kenji Fukuzawa from the Department of Micro-Nano Mechanical Science and Engineering, Associate Professor Eijiro Maeda from the Department of Mechanical Systems Engineering, and Associate Professor Hisataka Maruyama from the Department of Micro-Nano Mechanical Science and Engineering for kind agreement with being my doctoral committee member.

I would like to personally thank Associate Professor Taisuke Masuda, Assistant Professor Shinya Sakuma, Assistant Professor Seiji Omata, Assistant Professor Yuichi Murozaki and Research Fellows Hashim, Gallab, Bilal for their kind advice, help and supports. And, not to forget, Ms. Tsukamoto, for her kind help for my study abroad in Japan. Many thanks to all Arai's lab members for their advice and supports.

My greatest gratitude must forward to my family especially my father, Hj. Mohd Noor Ahmad and my late mother Hjh. Zainin Hasan Basri for continual support and prayers. Special thanks to my beloved wife Rasidah Abdul Wahab for sharing the happiness and hardship together and children

Abdul Wahab Anas, Fatimah Anas and Maryam Anas who have been continually encourage and motivates me to finish my doctoral journey.

ABSTRACT

The most common blood examine in clinical medicine is white blood cells (WBCs) count. Various diseases cause changes in the blood composition or cell populations, and therefore, the analysis of blood is essential in clinical diagnosis. Furthermore, WBCs provides information about health status, such as WBCs count is changing due to diseases commenced. The WBC subpopulation cells counting such as lymphocytes, T and B cells are very important to determine the health condition, specifically the immune system. Current trends of cell counting instruments are moving forward to have featured such as portability including miniature system, cost-effectively including sample processing, system management and maintenance. Moreover, the result produces are rapid, reduces delays of treatment, and provides better monitoring system in the limited resources area. Conventional system used for this cell separation and counting task are accomplished using flow cytometry. The main advantages of flow cytometry are able to analyse simultaneous parameters and provides high throughput. However, despite all the advantages, the instruments are costly (operation and maintenance), sophisticated system, often bulky in size and required a highly trained specialist to operate them. Hence, microfluidic provides an alternative technique of cell separation and counting. Moreover, this technology offers cost reduction, device portability, very small sample volume, disposability device and suitable for point-of-care applications.

We proposed a simple microfluidic device for cell separation and counting applications. The device comprises of microfilters that serve as the filtration mechanism based on sizes and deformability. Conventional

microfilters mechanism suffers from device clogging. Thus, a simple solution to eliminate this problem by utilizing a gradual filtration concept, and microfilters escape route. The microfilters gap size gradually decreases from 15 μm to 3 μm to facilitate the deformability-based separation. Leukocytes have various sizes; hence, they can be separated by microfilters directly from whole blood samples without any cell clogging, and they do not require samples pre-processing such as centrifugation or red blood cell lysis which is tedious and costly. As a result, we succeeded to achieve that our technique able to separate WBCs from whole blood with a high efficacy of 99%. Moreover, the repeatability test of the proposed device shows low coefficient of variations with only 2.77%. Furthermore, the developed imaging system and a simple cell counting algorithm gave a statistically significant correlation and agreement with standard laboratory flow cytometer method.

In conclusion, the proposed method allows a very low sample processing, provides a short time of sample pre-treatment (less than 20 minutes), simple technique in reducing device clogging caused by the cells, and good agreement with a conventional instrument. The use of microfluidic technique for cell counting and deformability study seems very promising.

CONTENTS

LIST OF FIGURES

LIST OF TABLES

Chapter 1

Introduction

1.1 Microfluidic Cell Counter

Since 1950s, the microfluidic technology has been introduced for commercial application such as an inkjet printer. The mechanism behind of this printers is based on microfluidic; comprise of very small tubes for transporting the ink for printing. The developments of these technologies contribute to many of the key advances applications including life sciences, medicine, manufacturing as summarised in Figure 1.1.

The term miniaturized total chemical analysis systems or μ-TAS was coined by Manz [1], describes the integration of different laboratory steps into a single microfluidic device. Over the years, the term μ-TAS has been interchangeably used with the term lab-on-a-chip (LOC).

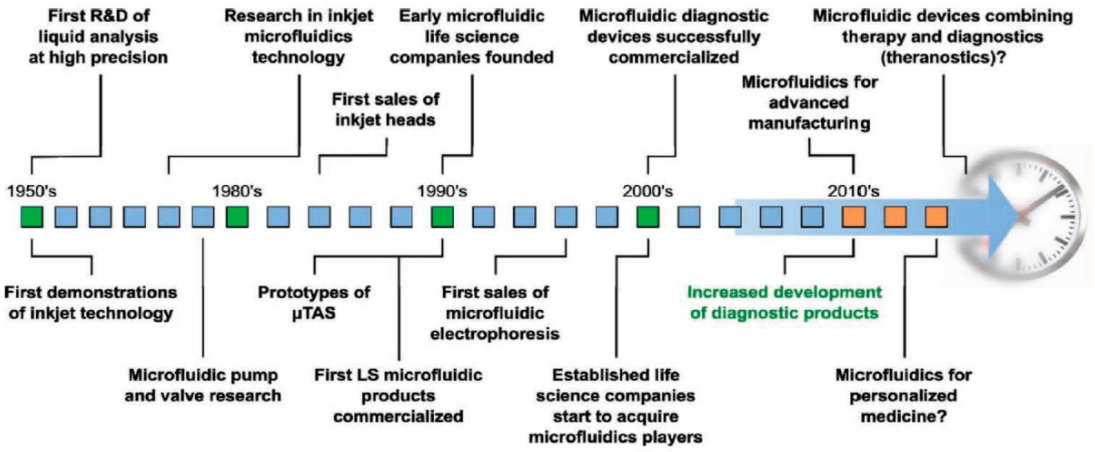

Figure 1.1 The timeline of the microfluidic technology evolution. Republished with permission from Gervais et al. [2].

The rapid advances in microfabrication and nanofabrication, the emergence of new materials and technologies have contributed to powerful tools that have helped develop many areas, including life sciences research and industries [3][4]. For example, applications of microfluidic cells sorting or separation have increased in the number of usage in medicine, biotechnology, and cellular biology [5][6]. This LOC cell counter offers simplicity and flexibility for easy to set-up and low maintenance compared to standard instruments [7]. Furthermore, results or analysis from LOC devices could be achieved in a short time thus reduces delays of medical treatment etc. The timeline of cell counting methodologies is shown in Figure 1.2.

Example of conventional method cell counting and sorting tasks accomplished using flow cytometry, including fluorescent-activated or magnetic-activated based [8][9]. The basic principles operation of flow cytometry is suspending cells in a stream of fluid flowing them through the detector (optical or magnetic). The main advantages of flow cytometry are simultaneous analysis (multiple parameters analysis) and high throughput [10]. However, the major disadvantages of the instruments are costly (operation and maintenance), sophisticated system, often bulky in size and required a highly trained specialist to operates the equipment. These factors caused limited use in areas and fields such as bedside testing, patient self-testing, low-resource area, e.g., rural area and global diagnostics [11]. Moreover, this instrument could cause cell death and having limited quantitation capability.

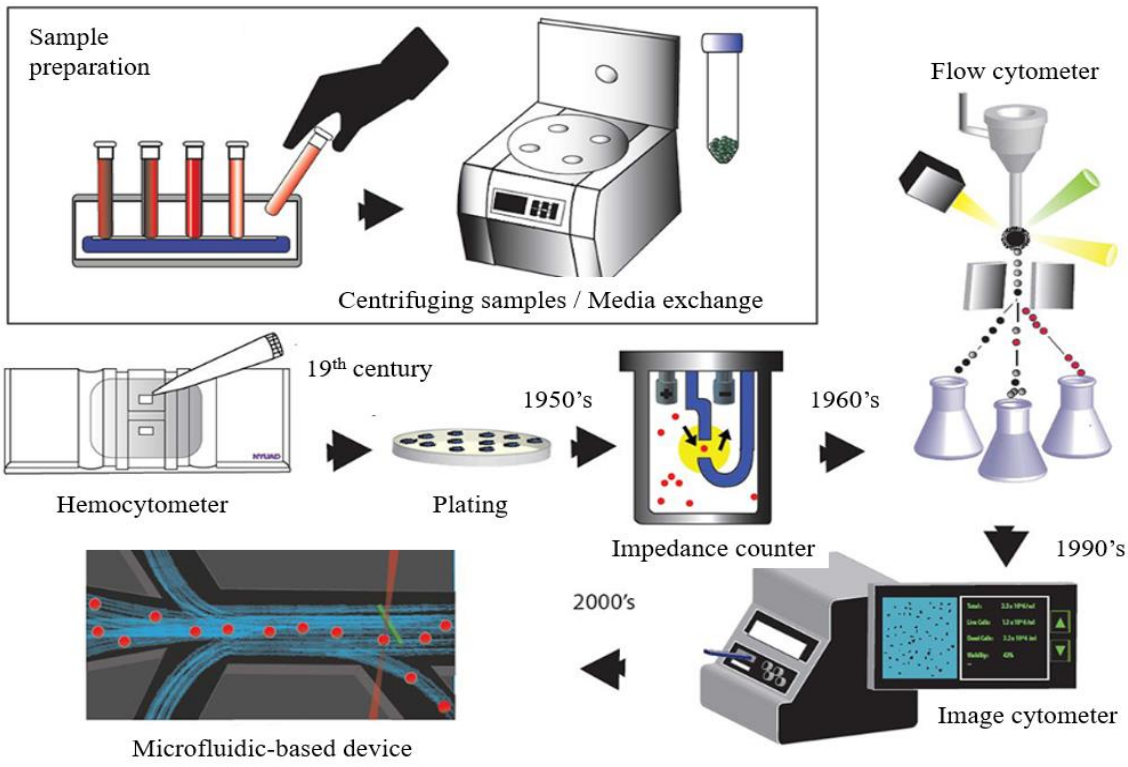

Figure 1.2 Evolution of various cell counting and detection technologies.[12]

Hence, microfluidic could provide an attractive alternative technique of cell sorting (Figure 1.3). Moreover, this technology offers cost-effective, device portability, smaller sample volume, disposables microfluidic device and suitable for the point-of-care application. For example, a microfluidic-based flow cytometry where microfluidics and flow cytometry are integrated

to enhance functionalities on the microfluidic device offers greater advantages over conventional techniques [13] [14].

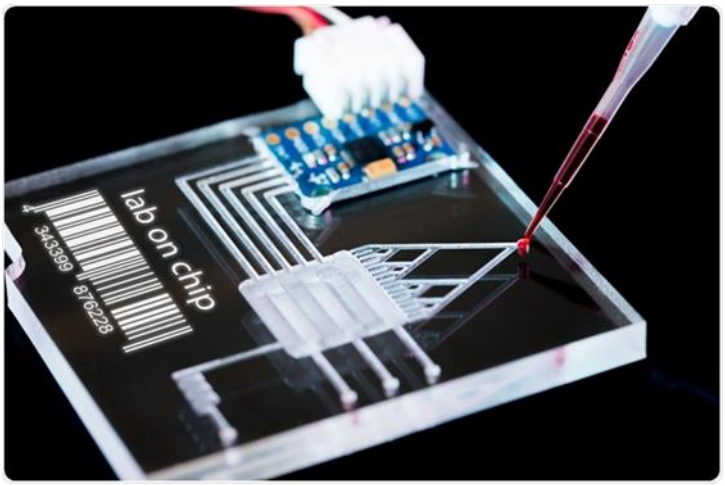

Figure 1.3 Example of a microfluidic device [image adapted from https://www.news-medical.net/life-sciences/Benefits-of-a-Microfluidic-System.aspx]

1.2 Blood: A Major Disease Biomarker

Body fluids include blood in humans are essential for life. Blood circulates through the body and carries essential substances such as nutrients and oxygen to the body's cells [15]. It also carries waste products away from the tissues metabolic process through blood circulation. Blood cannot be made or substitute or manufactured. A blood transfusion is the only way to introduce blood to the body after an injury or illness. Blood is well known as major disease biomarker [16][17]. Blood is heterogeneous, contains a mixture of cells types (e.g., red blood cells, white blood cells) and biomolecules (e.g., antibodies, proteins, plasma) (Figure 1.4). Composition of blood changes by diseases, and therefore, the analysis of blood is essential in clinical diagnosis [18][19].

The white blood cells (WBCs) play essential roles in the immune system for protection over illness and disease. WBCs flow through the bloodstream seeking foreign bodies, like viruses and bacteria and attack it. It also could go into the tissue by leaving the blood stream to fight the foreign bodies. Thus, the populations of WBCs are affected by diseases which could be diagnosed form this information. Even though there are many ways to test blood, the most widely used and as a standard test in clinical medicine are the full blood count or complete blood count (CBC) [20]. CBC generally includes RBCs, WBCs, platelets, haematocrit, haemoglobin etc. If these components are in abnormal range values, this is an initial indication that diseases or virus infections have occurred and further specific test are required to identify the type of infections, diseases etc. [21][22]. Table 1.1 shows the typical composition of adult human blood.

Current typical blood analyser is not suitable for further determine WBCs subpopulation [23]. The limitation of this typical blood analyser where not be able to accurately provides the measurement of the cells phenotypes, for example lymphocytes (T, B and NK cells) population. This is because of the principle of blood analysers operation is based on Coulter principle (electrical impedance) where the impedance is varied by cell morphology (size, shape) thus cannot distinguish between the similarly-sized granular WBCs. Therefore, details on cells phenotypes population only could be determined form state-of-the-art flow cytometer [24].

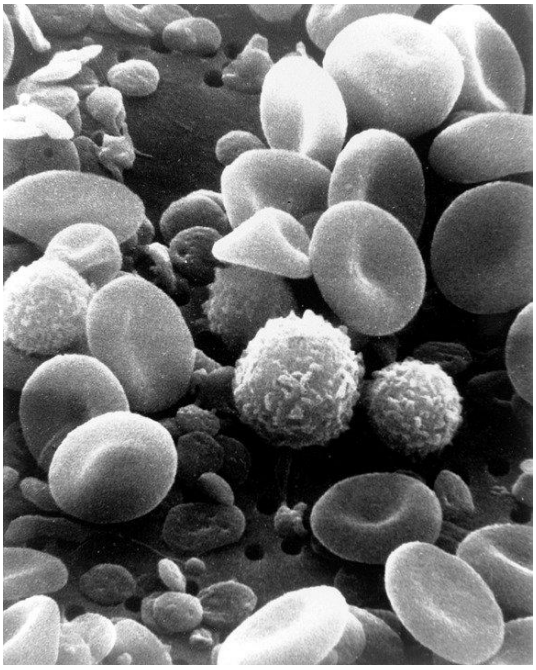

Figure 1.4 A scanning electron microscope image of blood cells. RBC (disc-doughnut shaped), WBC (spherical shaped) and platelets (small-disc shaped). [image adapted from http://en.wikipedia.org/wiki/White_blood_cell]

Table 1.1 Typical composition of adult human blood [37]

	WBC Type					Other Cell	
	Granulocytes			Non-granulocytes		Red blood cells	Platelets
	Basophil	Eosinophil	Neutrophil	Lymphocyte	Monocyte		
Size (μm)	10-14	14	15-17	6-15	15-20	7.5-8.5	2.3
Count (cells/μL)	25-1000	50-400	1,800-7,700	1000-4000	100-800	4,000,000-6,200,000	150,000-400,000
WBC Percentage population	0.5-1	1-4	40-60	20-40	2-8	-	-

1.3 Conventional Blood Cell Counter

Before the introduction of automatic cell counter in the early 1950s, the clinical tests of the blood relied on manual blood smear image observation using an optical microscope [25] (Figure 1.2). The blood smear sample preparation and observation were tedious and time-consuming. Moreover, only trained haematologist could do the analysis and interpretations of the

results are varied between people, which lead to imprecision analysis [19]. Therefore, a standard automated tool is required to solve the limitations in manual blood analysis method. Furthermore, the automated counter had become standard in large clinical laboratories that required high throughput process and analysis [26].

Currently, there are three principles of cell counter in the automated system, including Coulter principle, image analysis and flow cytometry [25] (Table 1.2). Coulter principle is using impedance measurement where blood is passing through a small orifice and changes of electrical conductance is measured. However, this principle has a limited analysis which only can measure 3-type of WBC differential (monocyte, granulocyte and lymphocyte). Moreover, due to overlapping count between granulocyte (neutrophils, eosinophils and basophils), counting of sub-populations of WBCs using this method couldn't be performed [25]. However, the automated blood counter using Coulter principle still widely being used because it is cost-effective, fast processing and reliable such as to determine general WBCs and RBCs counts.

On the other hand, imaging techniques require staining of blood samples for sub-populations analysis such as WBCs (lymphocyte, monocyte, neutrophil, eosinophil and basophil). Although the method suitable to determine the cell phenotypes, it is not popular compared to automated blood counter such as Coulter blood analyser. The process of cell identification usually been performed using standard or fluorescence microscopy. At first, the cell image was taken, and further analysis such as cellular features information (cell size, nucleus shape etc.) will be performed. However, this method is suffered from low throughput, accuracy and required tedious sample pre-treatment steps [27][28].

The basic principle of flow cytometry is the passage of cells in single file

are presented to the laser so they could be detected, counted and sorted. Sample are fluorescently labelled and excited by the laser to emit light at different wavelengths. The advantages of a flow cytometer are high throughput process, be able to analyse subpopulations from the heterogeneous population. However, a highly trained operator or expert are required not only to analyse the results but including designing of optimal immunophenotyping for multi-detection application which often having overlapping of excitation and emission signals (fluorescence), suitable dyes and staining techniques. In conclusion, although the conventional analysers are suitable for lab-based operation, the cost still high, bulky instrument size, and limited functions are always a challenge. Hence, microfluidic technologies represent a promising alternative methods to conventional laboratory methods which offers a great advantage over the conventional method.

Table 1.2 Summary of the conventional blood cell counting principles, Coulter principle, image analysis and flow cytometry

Methods	Detection Principle	Sample Labelling	Capability			Accuracy	Throughput
			CBC	WBCs count	WBCs Differential		
Coulter	Electrical impedance	Label free	Yes	Yes	3-type	High	High
Imaging	Optical image	Needed	Yes	Yes	5-type	Low	Low
Flow cytometer	Optical (scattering, absorption,fluroscence)	Label free: scattering Label needed: absorption,fluroscence	Yes	Yes	WBCs subtypes	High	High

1.4 Need of Point-of-Care Device for Cell Counting

Point-of-care (POC) refers to a diagnostic device which obtains fast results near-patient rapidly during consultation. For example, devices used in patients' home or could be used anywhere even at limited resources area or facilities. There are numerous, commercialized POC device applications

available [29]. Such for example, an application of blood count. A traditional blood count diagnostic occurred in the complex laboratory. Therefore, over the decades, growth of POC is likely to continue, the manufacturer has been pushing to improves in healthcare delivery which are aimed providing a cost effective devices that is suitable to be used or diagnose closer to patient. As an example, one of the healthcare manufacture, Becton, Dickinson and Company (BD) that manufactures and sells medical devices has developed a FLU detection device. Conventional diagnose of FLU infection based on visual interpretation. Visual interpretation required a highly trained lab technician, the evaluation process is time-consuming and tedious, these include sample preparation, observation and total management (sample collection, storage, disposal etc.). Furthermore, the results at least ready after 2-4 hrs for a single patient [30].

Another critical application needs POC technologies is monitoring HIV infection and antiretroviral therapy (ART) by CD4+ T-lymphocytes (CD4+ cells) cell count. According to the United Nations Program on HIV/AIDS (UNAIDS), the number of people with HIV infected is approximately 37.9 million across the globe with HIV/AIDS in 2018 [31]. HIV caused CD4 levels depleted and weakening the immune system, which leads to AIDS and death caused by cancer diseases and other infections. ART treatment slows the AIDS progression by reducing viremia. Therefore, it is critical to determine the population of CD4+ cells upon diagnosis of HIV and before starting ART (monitoring the therapy efficacy). The current standard methods for counting CD4+ cells are based on Flow cytometer, manual counting and commercial available CD4 test device [32]. However, the major advantages of all available methods are a costly instrument (e.g., Fluorescence-activated cell sorting (FACS)). The FACS instruments uses sophisticated optical-based for cells

detection. Fluorescence-labelled sample cells are pass through a narrow channel where light illuminates the cells in the channel. As a result, light scatters, or emission by the cells is precisely measured by the detector. Thus, based on the light detected, FACS able to sorted using electrical charge method of targeted cells. The results are presented as histogram or dot-plots represent the intensity of light detected. Some limitations of this system are time-consuming caused by the sample preparation and management process, and tedious (long incubation time, need of sample storage), limited lifetime (e.g., strip based detection) and many more. Furthermore, some methods (e.g., manual observation or strip-based detection) is suffering from accuracy compared to conventional FACS cell counting.

New technologies and benefits of microfluidic-based diagnostics have played an essential role in the crucial technological process of POC, that could provide less diagnostic time, and high precision testing results. Furthermore, the microfluidic-based device requires a small volume of clinical samples and reagents, which reduce the operation cost, ease of operation (minimally-trained operator) and suitable to be performed outside a laboratory or poor-resource setting. Thus, the microfluidics-based device offers excellent prospects to make POC as an essential diagnostic tool.

1.5 Microfluidic Cell Separation Methods

Currently, cells separation and cell counting are accomplished using conventional flow cytometry system. As discuss earlier, the process of cell counting using this method are tedious and costly. Thus, alternative methods such as using the microfluidic device are promising without reducing the accuracy and offer a cost effective system. There is serval as methods to

separates and counting cells using a microfluidic device such as passive and active techniques. These separation methods are separated using a method such as passive, active separation and combinations passive and active techniques. Passive cell separation techniques are relying on the flow field, channel structure and interaction between cells usually do not require external forces.

On the other hand, active techniques require external fields which offers better performance compared to a passive method. However, the active microfluidic device and systems are much more complicated than a passive system. Table 1.3 shows a comparison between passive and active cell separation methods.

Table 1.3 Comparison of microfluidic cell separation techniques

	Separation technique	Mode of separation	Separation criteria
Passive	Mechanical Filter	Size exclusion	Size, deformability
	Microstructure	Microstructure perturbation of cell flow	Size, density, deformability
	Hydrodynamic	Streamline manipulation	Size, shape
	Inertial	Lift force and secondary flow	Size, shape, deformability
	Deterministic lateral displacement	Migration in micropost array	Size, shape
Active	Magnetic	Differential magnetic mobility	Magnetic susceptibility
	Acoustic	acoustic radiation force	Size, density, compressibility
	Optical	optical lattice	Refractive index, size

	Electric	dielectrophoresis	Polarizability, size
	Gravity	sedimentation difference	Size, density

The microfluidic cell separation using passive technique particularly using the mechanical filter will be discussed. Although there are numerous methods of cells separation using microfluidic platform, our purposed are more towards simplicity of device including device fabrication, reconfigurable device for specific purposed, device operation and sample preparation. Therefore, the passive cell separation is best suited method due to its simplicity system including operation, cost etc. In particular, mechanical or size-exclusion filtration is a straight-forward cell separation based on cell size, shape and deformability technique. Furthermore, this technique provides advantages over other passive techniques where it is based on simple filtering structure (e.g., micropillar, cavity or membrane) relatively simple fabrication with simple structure, simple system integration and lower maintenance. Therefore, this technique is suitable to be implemented in the related application such as in clinical analysis which required a rapid sample processing, provide a fast result and high throughput. Moreover, simple system is required to be used in limited facilities or healthcare resource.

1.5.1 Mechanical Filtration

The Mechanical filtration, also known as size exclusion filtration comprises of a series of linear arrays of micropillars or membrane (pores or cavity) array that enables highly efficient separation cells by size, shape and deformability. Furthermore, the filters such as micropillars including microstructures filter size or membrane pores size can be precisely controlled

depending on the target cells or particle which need to be filtered [33]. However, the conventional mechanical filtration design including dead-end filtration, microcavity, 3D structure, are usually avoided since the cells are captured or trapped within the same direction of flow. Thus, this will have caused an accumulation of cells within the micro pillars or membrane pores, which results in deterioration of membrane performance [34-36].

For example, a microfluidic device contains microcavity array for counting WBCs from small volume of whole blood have been developed by Hosokawa et. al. [37] (Figure 1.5 (a)). The device equipped with a size-controlled microcavity (3 μm pores size) array for sub-microliter (1 μL) of whole blood. They successfully recovered is 90% of WBCs in the whole blood sample. Although the method purposed is straight forward separation technique, the sample required a high dilution to reduces cells (RBCs) clogging. Moreover, there still some of the WBC passing through the filter due to pressure and device size influenced.

A similar cell separation concept to Hosokawa et. al., developed by many researcher has shown that mechanical filtration method provides simple technique for many suitable applications including, tumour cells [38-40]. For example, Lee et. al. [39] developed a microslit filter to capture circulating tumor cells (Figure 1.5 (b)) and Yusa et.al. developed a microcavity filter for isolation of circulating tumour cells (CTCs) rapidly using 3D palladium filter [41] (Figure 1.5 (c)). The filter composed lower layer (pores) and upper layer (pocket) with size of 8 μm and 30 μm respectively. They successfully recovered more than 85% of CTCs from whole blood sample. The system is simple which uses gravity flow for cell separation. Clogging device by blood cells are reduced by pores size which blood cells (RBCs and WBCs) could pass through. However, the device still captured some WBCs if the number of pores

is lower, thus, increasing of filtration area will increased pores number to reduced cells clog and the device fabrication process must be precisely control.

Virginia et.al., separates WBCs using a cross-flow technique from whole blood sample [42] (Figure 1.5 (e)). Cross-flow could reduce the cells clogging by flows tangentially across a membrane surface. Smaller cells (E.g. RBCs) than the cross flow membrane pores pass through the membrane, while larger cells (e.g., WBCs) suspended particulates remain in the main stream [43]. Therefore, cells with different size could be separated efficiently than dead-end filtration [44-46]. However, the separation efficiency of this technique is usually limited. This is because only the particles or cells reaching the filtering area being sorted. If the channel is wide or the sample are too concentrated, the efficiency become more worst [47]. Several techniques are proposed to enhanced the cross-flow have been developed by many researchers. For example, Sethu et al, changing the cross-flow filtration pressure by adding a diffuser channel to pushed cells towards the filters efficiently [48] (Figure 1.5 (f)). Chiu et al, enhance the separation process by adding hydrodynamic focusing. This technique will push the cells towards the filters and separation of cells become more efficient [47] (Figure 1.5 (d)). However, hydrodynamic focusing increased shear stress, damaged the cells and reduce separation performance.

Swee et al. developed multiple arrays of crescent-shaped filter (crescent trap) structure to improve the efficacy of cell capture by mechanical filtration [49]. (Figure 1.6 (a)) The principle is simple and straight forward. Cells are flowed through the crescent-trap and get trapped if no obstacle (no trapped cell). If the trap is filled with cell, then the flow path-line changed (divert) to next level of crescent filter. Thus, this device shows success in reducing device clogging. Although the methods are promising, limitations of the device are

unable to process multi-size of cells in a heterogeneous sample, and only suitable for large cells and stiffer cells. Smaller and softer cells tend to escape through the crescent-shape filter.

Another simple technique for cells separation develops by Wei et. al. that utilizes porous membrane [50] (Figure 1.6 (b)). The membrane filter consists of multiple pores sizes filters of a 3D microfluidic structure. Thus, the porus membrane allows the microfluidic device to produce a series of size fractions from a whole sample within a single microfluidic device. The principle is similar to dead-end and cross-flow operation where smaller cell size are passing through the porus membrane with larger size than the cells and bigger cells are captured or trapped. The technique shows that the captured cells (RBCs and WBCs) results efficiency is 99%. However, the major disadvantages of this device are the flushing and collecting of the samples must be frequently taken to prevent cells clogging. Thus, additional pump for controling the pressure and valves made the system more complicated.

On the other hand, gradual size filtrations could enhance cell separation based on dead-end filtration technique. It was firstly introduced by Mohamed et al. for separating circulating tumour cell (CTC). The device comprises a varying filters gap widths to separate cells based on size and deformability [51] (Figure 1.6 (c)). Their application is to separate circular tumour cells (CTCs) from mixed with whole blood. They presented that the varying channel gap filtration successfully separated larger cells (e.g., CTCs) from a whole blood. Although the cell separation is succeeded, the clogging effect still exists due to overlapping size (similar sizes) of some CTCs and WBCs, and not totally reduced.

Thus, later, McFaul et al. developed a ratchets structure for separating cells [52] by the cell size and deformability. They introduced the reversed flow

condition to unclog the constrictions (funnel shape), small and deformable cells are unable to pass back through (Figure 1.6 (d)). They also include multiple linear arrays of funnel constrictions with different sizes of funnel pores size to separates cells by size and deformability using the microfluidic device. Therefore, the oscillatory flow mechanism improves the selectivity of traditional filtration methods. However, although the technique is promising, the microfluidic system is complicated. They required a precise control of flow and pressure system which made the system complicated and need to remove (by centrifuging) RBCs to reduce the sample concentration (number of cells) which influenced the cell separation performance.

The concept fluid flow oscillatory to reduce device clogging based on mechanical filtration similar to McFaul et. al. has been utilized for separating tumour cells by Yoon et. al. They developed a clogging-free microfluidic device based on lateral flow technique [53]. The principle of clogging-free device is simple and straight forward. By introducing a mechanical oscillation to the fluid flow, which released the aggregated cells at the filter (Figure 1.6 (e)). Smaller cells will be pass through while larger cells are trapped at the filter. The major disadvantages of this technique is overlapping target cells with blood cells (WBCs) due to similar sizes is difficult to be separated.

Another similar concept based on fluid flow manipulation is using fluid flushed back and forth developed by Cheng et al. to reduce cells clogging problem at filter membrane [54]. The principle is simple, by using a bidirectional motor pump, the fluid flow is flushed and force alternately to the filter membrane. Thus, the trapped cells in the filters (micropores) could be withdraw by flushing the membrane to prevent cells clogging (Figure 1.7 (a)). However, the device become more complicated which required pump controlling the flushed movement. Furthermore, it is not suitable for a high

concentration sample where the separation performance is effected by the sample condition.

Pang et al. developed a constricted structure for filtration for cells separation based on size and deformability with microvalves [55]. Also, the device is clogging free and have improved separation selectivity. The device consists of a funnel-like filter matrix (Figure 1.6 (i)). Although the microfluidic device could be able to separate cancer cells with more than 90% cells recovery and more than 80% of purity (target cell mixed with non-target cells) and clogging improved, the complexity of device operations including precision pressure and flow control by microvalves. Therefore, the major drawback of this method are required a complicated system for the operational. Moreover, the separation process requires frequent of repeating cycle-step of infusion, sorting and exclusion which is time-consuming separation process and not suitable for high concentration sample.

Sarioglu et al. developed a tumour cell separation microfluidic device based on triangular Pillar [56]. The purpose of the device to capture cluster tumour cells (CTC-cluster) from the unprocessed patient blood sample. Thus, the device could handle a high concentration of cells. The principle operation is similar to dead-end filtering where, the fluidic flow is perpendicular to the filtration structures (Figure 1.6 (f)). Smaller cells (blood cells) could pass through the filtration barriers due to the filter trap size is bigger than the size of blood cells. On the other hand, larger cells (cluster CTCs) are trapped at the filter. The cluster cells size is approximately having a minimum of 30 μm of size. Therefore, cluster tumour cells are easily being captured at the filters compared to blood cells where the cell sizes are smaller than the cluster tumour cells. The major drawbacks of this device are captured cluster cells

sometimes mixed with WBC (non-specific cell adhesion), and the device only suitable to separate a large size cells.

Masuda et al. proposed an open-channel microfluidic device for cell separation [57]. The device can separate circulating tumour cell (CTC) from whole blood. The principle of operation is straight forward. The sample is introduced from above of the trap pocket with diameter size is 32 μm. Trap pocket is formed form pillars which are arranged in a hexagonal pattern (Figure 1.6 (g)). CTC cells will be captured in the trap pocket while smaller cells, including RBCs and WBCs, are escaped from the trap pocket. The advantage of the open-channel device is the ability to isolate (cell picking) in-situ after the separation process. However, although the clogging of blood cells (RBCs and WBCs) is reduced, cells that were having similar size of CTCs such as large WBCs will also be captured at the trap pocket. Moreover, high shear stress occurred to the captured CTC cells due to high sample flow speed (up to 20 mL/h) during the separation process could resulted in damage to some softer cells. If the sample flow speed is too slow, resulting in the non-target cell captured which reduced the purity of single cell isolation.

Another example of mechanical filtration is using a 3D microstructure cell sorting developed by Xu et al. which performing multimodal cells size separation and clogging-improved microfluidic device [58]. The device that used arch-like microstructures for separating size based on cell size. The filter comprises two filters filtering sizes or can be configured more by designed based on arch-bridge-like (Figure 1.6 (h)). The cell separation principle is straight forward. Larger cell size than the filter size will pass through the filter by flowing on top (bypassing) of the filter structure (bridge). For smaller cells, cells will enter the filter and get captured under the bridge-filter. Although, this technique improved performance (clogging-free, the separation is only

base by size but not deformability. Cells have distinct deformability properties, even in the same population. Therefore, the limitations of this purposed technique only suitable for high stiffness cells only. Lower stiffness cells, despite the cell size still could be mixed with target cells. Thus the specificity is lower using this technique. Furthermore, clogging of cells could happen in high concentration sample where cell to cell interactions (cause by flow) is unpredicted.

Cell separation technique based on tuneable filtrations has been previously reported for many applications [59]. For example, a resettable cell traps are purposed to reduce clogging and improve selectivity and throughput have been developed by William et al. [60] (Figure 1.7 (c)). The device consists of the upper and lower flow channel. Upper channel is for sample flowing and the lower channel is for fluid-filled control. The two channels are separated by a thin diaphragm that can be deflected up or down by a pressure difference between the channels. Although the filtration concept of separation is simple, the device required a precision flow control pump and not suitable for a heterogeneous sample where target cells size is overlapping with non-target cells and might be wrongly separated. A similar works that utilizes tuneable filters for cells separation by Alvankarian and Burhanauddin for WBC separation form whole blood [61]. The microfluidic device consisting of arrays of mechanically control (by actuator) tuneable spacing pillars. The tuneable filtration system is used for analysis the suitable spacing conditions (filter gap size) for many applications. However, the device shown developed of WBC clogging and fouling.

Song et al. developed a tuneable filter modulated for reducing cell clogging during cell filtration process [62]. The filtration separation mechanism is based on the deformation of poly-dimethyl siloxane (PDMS)

tuneable membranes (Figure 1.7 (b)). The dimensions of the open area of the fluid channel (filters) could be changed based on the pneumatic tuneable deformation and thus determines the maximum diameter the cells which could pass through the microchannels. Although the tuneable channel success separates cell based on the size, cells clogging is still occurred. Therefore, a back-flush process was included which forced to remove the clogged cells at the filter area. This process unclogs the filters and improve recovery rate. However, back-flushed mechanism required additional pumps to control the flow fluid which caused the system more complicated. A similar work with back-flush device was developed by Cheng et al. [54].

Lee et. al. purposed a separation of CTC based on centrifugal-force-based size-selective device [63]. The device was developed utilize centrifugal forces to transport test samples from loading area to cell isolation chamber. The centrifugal force drive blood sample to the isolation chamber with a membrane filter where target CTCs are trapped (CTC size is larger than filter pores sizes). Smaller blood cells size such as RBCs, platelets and small size of WBCs are pass through the membrane (pores size is bigger than blood cells size) and straight to waste chamber. However, membrane clogging is the major drawback using the separation technique. To reduce the clogging effect, they performed sample dilution instead of RBCs lysis due to haemolysis caused target cell (CTCs) loss compared to sample dilution. However, the separated CTCs often contaminated with WBCs which size is similar to CTC using this technique. This is because only a portion area of membrane is used for separating cells due to centrifugal effect. Later, they further improved of this device to increase the separation efficiency and significantly alleviates clogging by introducing FAST (fluid-assisted separation technology) [64] (Figure 1.7 (d)). FAST disc concept utilize the entire filter membrane area for

cell isolation while non-FAST use partial of membrane for separation due to centrifugal force. Although this technique successfully separated CTCs rapidly (>3mL/min) and high recovery rate (>95%), the clogging was unavoidable for higher numbers of cells and contaminated cells such as WBCs.

Although all the purposed techniques developed to improved separation efficiency, rapid processing, removed cells clog etc. using mechanical filtration (Figure 1.5, 1.6 and 1.7), some common major drawbacks are complicated system setup including the need of precision flow or pressure control, actuators mechanism, sample needs to be diluted which not suitable to captured uncommon or rare cells in large populations and reduce throughput. Moreover, clogging issue using mechanical filtration including size, deformability, shape separation still a major challenge. Therefore, it is essential to develop a simple technique including device operation, sample preparation, provide rapid processing time, uncomplicated device system integration, fast result etc. which is suitable to be used in the clinical application including application at rural areas where limited healthcare resources are the major problem.

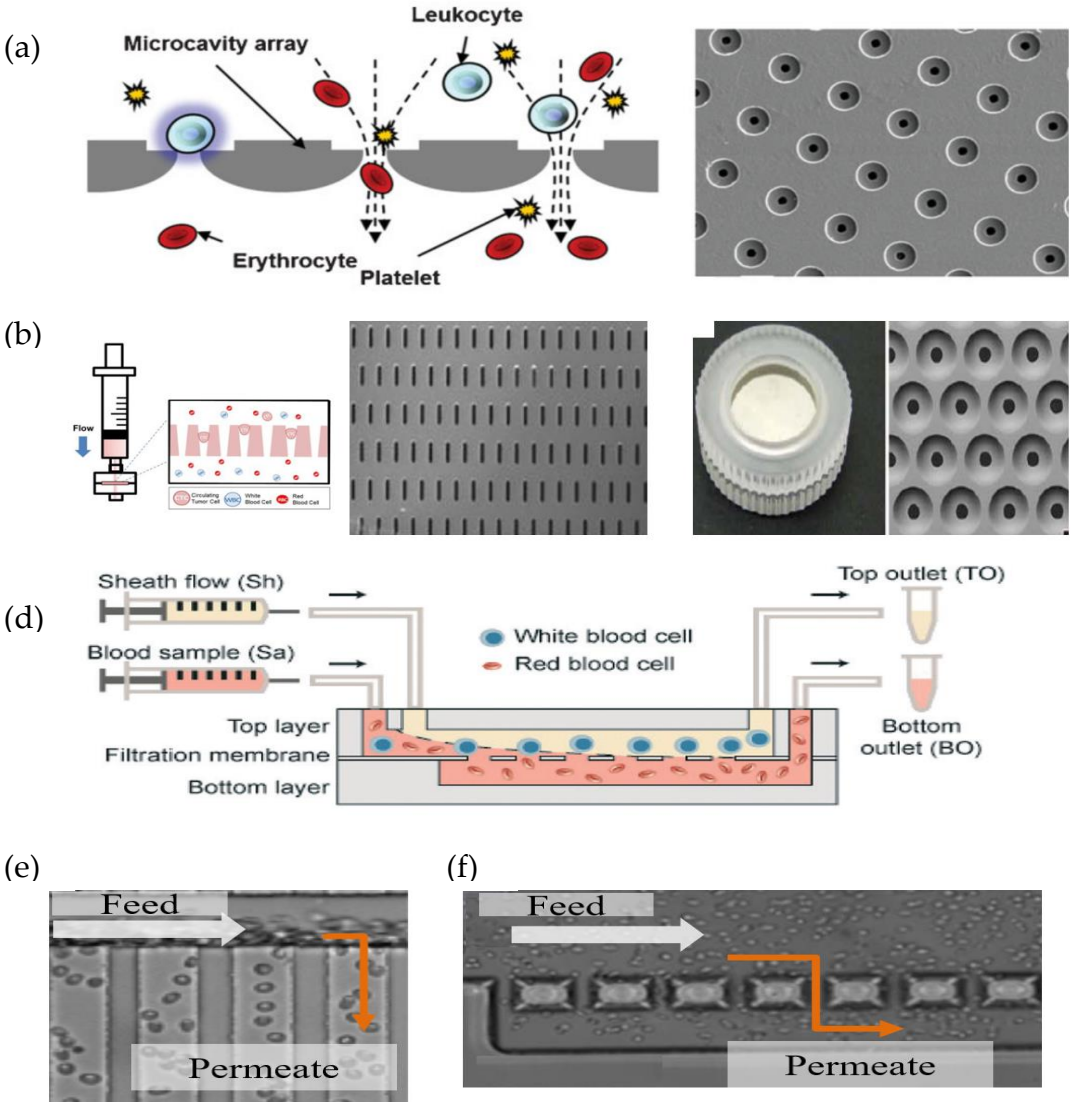

Figure 1.5 Cell separation by mechanical filtration. (a-c) Microcavity micropores filtration [37][39][41]. (d-f) Cross-flow filtration [43][42][44].

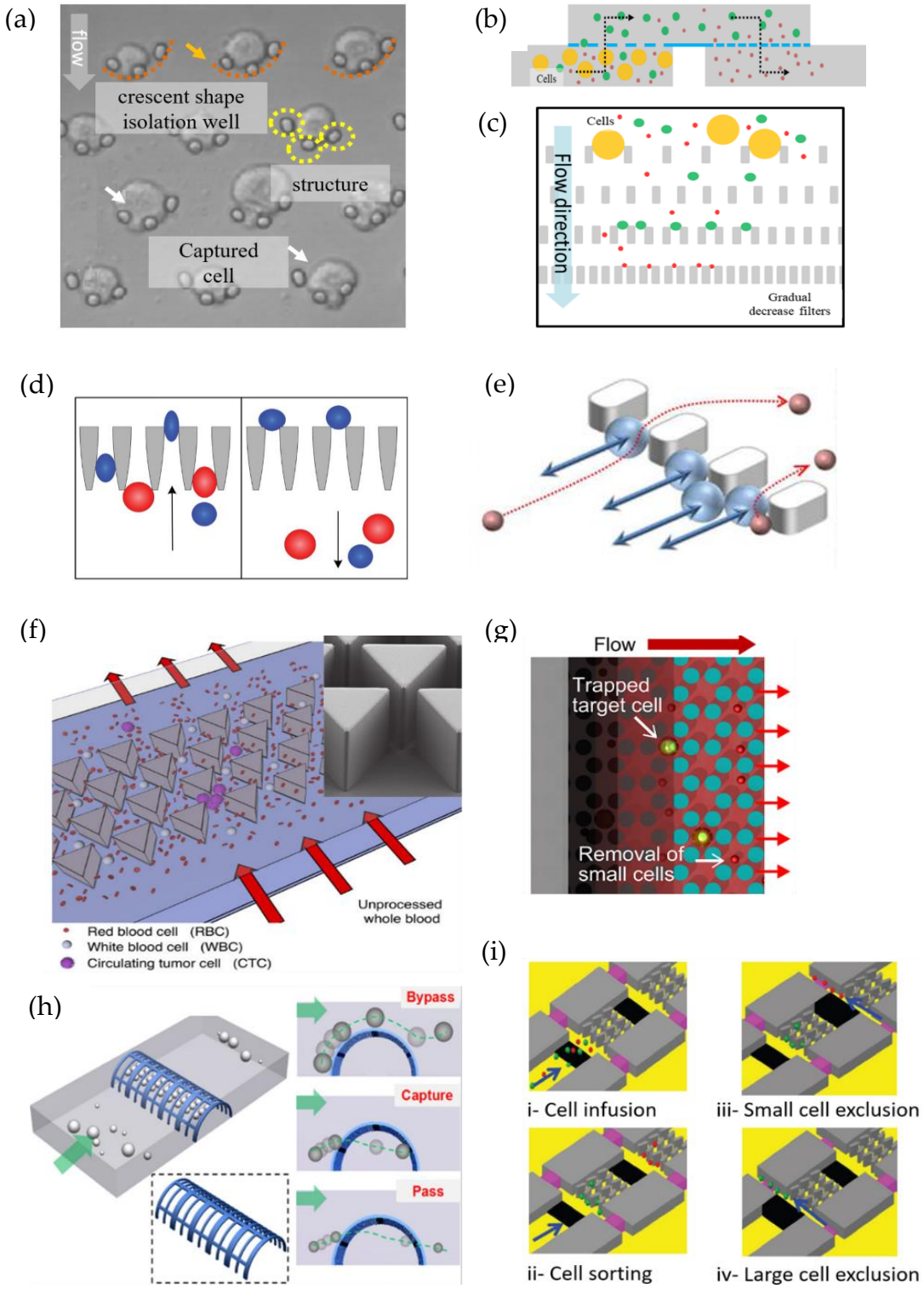

Figure 1.6 (a) A resent shape filtration [49]. (b) Membrane filter with multiple-pore [50]. (c) Gradual filtration [51]. (d and e) Oscillatory induced flow [52][53]. (f)Triangular pillar filtration [56]. (g) Pillar based open-channel filtration [57]. (h) 3D microstructure filtration [58]. (i) Microstructure-constricted filtration with pneumatic microvalves [55].

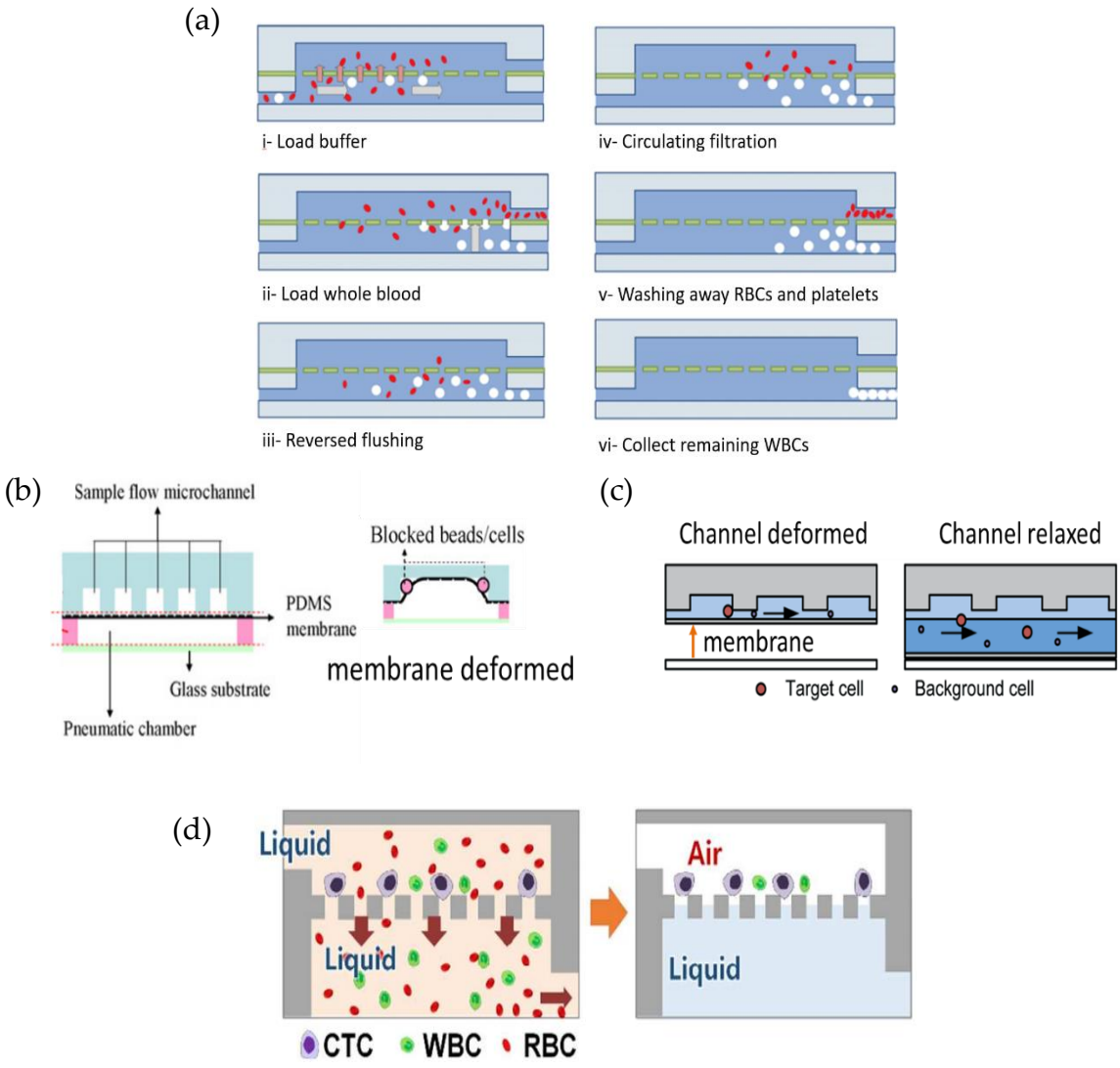

Figure 1.7 (a) Flushed and force alternately [54]. (b and c) Tuneable filters [60][62]. (d) centrifugal-force-based size-selective [64].

1.6 Thesis Overview

1.6.1 Research Motivation

A global trend shows that healthcare must be patient-oriented, providing a rapid diagnostics and test results, cost-effective and availed in more remote locations, emerging country or under developed regions of the world. One of this emerging country including Southern Africa is the world's highest population with a life-threatening epidemics and diseases such as tuberculosis (TB), malaria and Acquired Immune Deficiency Syndrome (AIDS). The people in this part of the world have a lack of health and sanitation awareness which cause these outbreaks. Patients need to be appropriately diagnose and monitor to prevent diseases spreading and losses of human life. Primary healthcare services and equipments are very limited in these countries (Southern Africa). Moreover, the facilities only available in the urban areas which requires basic infrastructure such as electrical, water etc. Thus, rural areas where a majority of the population are situated, unable to acquire much benefits from these urban areas healthcare facilities. Therefore, healthcare devices and systems such as point-of-care (POC) is feasible to allow a proper diagnostics [65][66].

Microfluidic system is an excellent to be used for a POC application. The microfluidic device enables a better cell sorting, straightforward cell manipulation and provide a simple system. A small volume of sample required compared to conventional flow cytometry which required a larger sample volume with tedious sample preparation, including Ficoll gradient centrifugation, haemolysis, labelling and many more. Furthermore, fabrication of the microfluidic device is reconfigurable to suit the application's requirements and could be made disposable. Applications such as complete

blood count used to evaluate health condition and diagnose a numerous disorders including virus infections, leukaemia and anaemia. For example, white blood cells including T (thymus) and B (bone marrow) cells provides information of the immune system, therefore, could be determined from specific blood count such as detection of the human immunodeficiency virus (HIV) etc.

1.6.2 Research Goals

The previous sections have discussed some of the advantages and disadvantages of conventional instruments such as flow cytometry and current microfluidic-based passive separation methods. Using microfluidic technology as the enabling tool, this research aims towards developing components for the point-of-care WBCs capture and cell counting. The research aims at achieving the following objectives:

1. *To develop a technique for WBCs separation based on mechanical filtration form whole blood. The separation of WBCs on the microfluidic device must be simple and clogging-free.*

   Blood is heterogeneous, contains a mixture of cells types such as red RBCs, WBCs and platelets. To determine the WBCs and its subtypes population, cells separation is the first step process. Conventional microfluidic-based cell separation using mechanical filtration is a straight forward manipulation of cells form its biophysical properties and required no additional forces for manipulating cell or tedious fabrication of microfluidic device such as affinity-based. However, these mechanical

filtration methods often suffer from device clogging caused by the cells that stuck. Current techniques developed such as oscillatory flow is not suitable for continuous flow separation, time-consuming process, additional oscillatory pump etc. Moreover, the capture or separation of cells is not efficient. Therefore, the work aims to develop an improve microfluidic device for cell separation using mechanical filtration based on cell biophysical including size and deformability. To perform WBCs separation more efficient, eliminate cell clogging problem and require a small amount of sample volume. The approach will be able to separate and capture thousands of WBCs in rapidly and provide accurate cell count. The purposed device should be easy to use, and perform highly efficient capture of WBCs.

2. *To develop an imaging system for detection and counting of cells captured on the purposed microfluidic device.*

The principle for cell detection using microfluidic filtration technique is different from a conventional flow cytometer cell counter. It requires image sensing where cell image will be taken and further process. Thus, a custom imaging system need to be develop to image separated cells in the microfluidic device. The imaging system must be sensitive enough to detect a low emission light (fluorescence) from labelled (fluorescence labelled) cells. Moreover, a multiple-detection of cells are required to determine WBCs sub-populations where multiple fluorescence labelled will be used. Therefore, the imaging system must be suitable to be used for multiple-fluorescence detection. On the other hand, cells must be able to detected from the captured images. Thus, a suitable algorithm must be developed to detect and count the cells accurately.

We proposed a colour thresholding methods which is suitable and simple, compared to others available methods.

In conclusion, the research aims and objectives pointed to provide a solution for some limitations (e.g., clogging, additional mechanism to unclog, overlapping captured cells at the filter, etc.) using conventional cells separation technique. Furthermore, overlapping cells are common problems in conventional filter-based microfluidic device for cell separation. The cells are captured at the same position at the filter caused cells overlapped and developed of cells clogging on the device. Overlapped cells image caused difficulty to determine cells types and count. This overlapping decreased the accuracy performance of cells counting on microfluidic device. Thus, simple technique for cells separation, imaging and cells detection is preferable to be used for many applications (e.g., cell analysis and counting) suitable without reducing the performance (comparable to standard method instruments used).

1.6.3 Dissertation Outline

This thesis reports a newly developed microfluidic device for cell separation, detection and counting. The principle of cells separation is according to cell biophysical features (size and deformability) based on mechanical filtration method (Figure 1.8).

In chapter 2, the proposed microfluidic device for size and deformability based cell separation will be described. The new developed concept of clogging-free device, and device fabrication process, including microfluidic device design and principle operation, are also explained.

In chapter 3, the hardware of custom imaging system used to detect the separated cells on the microfluidics device based on fluorescence detection

(immunofluorescence) and for cell imaging will be described. The image processing algorithm for cell detection and automatic cell counting are also discussed.

In chapter 4, the application of WBCs separation directly from whole blood using the proposed clogging-free microfluidic device will be described. In addition, the sample flow speed used to determine the efficacy of WBCs separation and captured distributions over the filters are also discussed.

In chapter 5, the application of T and B lymphocytes separation and detection using the purposed microfluidic device will be described. The cells count and ratio of T and B lymphocytes are compared with conventional instrument flow cytometry are also discussed.

In chapter 6, all the research findings and conclude with limitations of the microfluidic device and directions for its future development are summarized.

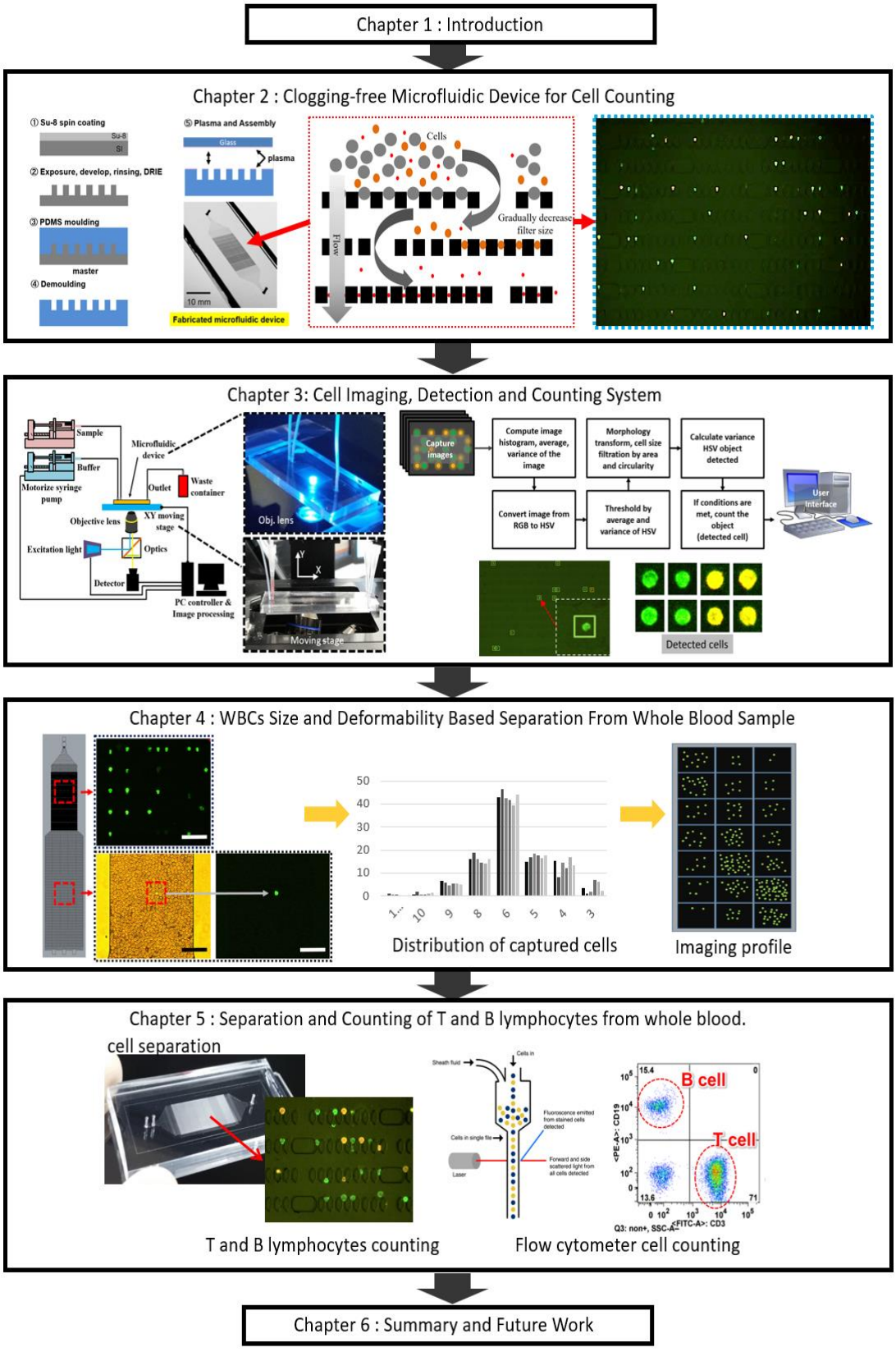

Figure 1.8 Dissertation Outline

Chapter 2

Clogging-free Microfluidic Device Based on Passive Separation Method

2.1 Introduction

In this chapter, the passive cell separation methods are described. Particularly, on passive separation based on mechanical filtration method. Although there are numerous passive cell separation methods as described in chapter 1 (Table 1.3), mechanical filtration is the most straight forward method of operating cell separation principles. Therefore, these methods are suitable to be used in many applications including separating of cells based on size, shape and deformability for example as cancers cells enrichment etc. This chapter is divided into several sections. Introduction to passive cells separation techniques, its advantages and disadvantages, the current development and proposed techniques to eliminates device clogging and the conceptual of the proposed technique. The microfluidic device design, the fabrication process of the purposed devices, preliminary experiment for observation of clogging effect using the purposed device, and the conclusion.

2.2 Passive Cells Separation Methods

Passive techniques offer simple structure and required no external forces (e.g., acoustic, optical, electrical, magnetic etc.) for cell separation and

sorting. As an example, mechanical filtration type cell separating is usually based on cell biophysical features including size, shape and deformability. The separation method can be divided into three main categories (Figure 2.1); membrane including microcavity or pores [33,41], pillars [48][49][51[67], weirs [68-70], cross flow [42-48]. The mechanism of these filtration methods can be classified based on the direction of the flow, such as dead-end technique which cell filtered having similar direction to the sample flow or cross-flow technique which flows tangentially across a membrane surface. In addition, the filter size (constrictive area) can be precisely controlled depending on the target cells physical size.

The fundamental separation principle of these size-based separation methods including pores, pillars and weirs are similar to the sieving concept where cells with smaller than filter size allow to pass through (unfiltered) the filtration, while larger size cells than the pores size will be filtered or captured. The flowing of the cells in the suspension or sample is driven by either positive pressure (push) or negative pressure (vacuum) through the filter. However, cells under pressure are not in static shape; cells are deformable in response to the force, which they could change shapes extensively, e.g., elongated. Deformability of cells is different from the cells types where deformability depends on the cellular properties including cell membrane and content [71].

On the other hand, the principle of cross-flow filtration which the feed flow and the filtration flow direction are at a 90° angle. Cells are flowing through a channel, the bigger size cells than the membrane size being trapped in the filter and the smaller size being released at the other end [43]. Crossflow filtration performs better than dead-end filters (pores, pillars and weirs), where it reduces the clogging effect.

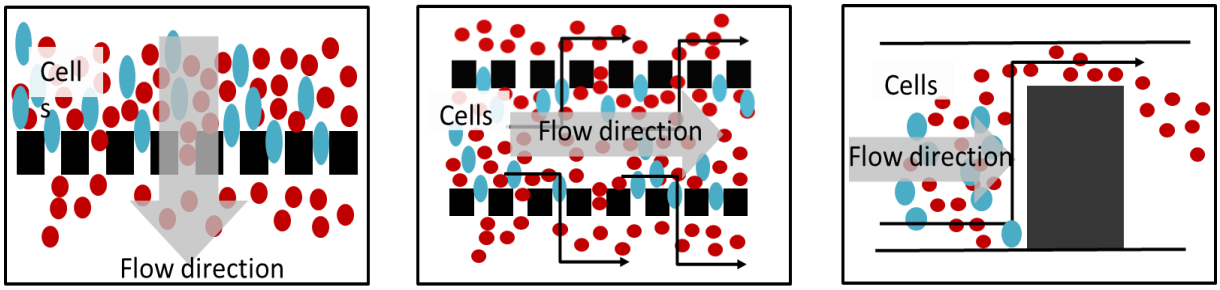

Figure 2.1 Passive mechanical filtration techniques based on size and deformability cells separation methods. Cells are separated or filtered by its biophysical properties. (a) The dead-end filtration (pores or pillar type). (b) Cross-flow filtration. (c) Weir filtration.

2.2.1 Advantages and Disadvantages of Cells Separation Based on Filtration Methods.

In 1964, S.H. Seal successfully separated large tumour cells or CTC from whole blood using mechanical filtering technique [72]. Till date, many have shown that filtration methods could provide simplicity, including device fabrication process, easy to be used and straight forward separation process. Furthermore, the methods also provide high throughput, and captured cells could be directly used for downstream analysis. However, due to device clogging caused by high cell concentration, poor specificity (overlapping filtered of cells) and purity (similar size of cells but with different types being captured) issues and unable to handle large sample volume caused these methods less popular than active separation methods. Although the crossflow filtration method could manage the effect of cell clogging problem, the high flow rates used, and improper separation in crossflow feed can damage a shear sensitive cells and decreased separation efficacy.

All these limitations caused the separation methods less popular in the highly selectively applications; for instance, separation of circulating tumour cells, cancer cells and rare cells require high selectivity, purity and also viability for further downstream assays. Furthermore, overlapping of cells

such as white blood cells with cancer cells caused major problems. Further additional process is required such as immune cells identification due to similar cells size, deformability properties etc. [73]. Hence, these major drawbacks and limitations of these mechanical filtration methods caused most of the applications of cell separations are shifted to more high efficacy and practicality as offers by active methods of cell separation [74].

2.2.2 Technique Developed to Reduce Device Clogging

Currently, few techniques were developed to reduce the problems using mechanical filtration techniques. As an example, a multi-level filtration such as gradual size filtration introduced by Hisham M. et al. [75]. The method successfully separated neuroblastoma, WBCs and RBCs at specific filter size. Others methods which discussed in the previous chapter such as an introduction of an oscillatory flow to the filtration mechanism, back flushed flow and a tuneable microfilters. However, these techniques require an additional mechanism which increased system complexity.

Therefore, it is essential not only to reduce clogging effects but also to minimize the system cost (from additional mechanism to reduce device clogging effect). In our purposed device, dead-end filtration method is enhanced by adding an escape route at the filtration. The escape route reduced the pressure and offered an alternative flow during the accumulation of the cells at the filters. The principle of escape route allowed sample flow through it when filters are occupied or captured cells. The direction of flow changed by this condition. If no cells captured at the filters, the sample will flow through it until cells being captured (Figure 2.2). Therefore, the microfluidic

device could not be clogged. This anti-clogging concept is simple and straight forward just manipulating the sample flow in the microfluidic device.

In addition, multi-size cells separation based on gradually size decrease filtration is incorporated with an escape route technique was used to enhance the anti-clogging effect (Figure 2.3). The gradual size decrease filtration was firstly introduced by Hisham M. et al. [75], for isolating of rare cells from biological fluids. The technique successfully separates cancer cells, WBCs and RBCs at specific filter size. Blood cells are having a broad range of cells sizes and deformability. The principle of cells separation using gradually decreased filters is based on the cells sizes and deformability. Larger cells are captured at early filter stages because filters size are bigger and smaller cells are captured at end stages with smaller filters size. Therefore, multi-size filtration is a suitable technique to reduce cells clogging effects and separates cells based on the size and deformability effectively. Figure 2.2 shows the conceptual of the clogging-free microfluidic device.

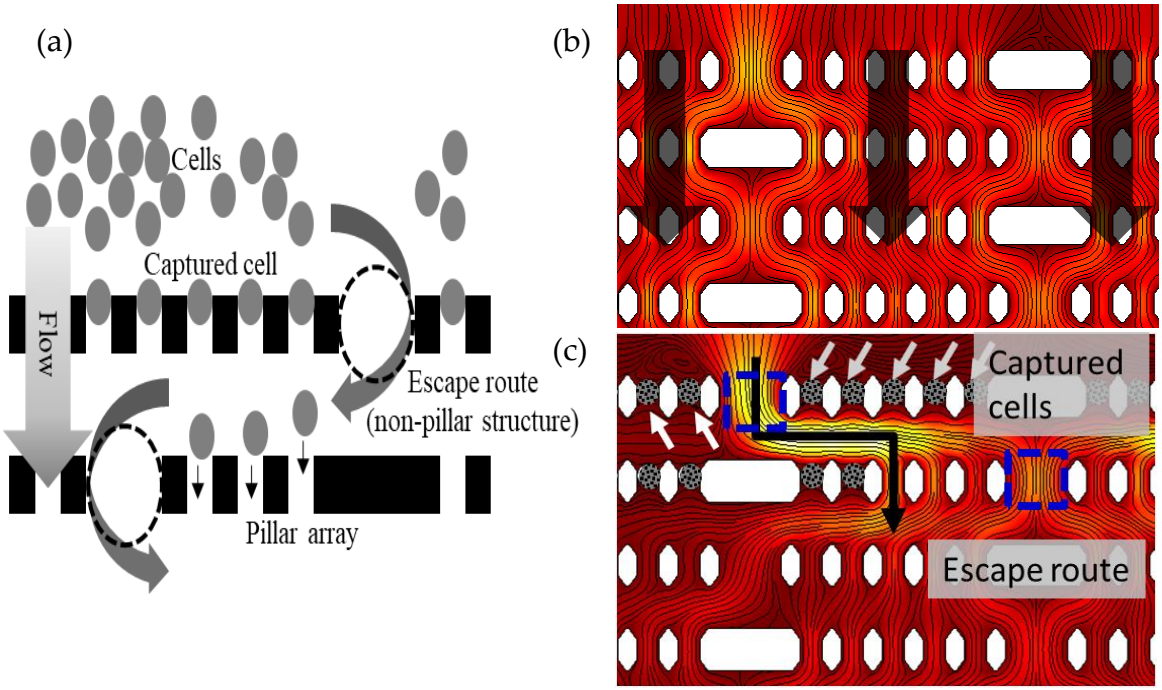

Figure 2.2 Clogging-free microfluidics device. (a) Cells are captured at the pillar based filters. When the filters are occupied with cells, others uncaptured cells will flow to other uncaptured filter area and through the escape routes. This technique will eliminate device clogging effectively by manipulation of flow. (b) Flow simulation example shows the flow pattern without any cells captured at the filters. (c) When filters captured cells, flow will be diverted to the escape route or empty filter space.

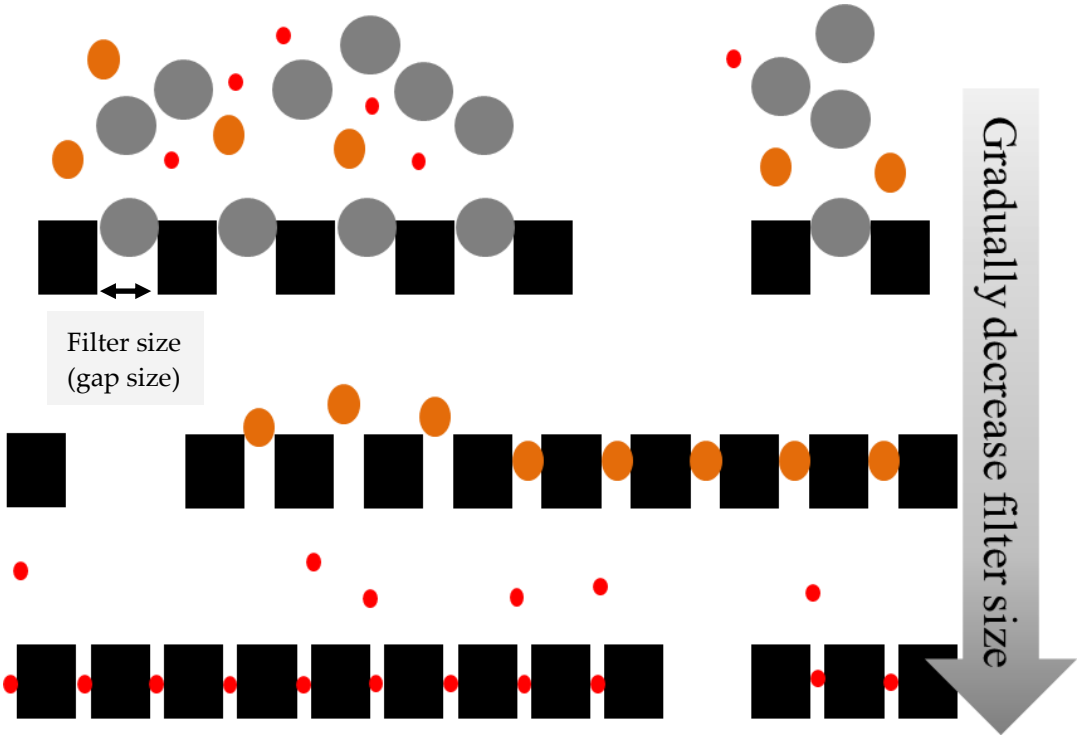

Figure 2.3 Gradually decrease filters size to capture cells based on size and deformability. The filter size from 15 down to 3 um are suitable to separate blood cells components including WBC. Unwanted smaller cell size cells such as RBC and platelets are able to passing through the filters

2.3 Microfluidic Device Design

Two types of the microfluidic device were developed for different applications and studies. The first, is to study the distribution of captured cells of WBCs or leukocytes from whole blood. The second device is to determine (cell counting) the sub-population of WBCs, T and B lymphocytes from whole blood. The cell separation mechanism based on mechanical filtration, i.e., pillar based, design for both devices are similar. The differences between these design were the sample outlet condition, where first design have sample waste area on the device and the second design sample waste is outside the device (Figure 2.4).

The first microfluidic device comprises two sections: the first section separates the targeted cells from the whole blood sample and the second section collects the remains of the processed sample (sample waste). For the second microfluidic design, we excluded the second section (Figure 2.4). The separation area comprises micropillar arrays with gap widths in the range from 3–15 μm [76]. The design details of the microfilters are outlined in Table 2.1. Larger microfilters gap sizes (e.g., 10 μm and above) are designed to capture larger CD45+ cells, including neutrophils, basophils, eosinophils, and monocytes, with sizes ranging from 10–35 μm. Smaller cells, such as lymphocytes, are more suitably captured by smaller gap sizes. Unfiltered or uncaptured cells, for example, RBCs and platelets, could pass through the microfiltration, as the deformability of RBCs (e.g., ability to contort, twist, and change shape) can result in cell sizes as small as 3 μm [77].

The preliminary experiments confirmed that micropillar filtration using a filter gap size of 2 μm caused RBC clogging in the device (data not shown). Therefore, we chose 3 μm as the smallest filter size. The escape routes in the microfilter arrays prevent cell clogging and fouling on the device during the filtration process. The width (Wsa) and length (Lsa) of the separation area are 10 mm and 20 mm, respectively. The waste area is 15 mm wide (Wwa) and 30 mm long (Lwa) and contains pillars for supporting the roof to prevent collapse. The support pillars' width (Wp3) and length (Wp4) sizes are 100 μm and 800 μm, respectively. The distance between the support pillar-to-pillar (Wp1) and line-to-line (Wp2) are 200 μm and 120 μm, respectively. The height of the microfluidic device is approximately 40 μm. Thus, the total volume is 8 and 18 μL for the separation and waste area, respectively, and the approximate total volume of this device is 26 μL. Thus, the sample volume for the device must be less than 18 μL (e.g., 10 μL) to prevent the sample overflow (i.e., going

out) at the outlet. For similar reasons, the waste area was also designed to be larger than the separation area. The waste area design on the microfluidic device will eliminate problems, such as improper sample flushing to the reservoir (e.g., a waste container), that occur when using a conventional microfluidic device (Figure 2.5). These problems could lead to missing cells and/or cells adhering to the microfluidic tubing wall or container. In addition, sample residue is tedious to process, and processing would involve transferring, which causes cells loss. Therefore, the sample waste collection on-chip design will significantly reduce errors in the cell counting process, particularly for applications that demand precision. Table 2.1 shows the sizes and dimensions (separation area design) of the purposed device.

Table 2.1 Microfluidic device separation area (filters) dimensions

Gap size (µm)	No. of microfilters line	line-to-line size (µm)	Microfilter length (µm)	Microfilter width (µm)	Escape route width (µm)	No. of escape route per microfilter lines	Wall width size (µm)
15	12	25	20	14	-	-	-
14	12	25	20	14	30	13	200
13	12	25	20	14	30	13	200
12	12	25	20	14	30	13	200
11	12	25	20	14	30	13	200
10	12	25	20	14	25	13	200
9	48	25	20	14	20	49	48
8	60	25	20	14	20	50	48
6	60	25	20	14	20	53	58
5	60	25	20	14	15	57	44
4	48	25	22	20	14	47	54
3	40	15	22	20	6	33	42

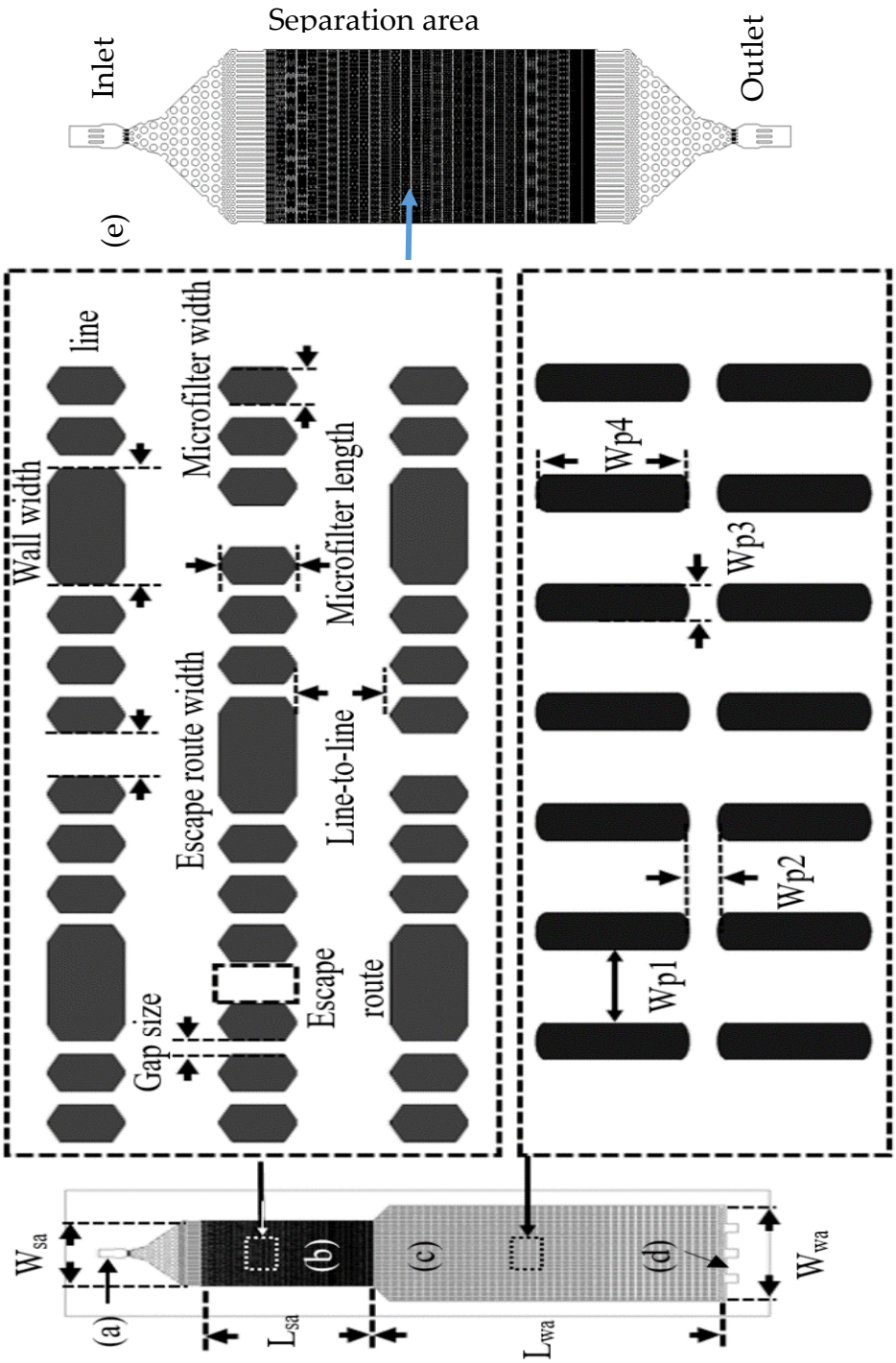

Figure 2.4 Top view of the schematic diagram of the microfluidic device. (a) Sample and buffer inlet port. (b) Cell separation area with microfilters, gradually narrowing filter size. (c) Sample waste area. (d) Air outlets. (e) Schematic of second microfluidic device without sample waste area. The separation area design and dimensions are similar to first device

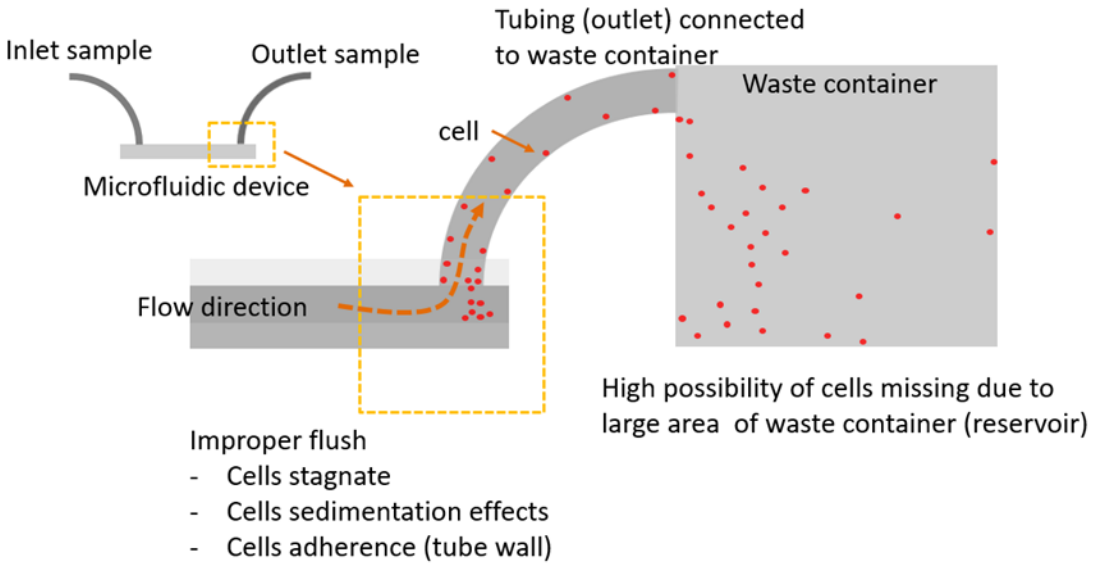

Figure 2.5 Conventional microfluidic device setup with sample outlet connected to container (reservoir). Improper sample flow to the container caused in accurate cell determination and sample transfer caused possible of missing cells, adherence of cells at the wall and difficulty to recover cells for further analysis etc.

Microfluidic Device Fabrication

The microfluidic device consists of polydimethylsiloxane (PDMS) and a glass plate (Figure 2.6). The PDMS part was fabricated using a standard soft lithography process. Firstly, a photomask was made using a laser printer (DWL66FS, Heidelberg Instruments Mikrotechnik GmbH, Heidelberg, Germany). Next, a high-contrast epoxy-based photoresist (SU-8 3025, Microchem, Corp., Newton, MA) was spin coated to a thickness of 40 μm on a 525-μm thick Si wafer (2000 rpm, 30 s). The Si wafer was soft baked for 40 min at 75 °C. The spin-coated wafer was exposed using a mask aligner (MA-6, SUSS MicroTec AG, Garching, Germany) for 35 s. The post-exposure bake was at 65 and 95 °C for 1 and 5 min, respectively. The Si wafer was developed and dry-etched by a deep reactive ion etching system (D-RIE, RIE-800, Samco, Kyoto, Japan). Octafluorocyclobutane (C4F8) was used for the passivation of

the Si mold to create a non-adhesive surface during the PDMS demolding process. The PDMS microfluidic device was prepared using a PDMS pre-polymer (Silpot 184, Dow Corning Toray Co., Ltd., Tokyo, Japan) mixed at a 10:1 (w/w) ratio with a curing agent. The PDMS was poured into the Si mold and baked at 75 °C for 1 h. The cured PDMS was demolded and treated with O2 plasma (Cute- MPR, FemtoScience, Seoul, South Korea) to facilitate the PDMS surface modification for the glass bonding process. The fabricated microfluidic devices are shows in Figure 2.7.

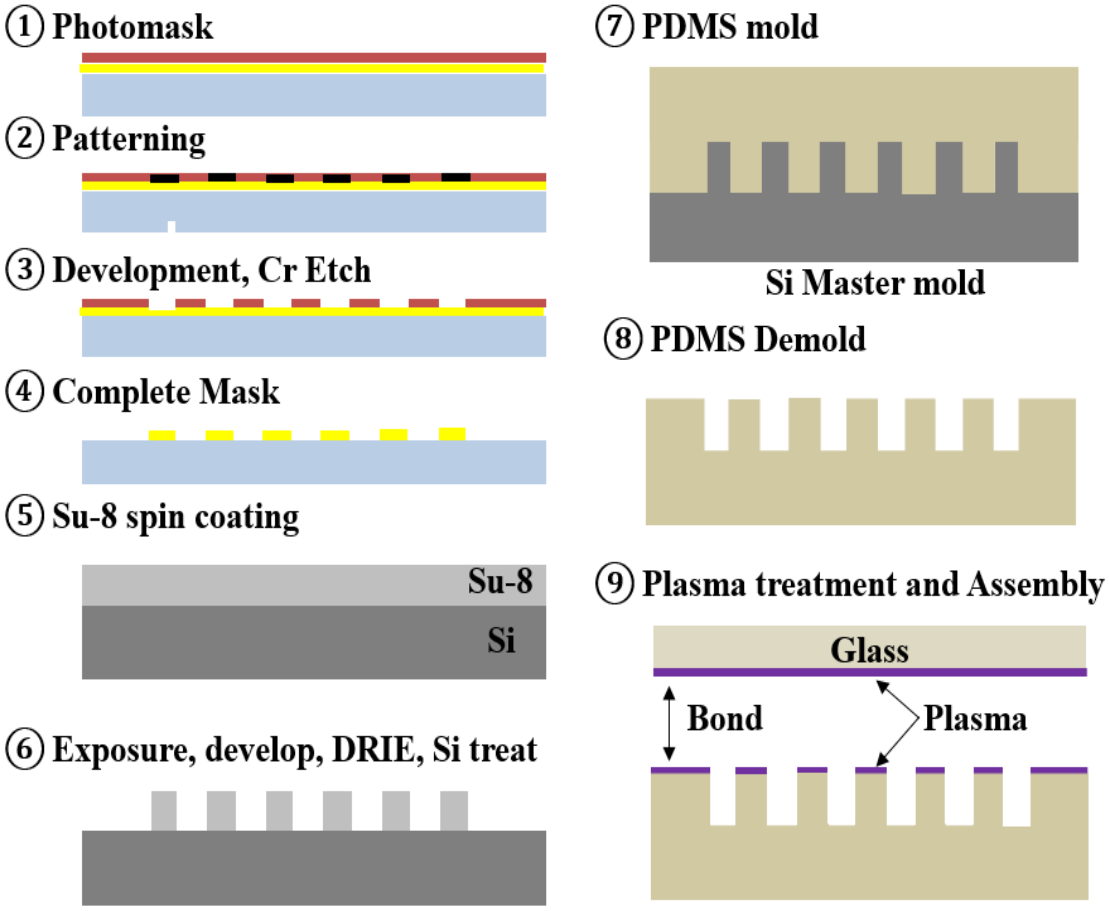

Figure 2.6 Microfluidic device fabrication process using photolithography and soft lithography techniques

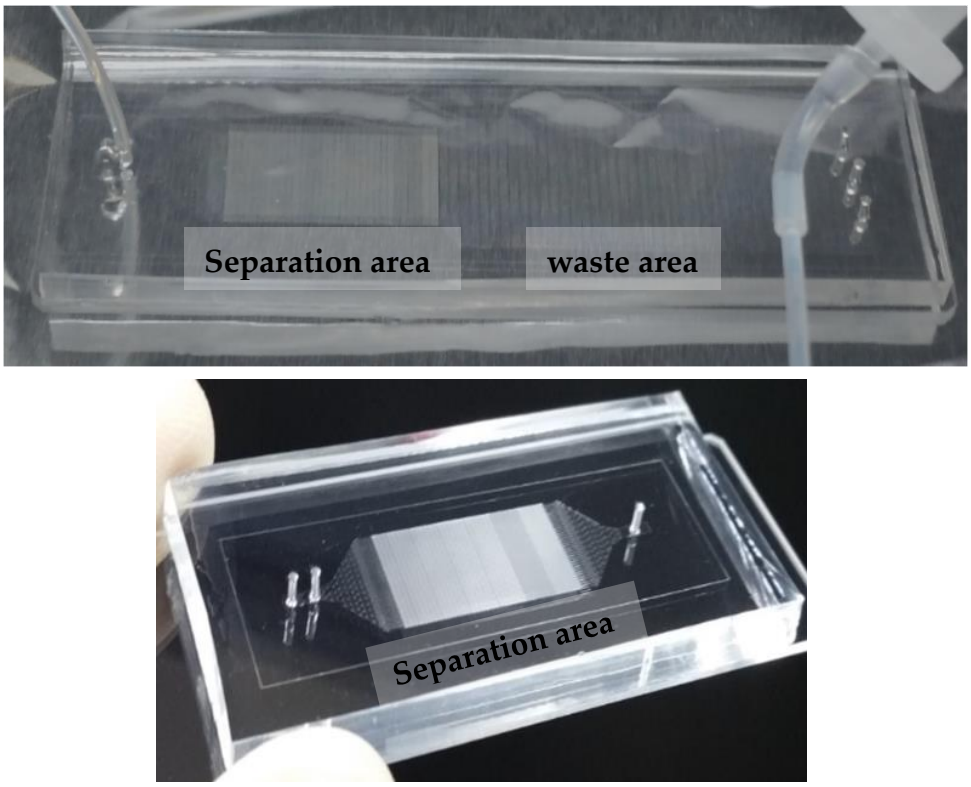

Figure 2.7 Fabricated microfluidic devices. Top and bottom images are the first microfluidic device (with waste area) and second microfluidic device (without waste area), respectively

2.4 Preliminary Results and Observations of Device Clogging Effect

In this preliminary experiments, there are no analysis performed on the experiment results. The main objective is to observe the microfluidic device clogging-free efficacy. The WBCs is used for the target cells separated from whole blood. The sample preparation and fluorescence labelling (immunofluorescence) and sample introduction to the microfluidic device will be discussed in details in chapter 4. In the observation, the microfluidics device does not have clogging problem by using 1 and 2 μL of sample volume (10 μL diluted prepared sample approximately equal to 1 μL of whole blood) (Figure 2.8). However, the device starts to build cells clogging when a 3 μL of blood

sample is used (Figure 2.9). Form the observations, we concluded that within the design dimensions (separation area) proposed, the concentration of WBC plays an important role in building up clogging on the filters. At 3 µL of whole blood volume, we estimated about 18,000 of WBC (1 µL is about 6000 WBC, determined from a healthy donor sample blood count). Therefore, in our

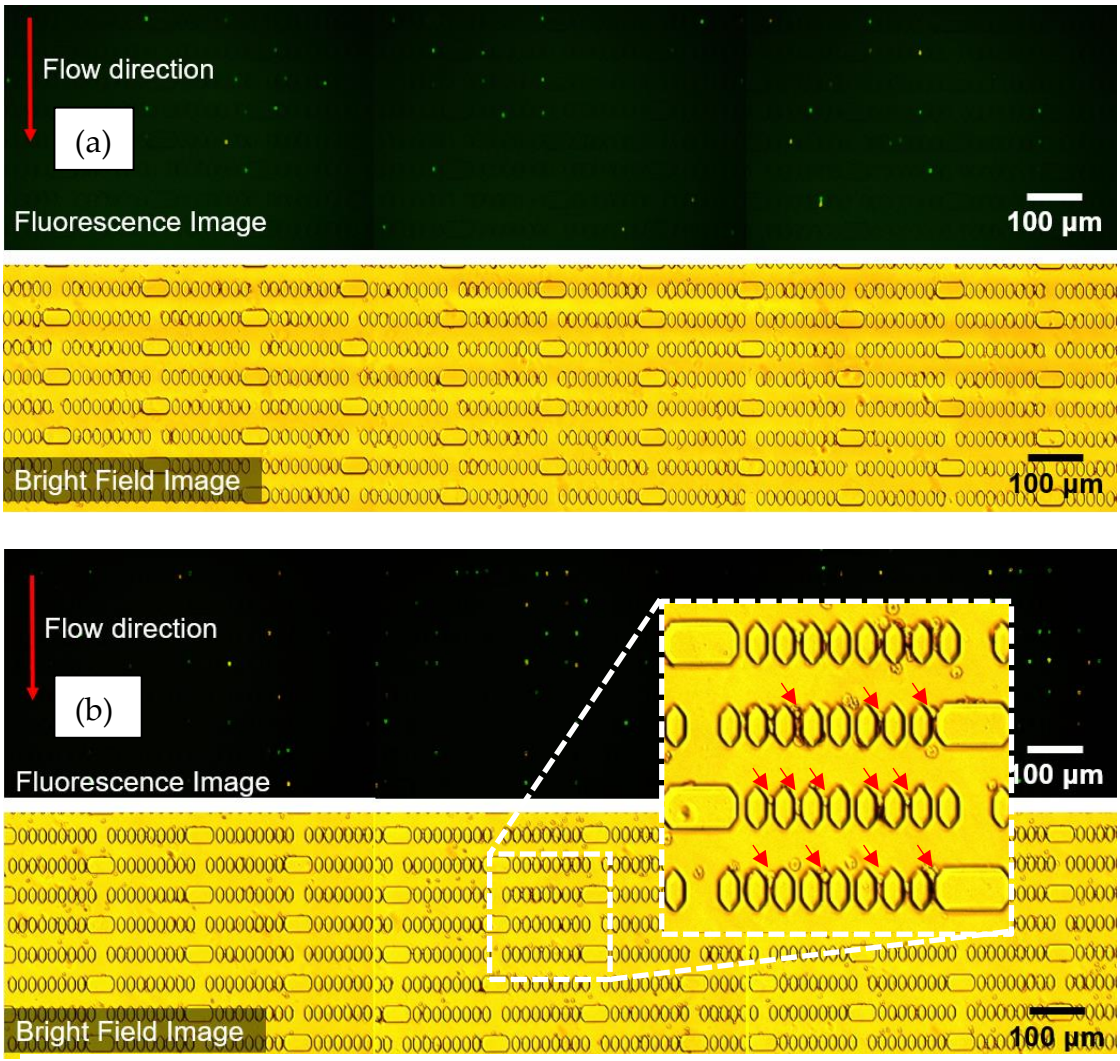

Figure 2.8 Microfluidic device show no clogging (cells clogging) using 1 µL (a) and 2 µL (b) of whole blood. The bright field images confirm the results. Images was taken at 6 µm gap size, centre of microfluidic device for comparison. Red arrows show the captured cells

applications, we limited the concentration of WBC by using a lower volume of whole blood sample to reduces the clogging effect.

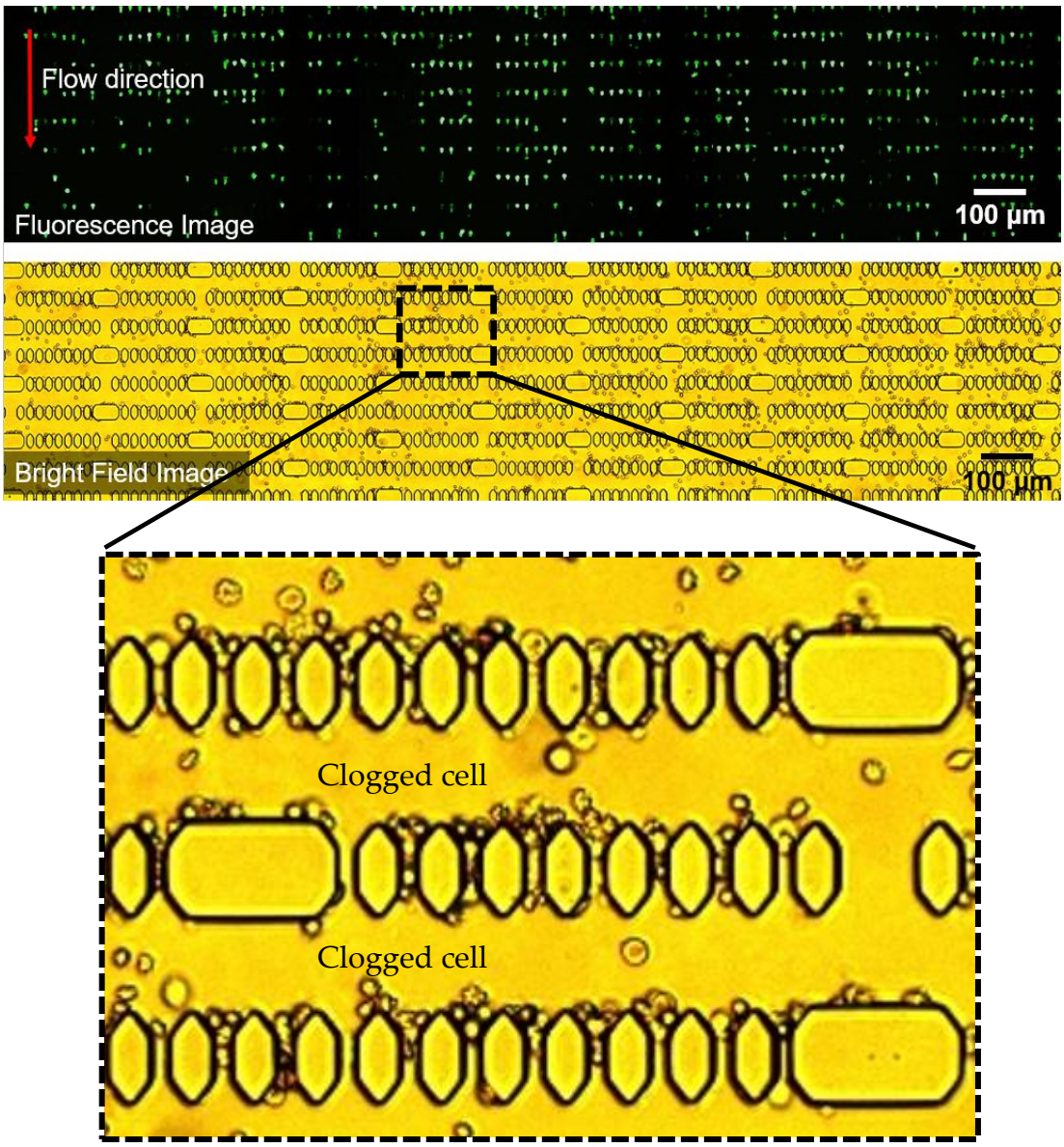

Figure 2.9 Microfluidic device show device clog build-up (cells clogging) using 3 µL of whole blood. The bright field images confirm the results. Images was taken at 6 µm gap size, centre of microfluidic device for comparison.

2.5 Conclusion

The concept of the clogging-free device is relatively simple compared to current techniques that require oscillatory flow, adjusting filter, and complicated device fabrication process. By introducing the escape route (empty spaces in the filters array), manipulation of fluid flow will help to reduce the pressure by choosing an alternative way which significantly eliminates device clogging. Observation in the preliminary test shows promising results where the device could handle up to 2 μL (20 μL of a diluted whole blood sample) of the whole blood sample. Further, increased sample volume, e.g., 3 μL is not recommended as the device filters start to build cells clogging. This clogging build-up is expected because of the dimensions of the developed device is limited to 10 mm X 20 mm (width × length) of separation area is small to manage a high concentration cells. Hence, with simple fabrication process, straight forward operation, the purposed device could be useful for many cell separation applications.

Chapter 3

Cell imaging, Detection and Counting

3.1 Introduction

In this chapter, the microfluidic device of cells detection algorithm is described. Cells are identified from their immunofluorescence. WBC are recognized by CD45 Fluorescein isothiocyanate (FITC). For lymphocytes, T and B cells are recognized by CD3+ FITC and CD19+ Phycoerythrin (PE), respectively. This chapter is divided into four sections. The custom-developed imaging system for cell detection, Cell scanning and image capturing system, the algorithm to perform cell counting from captured cell image and conclusion.

3.2 Development of Custom Imaging System

To establish a high-quality fluorescence imaging, the selection of system including optical, light source and detector (camera) are critical [78]. For example, selection of a light source, i.e., excitation light, such as xenon arc lamps, lasers, and high-power LEDs types must be suitable to the application. The light source used in a fluorescence microscopy and imaging applications must emit from the fluorophores present at the sample at the specific wavelengths. The intensity of excited source light must be high enough to stimulate as much fluorescence emission as possible. Source light such as

mercury arc lamps are expensive and suitable to be used for broad-spectrum compared to lasers and LEDs. However, the arc lamp has a short lifetime, which is a few hundreds of operation hours. Moreover, arc lamps required a wavelength selective excitation filter. This excitation filter allows only a specific wavelength to pass through it. Hence, the system becomes more complicated. On the other hand, typical lasers and LEDs source light require no excitation filter because the wavelength is selective [79]. Even though laser light is more intense (high concentration light) than LEDs, the cost is higher than other excitation lights. LEDs excitation light are low cost, low power consumption, compact and provide longer lifetime. Moreover, LEDs technology currently, offers narrow emission bandwidth; therefore, the intensity is better, less noise and an additional excitation filter can be omitted. Furthermore, narrow excitation bandwidth reduces the emission curve overlapping. This narrow bandwidth will increase the signal to noise ratio (SNR) for sample detection [80].

The performance of the imaging system is not only relied or dependent on the hardware setup alone [81]. The quality of fluorochrome (fluorophore) used for the identification of the cell plays an important role in cells detection using imaging techniques. A fluorochrome is a chemical which can absorb energy from an excitation light source and emit photons at a longer wavelength than the source wavelength, which is detected by optical sensors. A good quality fluorochrome provides not only brighter light emit (fluorescence) but sustain photo bleaching resistant for a longer time.

There are two techniques to fluorescence labelled cell antibody, including direct, indirect, including indirect with amplification [82] (Figure 3.1). The selection techniques depend on the level of antigen expression on the cell surface. As an example, a highly expressed antigen suitable for direct

immunofluorescence staining. The process of staining is simple, where antigen with fluorochrome label, directly bind (antigen-antibody interaction) to the cell surface. However, the major disadvantage is the lower sensitivity of direct detection or the intensity of the fluorescence signal, for lower antigen expression. In contrast, indirect detection provides a higher level of sensitivity even for lower expression cells. The signals are more intense by multiple secondary labelled antibody binding to primary antibody binding. However, the use of a secondary antibody requires extra blocking steps and additional controls. Moreover, the process of labelling is time-consuming and expensive. For very low levels of antigens expression, indirect with amplification technique is required. Fluorescence signals are amplified by a large number of fluorochromes. Although, the major disadvantages of this technique required additional process steps, and it is a time-consuming process for labelling and expensive.

To provide simple sample preparation in this project, direct immunofluorescence labelling technique is most suitable. Even though the expression of cells differs, a suitable imaging system develop could increase the detection sensitivity (able to detect very low light condition). However, many factors could influence cell detection (fluorescence labelled) including excitation power, optical system, staining methods, detector and biological sample. Thus, imaging system must be properly developed to ensure cells could be detected even at very low fluorescence emission intensity.

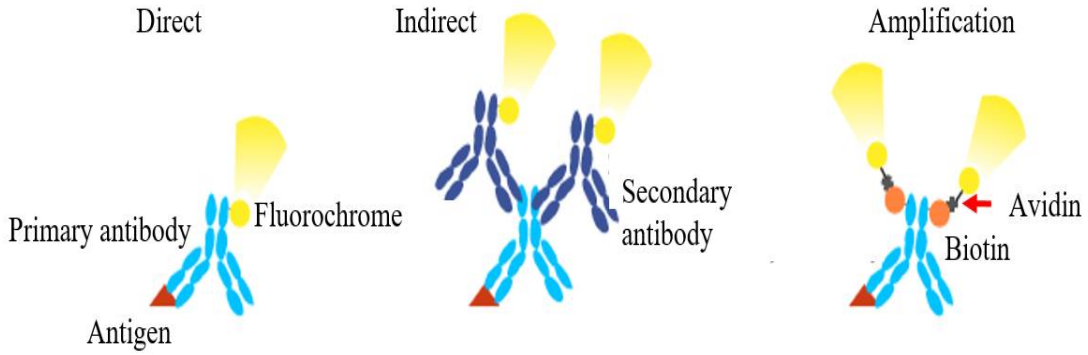

Figure 3.1 The immunofluorescence techniques for cell labelling. Light emitted intensity for direct method is lower than indirect method. Amplification technique increased the intensity of emitted light. [image adapted from https://www.mblintl.com/products/labeled-antibodies-mbli/]

The imaging system is carefully developed to meet optimum performance of cell detection. A 488 nm light source (Lumencor Inc., Beaverton, OR, USA) provides high performance and stable, suitable for optimum excitation of FITC and PE fluorescence emission with a dichroic mirror (DM505, Olympus, Japan) with a long-pass filter (505 nm) for multi-colour fluorescence detection. A 10X super-apochromatic objective lens (UPlanSapo, Olympus, Japan) is used for cells imaging. To ensure a good signal to noise ratio for signal detection, an emission band-pass filter is installed in the optical system with selected wavelength range 500–650 nm (Semrock, Rochester, NY, USA) is used. A narrow band-pass filter used is similar to that used in a flow cytometer system to reduce the background noise and spectral overlap (spillover signal). A filter with too wide spectrum may lead to an excess of background noise, leading to false results. If it is too narrow, it will reduce the detection sensitivity. Preliminary result in the system evaluation found that cell detection was compromised if we limit the detection filter (narrow bandwidth) spectrum band and therefore a wide range filter (500–650 nm) was selected to cover the entire FITC and PE fluorescence

emission spectrum band (Figure 3.2). Moreover, the relative intensity of fluorescence light emission depends on the expression of cell surface antigen

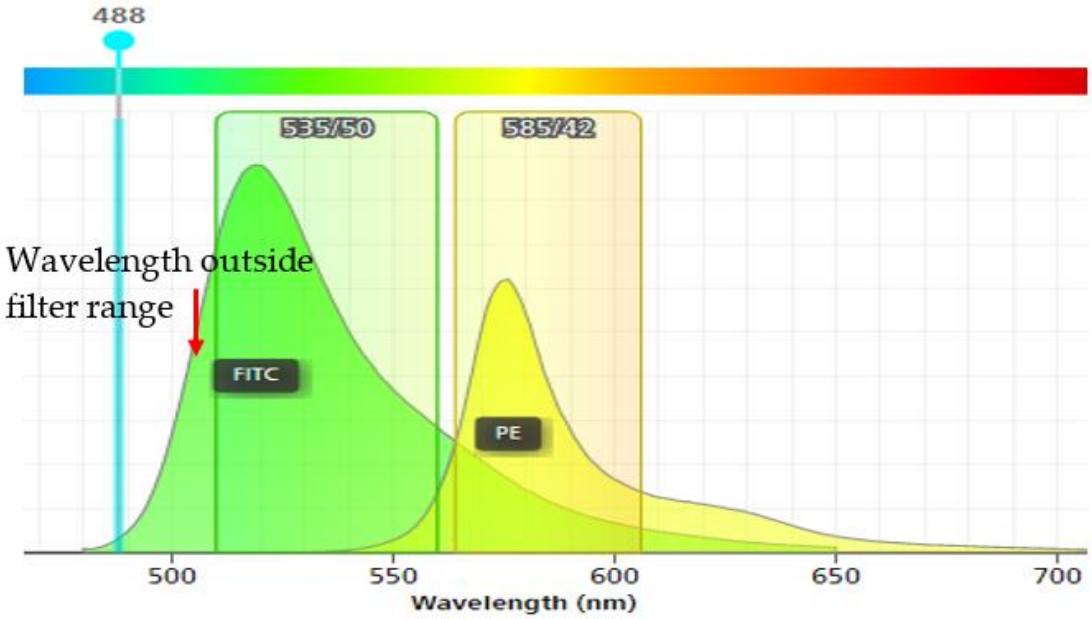

Figure 3.2 The spectrum fluorescence light emission. Excitation light at 488 nm (blue) and light emission are fluorescein isothiocyanate (FITC) and Phycoerythrin (PE). Flow cytometer filters available for maximal broad FITC detection is 535/50 nm and maximal broad PE detection is 585/42 nm. Overlapping of spectral is clearly can be seeing for FITC. The wavelength (emission light) outside the filter could not be detected. [image adapted from https://www.bdbiosciences.com/en-us/applications/research-applications/multicolor-flow-cytometry/product-selection-tools/spectrum-viewer]

[83] and the type of fluorochrome [84]. Although a wide range of emission band (500-650 nm) is used, overlapping spectra between FITC and PR fluorescence still occur (Figure 3.3). This could contribute to the error in cell counting where FITC and PE could not be distinguished properly. However, it could have been minimized by developing a robust image processing algorithm to reduce the error. This algorithm will be explained in details in next sub chapter, 3.4.

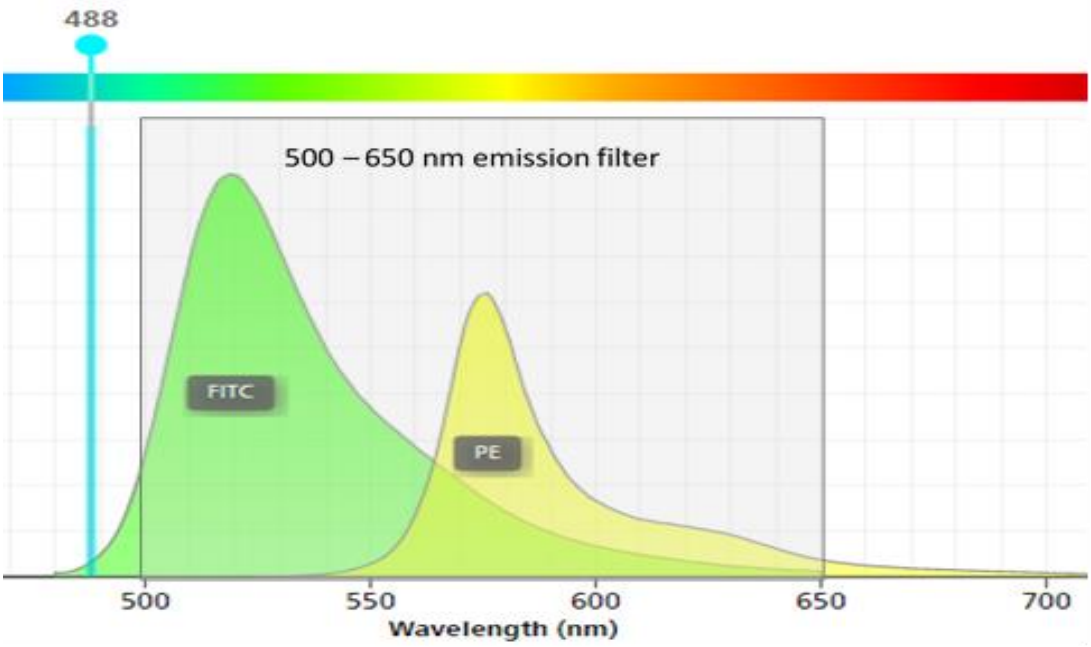

Figure 3.3 Emission filter with 500 – 650 nm spectral range increased the detection (FITC and PE) of labelled cells. Overlapping or spill over wavelength could be reduced by image processing algorithm. [image adapted from https://www.bdbiosciences.com/en-us/applications/research-applications/multicolor-flow-cytometry/product-selection-tools/spectrum-viewer]

3.3 The Cells Scanning and Imaging System

After a sample being processed (sample flow completed), cells will be separated at the separation area in the microfluidic device. To detect and analyse the separated cells, an automatic system is required to scan and capture the image of the separation area The scanning system, including precision moving stage (microfluidic device stage). The imaging system compromises the optical system, including detector as described earlier. There are two motorize system used to control the custom moving stage with X-axis and Y-axis for scanning the microfluidic device area with a 2 μm per-step resolution (Chuo Precision Industrial, Tokyo, Japan) used in the system. The motorized system is controlled automatically by the custom-developed

program. Initially, the motorize position will be calibrated before the scanning process. This is done manually by setting the coordination at first position area of the microfluidic device (Figure 3.4).

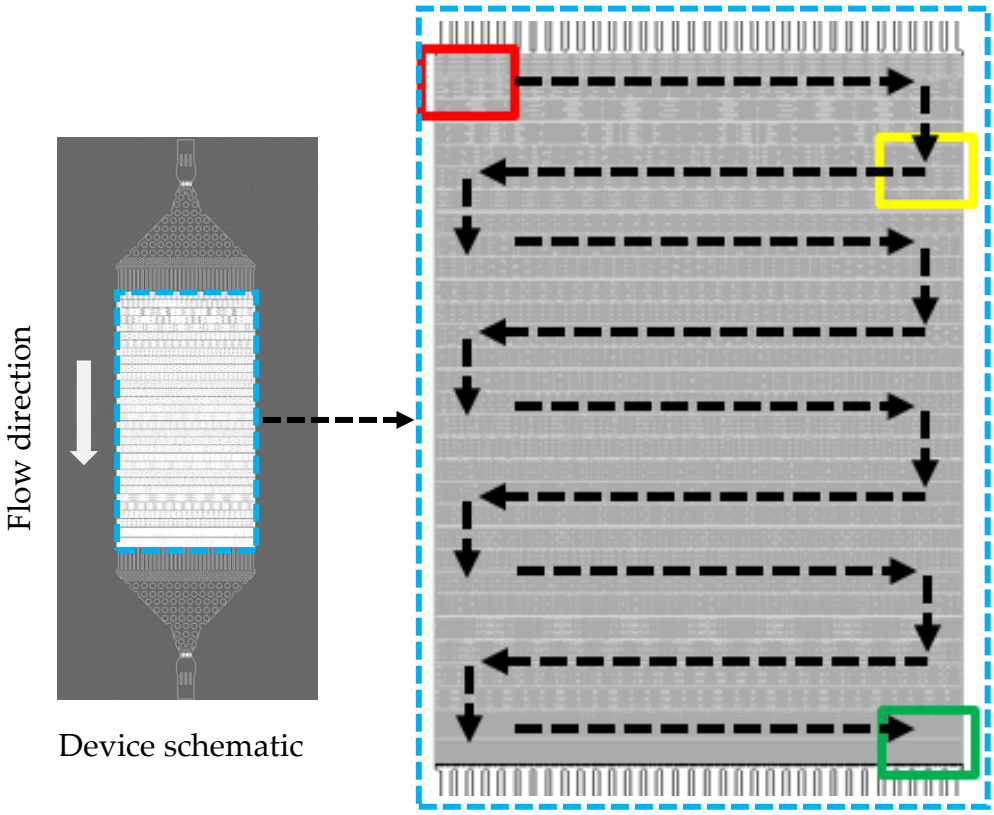

Figure 3.4 Illustration of cells scanning on the separation area in microfluidic device. The initial motorize moving table position (red box) are set manually. The scanning and imaging performs by motorize X-Y moving table and automatically stop at the last separation area (green box).

The intensity of fluorescence emission signals from the cell are sometimes very weak. It is also depending on the expression of antigen on the cell surface. Thus, a high sensitivity light detector is required. After several evaluations of sensors selection, we choose a high sensitivity RGB CMOS camera (ASI178MC-Cool ZWO, China) because it provides a low noise image. The colour camera is necessary for fluorescence microscopy to detect multiple fluorescence light signals. In FACS instruments, the fluorescence signal

detection uses different principle. It commonly used photomultiplier tubes (PMT) as a detector. Each PMT in the FACS needs specific wavelength filters depends on the number of colours offered by the system. Furthermore, RGB camera provides advantages of multi-colour detection compared to a monochrome camera. Furthermore, the camera provides a larger picture size resolution (6.4 Mega Pixels, 3096 x 2080). The camera provides high sensitivity light sensor (IMX 178, Sony, USA) are suitable for a very low light condition such as fluorescence imaging application. In addition, the relative response or spectral sensitivity of this sensor provided a high sensitivity for detecting FITC and PE signals (Figure 3.5). In addition, the large picture size (3096 x 2080) with 2.4 μm size of each pixel, suitable to a captured large area on the microfluidic device which improved the scanning time of cell separation area. Covering the entire cell capture area requires 503 images (Figure 3.4), and this process takes about 15 minutes (1 image about 1.8 seconds capture time) to complete. A CMOS detectors provide low-cost, low-power consumption and low noise compared to CCD detectors [85]. Figure 3.6 shows the diagram of the custom imaging system for the detection of WBCs.

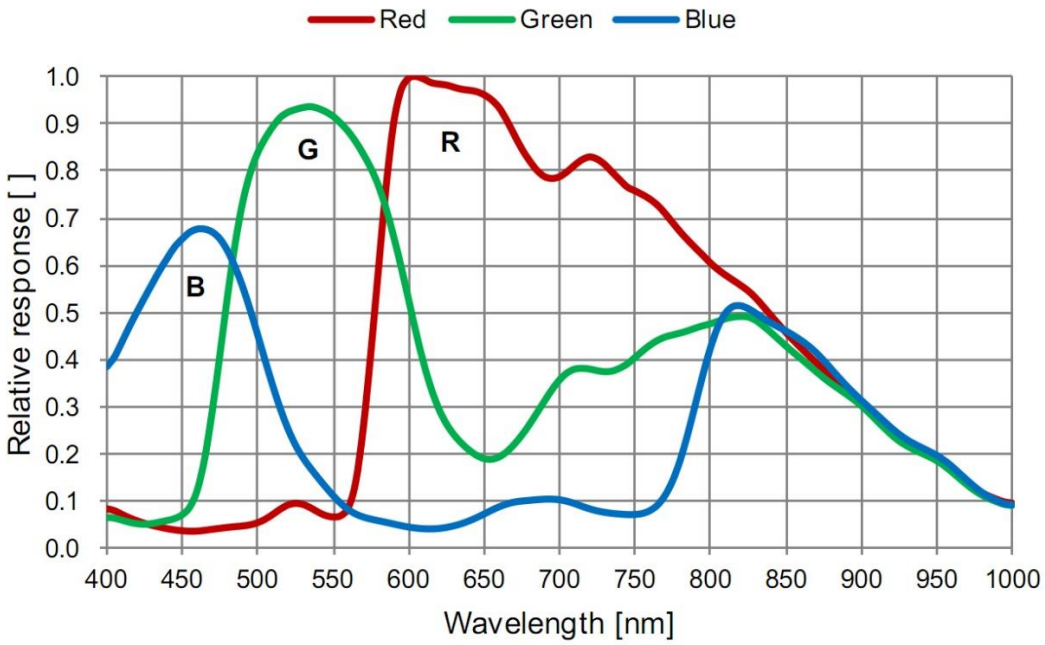

Figure 3.5 Relative response (normalized responsivity spectra) of IMX178 image sensor. The sensor performance is suitable to detect FITC and PE signals wavelength range from 470 to 650 nm. [image adapted from https://en.ids-imaging.com/sony-imx178.html]

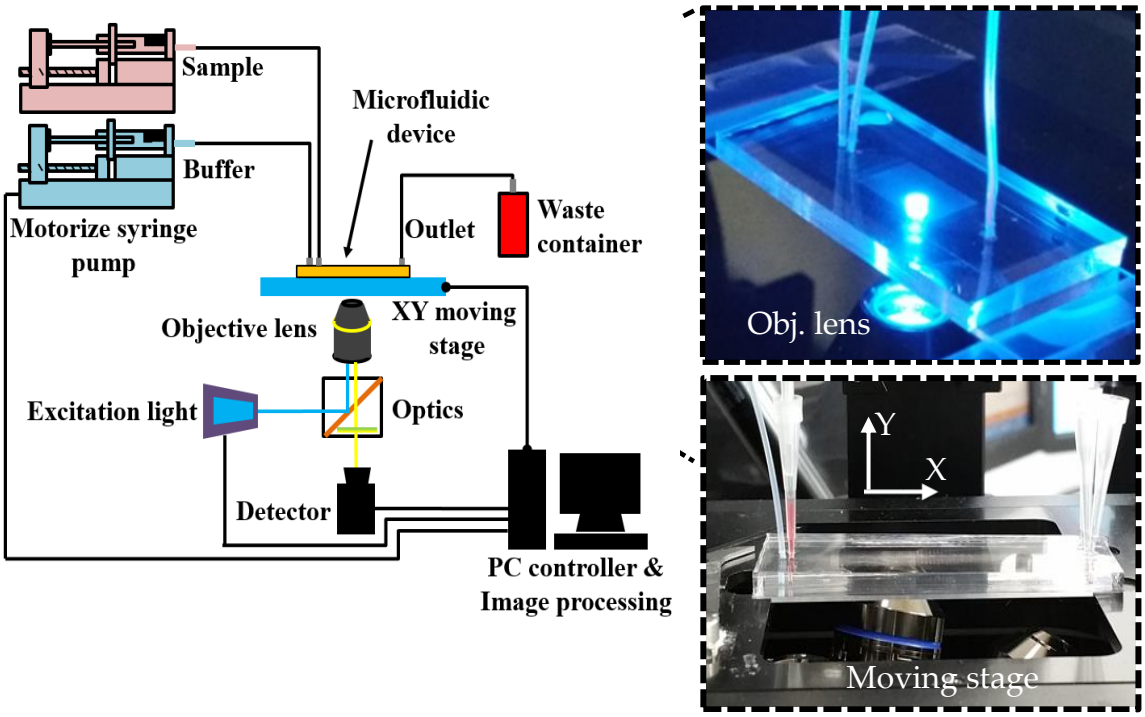

Figure 3.6 The schematic diagram of custom imaging system for scanning and detection of cells

3.4 Image Processing Algorithm for Cell Detection and Counting

Automatic cell counting usually consists of four major processing steps, including pre-processing, segmentation, feature extraction and classification. The pre-processing step often includes image enhancement of acquired image where noises or distortions such as non-uniform background, a variation of brightness or colour information in images. The pre-processing step is essential to some image features for the segmentation process. Feature such as shape, texture and colours etc. are usually used to segmented the interest or target object in the image.

The cell detection and counting for the imaging system; Block diagram of the developed algorithm (Figure 3.7). We used a simple thresholding

method which processed images faster using an HSV colour model [86][87]. HSV shows better performance in image segmentation compared to RGB or LAB [88][89]. In addition, the target cells such as WBCs, T and B cells are recognized by FITC (green colour) and PE (yellow colour) easily could be distinguished by manipulating the hue (H) colour component. Hue is colour angle where green colour (FITC) is between 121 and 180 degrees and yellow colour (PE) is between 61 and 120 degrees. Also, saturates (S) and value (V) components provides additional colour features such as colour intensity (in a percentage value; 0% means a shade of gray and 100% is the full colour) and brightness (in a percentage value; 0% is black, 100% is white). Thus, HSV colour space is suitable to be implemented for cells detection.

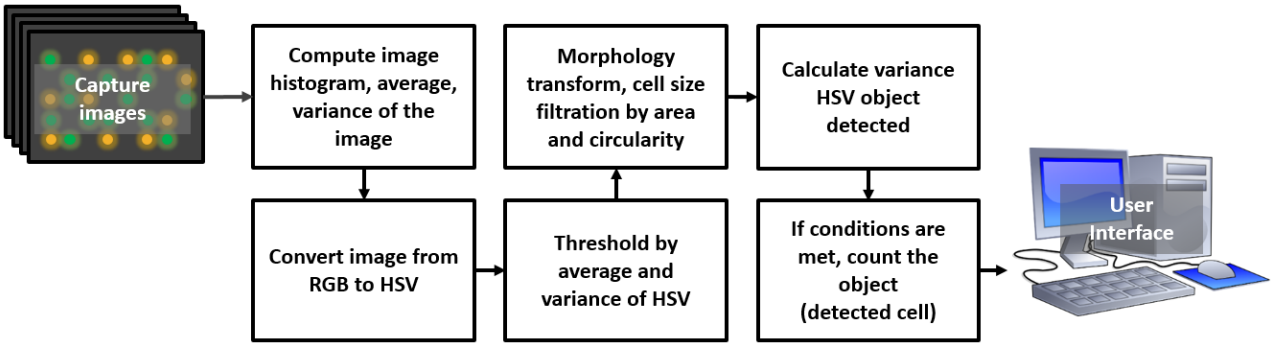

Figure 3.7 The block diagram of developed algorithm for cell detection.

The details image processing algorithm as follows (Figure 3.8):

i) Firstly, the background illumination on the captured image is not uniform due to noise (auto-fluorescence etc.) (Figure 3.8 (a)). A pre-process step required to make the background illumination more uniform. The foreground objects (cells (FITC and PE)) are removed using morphological opening. The opening operation removes small

objects that cannot completely contain the main element (cell image) structure. A disk-shaped structuring element for morphological opening is defined with a radius of 15 (pixels number), which does fit entirely inside a single cell.

ii) Next, subtract the background approximation image from previous step, from the original image. After subtracting the adjusted background image from the original image, the resulting image has a uniform background but is now a bit dark for analysis (Figure 3.8 (b)). Further image enhancement, including increased brightness and adding to the original image) (Figure 3.8 (c)).

iii) Next, performed image segmentation using HSV thresholding, the optimum threshold value for T and B cells for Hue (H) are 140° to 360° (green to red colour) and 360° to 120° (red to yellow colour), respectively. For Saturate (S) and value (V) for both cells (T and B cells) are 0 to 100 (%) and 10 to 100 (%), respectively (Figure 3.8 (d)).

iv) The thresholded HSV image, RGB image then converted to a binary image for further analysis. Additionally, a filtering process for binary image noise such as particles is performed using morphology dilate (increase) and erode (decrease) (Figure 3.8 (e)).

v) Performed blob detection on the binary image for identifying the binary object (cells) and blob counting (cell counting) (Figure 3.8 (f)).

vi) These process will be repeated for each captured images and results of cells count could be determined.

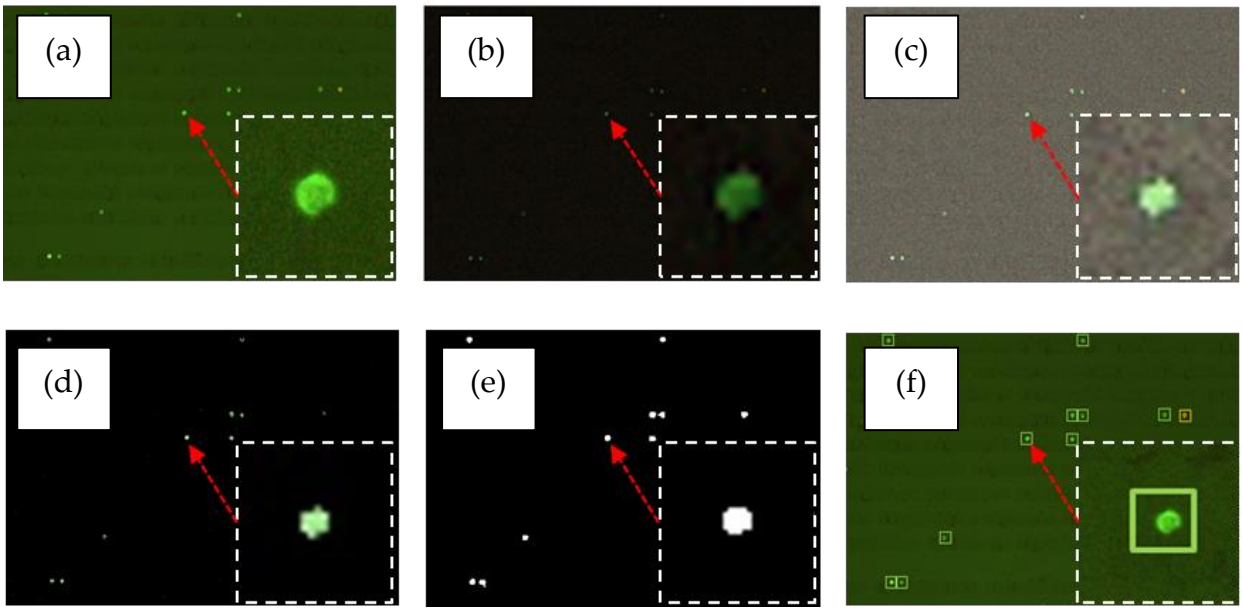

Figure 3.8 The image processing algorithm steps for cell detection and counting. (a) Original image captured. (b) Pre-processing image. (c) Image enhancement. (d) HSV thresholding. (e) RGB to Binary conversion, blob detection and blob counting. (d) The detected cells (T-cells (green), B-cells (yellow).

The detection of cells using the developed imaging system provide sensitive cell detection. A very low or weak intensity (fluorescence emission signal) of a cell could be successfully detected using the system (Figure 3.9). This is very important to reduce error in cell counting if the detection is not performed correctly, such for example in the application described in chapter 5 of determining T and B cells count and ratio in low volume sample. Therefore, a suitable imaging system not only depends on hardware performance such as optical, light source and detector. However, it also includes the performance of image processing algorithm. Combination of all these components may produce a reliable imaging system.

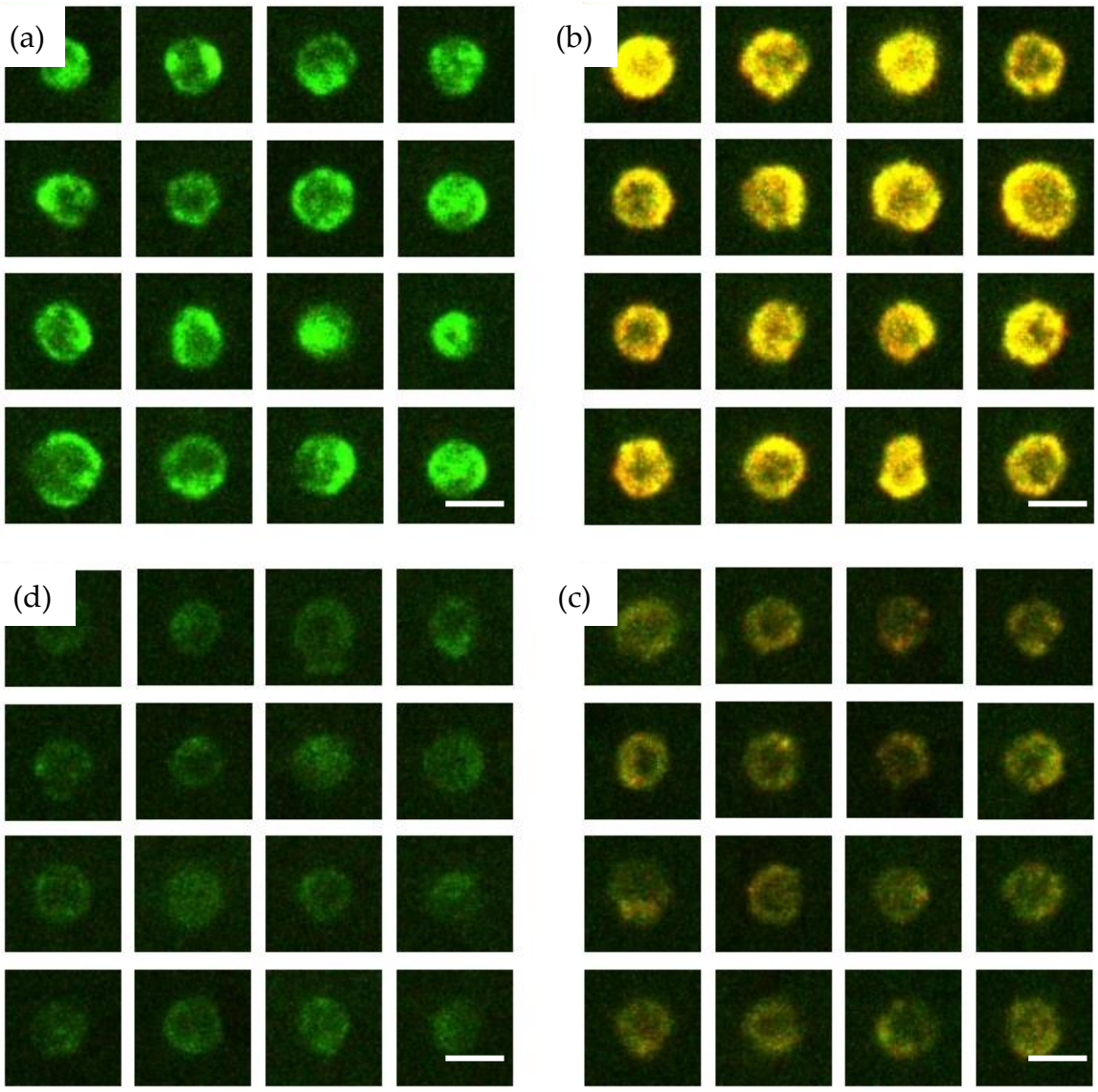

Figure 3.9 The detected cells images in the microfluidic device. The intensity of fluorescence highly depends on the system setup (hardware) and the expression of antigen on cell surface. (a) and (b), T-cells (green) and B-cells (yellow) with high intensity fluorescence emission respectively. (c) and (d), very low intensity of T-cells and B-cells images captured. Scale bars are 10 μm.

3.5 Conclusion

The developed imaging system, including the hardware system and the image processing algorithm, provides high sensitivity for cells detection. Although, the simple direct immunofluorescence labelling is used, the system is still able to detect and identify a low-intensity fluorescence signal. Moreover, the image processing algorithm using thresholding provides straightforward processing for cell segmentation and cell counting. In addition, the automatic thresholding is easy to performed when image background to foreground contrast ratio exists. Therefore, to developed a good performance of the imaging system, all the components, e.g., hardware, algorithm and target cell labelling, must be carefully taken into consideration.

Chapter 4

Investigation of WBCs Captured Cells Distribution on the Microfluidic Device

4.1 Introduction

In this chapter, the application of WBC cells separation based on size and deformability (mechanical filtration) using the purposed microfluidic device is described. The mechanical properties of cells, such as their stiffness response to applied stress, is generally determined by their microstructure. Previous studies have reported that cells in a diseased state have different mechanical properties than healthy cells due to a change in their physical structures. Therefore, the deformability of cells related to a health condition and as a biomarker are widely being studied currently. This chapter is divided into four main sections. Introduction including cell deformability and current methods of deformability assessment, limitation of existing methods and our approach, results and discussion and conclusion.

4.1.1 Cell Deformability as a Disease Biomarker

The mechanical properties and elastic models of cells, such as WBCs, were first studied nearly four decades ago. The cells can deform and change their shapes when pass through a very small area, even though the size of cells are bigger than the area [90]. Previous studies have found that the deformability of the WBCs changes due to disease-related conditions, and they

become more stiff (i.e., they are less deformable in patients suffering from diseases such as sepsis-induced disseminated intravascular coagulopathy [91], leukaemia (chronic lymphocytic leukaemia and acute lymphocytic leukaemia) [92], diabetes mellitus [93], Epstein–Barr virus, and severe lung injury [94]). Several studies have reported that diseases such as cancer (particularly lung and breast cancers) affect the deformability of cells (metastatic cells, in particular) depending on the stage of the tumour [95, 96]. Furthermore, the deformability of the cells also affects their morphological and morphometrical properties (relating to cell diameter and height) as well as elastic properties (Young's modulus) [93, 94]. These changes might be due to the altered cytoskeletal filament network (e.g., actin, microtubules, or lamins) organization of the cells [97, 98]. By understanding these properties, essential information may be obtained for further cell rheology studies crucial to understanding the disease and improving health. Additionally, the mechanical properties of the cells, such as elasticity, shear characteristics, compression, and deformability, reflect their states and functions and suitable as biophysical markers for the detection of pathological cell changes [91]. Therefore, the analysis of cell mechanical properties related to disease and drug treatments, specifically drug delivery, has attracted much attention [99-101].

4.1.2 Current Methods for Cell Deformability Assessment

Numerous techniques have been used to examine the biophysical properties of cells, particularly cell deformability. Examples include atomic force microscopy (AFM) [102, 103], micropipette aspiration (MA) [104, 105], optical tweezers (OTs) [106, 107], deformability cytometry (DC) [108–110], and microfluidic devices [111–114]. Although AFM is popular it causes lateral

instability under loads (i.e., cantilevers) in non-adherent cells such as passive human WBCs [115]. Additionally, a special mold is required to immobilize the cells. This requirement entails a high cost and the process is time-consuming [116]. OTs increase the local temperature due to the use of laser power, which might damage the cell structure and change the mechanical properties of the cells being analysed [117]. Thus, this technique has a disadvantage to assessing the mechanical properties of cells compared with MA, which reduces the potential for cell damage, provides a wide-ranging applications of a wide ranges of measurements, such as elastic coefficient, viscoelastic coefficient, etc. [118, 119], and offers a more straightforward measurement system. However, despite the advantage and wide-ranging applications of MA, the conventional technique still suffers from low throughput and is unsuitable for time-sensitive analyses that entail changes in the measurements over time [120]. DC could overcome the limitations of low throughput. This technique is based on contact modes, such as constriction channels [121][122], and non-contact modes such as a shear stress and pressure gradients [123]. Despite the advantages of DC, it requires a sophisticated system setup, including precision pressure control, a high-speed camera, a complex imaging system, and sample pre-processing. In general, DC is costlier than other techniques, such as microfluidic-based systems, analysis via lab-on-chip (LOC) and microTAS (μ-TAS). Therefore, for clinical applications such as sample pre-analysis (i.e., preliminary screening) of bulk samples, a conventional process might not be suitable. Furthermore, preliminary screening before a detailed analysis reduces the time and cost requirements, and detailed analysis can be performed only if required. Thus, a simple device and technique are required to provide a quick analysis result suitable for a clinical process. Various studies

have shown that microfluidic technologies for cell mechanical characterization provide advantages compared with other available techniques [124-127].

4.2 Limitation on Conventional Methods and our approach

Currently, the deformability of cells is determined based on the single-cell analysis. The single-cell analysis method provides high accuracy and reliable results compared with the bulk sample, where the measurement of the latter depends on the average value [125]. Although single-cell analysis provides precise information, the measurement system requires a complicated microfluidic structure design and sophisticated peripheral systems. Moreover, these cell characterizations or measurement methods are not suitable for practical clinical applications as they are monotonous and suffer from low throughput. Even though bulk analysis provides the average result, it could serve as a useful pre-analysis result, which reduces the clinical processing time. For instance, abnormal preliminary screening results could be investigated in more detail only if necessary. Therefore, preliminary screening could reduce tiresome work, expedite the measurement process, and, importantly, be suitable for clinical applications.

As described in chapter 2, the purposed clog-free microfluidic device, consists of multiple levels of filters, wherein the microfilter gap size is gradually narrowed. Our approach is to separate WBC directly from whole blood (bulk sample) using the proposed microfluidic device. RBC and platelets can pass through the filters and filtered or captured only WBC. The separated WBC is not only corresponding to the filters gap size but includes its deformability whether it can be pass through or captured at the filters. In addition, the sample flow speed is manipulated to investigate the captured cell

distribution. Changing the sample flow rate would increase hydrodynamic pressure. This pressure forced the cells to pass through the filters where higher cell stiffness is hard to pass through a smaller gap size compared to low stiffness cells, which easily deforms or squeeze through the filter. This work contributes to potential applications involving cell deformability as a biophysical marker for in-situ bulk sample analysis with high throughput, which might be useful in drug delivery and disease-related studies.

4.2.1 White Blood Cells Sample Preparation

Human blood samples obtained from healthy donors via venipuncture were placed in 5 mL K2-EDTA vacutainer (BD Vacutainer) tubes. 100 μL of each blood sample was placed in a test tube and gently vortexed at room temperature (24 °C). Then, 20 μL of CD45 antibodies (A07782, CD45- FITC, Beckman Coulter Inc., USA) were added to the test tube and incubated for 15–20 min at room temperature under the protection from light. CD3 and CD19 antibodies (BD Simultest™ CD3/CD19, BD Biosciences, CA, USA) were used for T and B lymphocyte identification. The sample was diluted 10 times with a phosphate-buffered saline dilution buffer (PBS, Sigma-Aldrich, St. Louis, MO, USA) containing 5 mM EDTA (Sigma-Aldrich, St. Louis, MO, USA) and stored in the dark at room temperature prior to performing the experiments. Figure 4.1 shows the process illustration. For dynamic observations (e.g., observations of high-speed moving cells), labelling fluorescence antibodies is unsuitable for the observation of uncaptured cells through the microfilters due to the intensity loss under excitation light exposure. Therefore, we labelled the test sample with the Hoechst 33342 nucleus labelling (10 mg/mL stock, Thermofisher, USA), which is more robust to the fluorescence emission

intensity fading compared with the antibody fluorescence reagent. To prepare the Hoechst staining solution, the Hoechst dye stock solution by dissolving the content of one vial (100 mg) in 10 mL of deionized water (diH2O) to create a 10 mg/mL (16.23 mM) solution. The stock solution is stored at 2–6°C prior to use. To use this stock, the prepared solution must be diluted in PBS (1: 2,000). Next, the diluted prepared solution is added into the sample (5mL:100mL). Then, incubate for 10-15 minutes, it is protected from light at room temperature (24 °C). The staining process is checked. If the staining is insufficient, (adding solution) the staining process is repeated. Figure 4.1 shows the illustration of sample preparation.

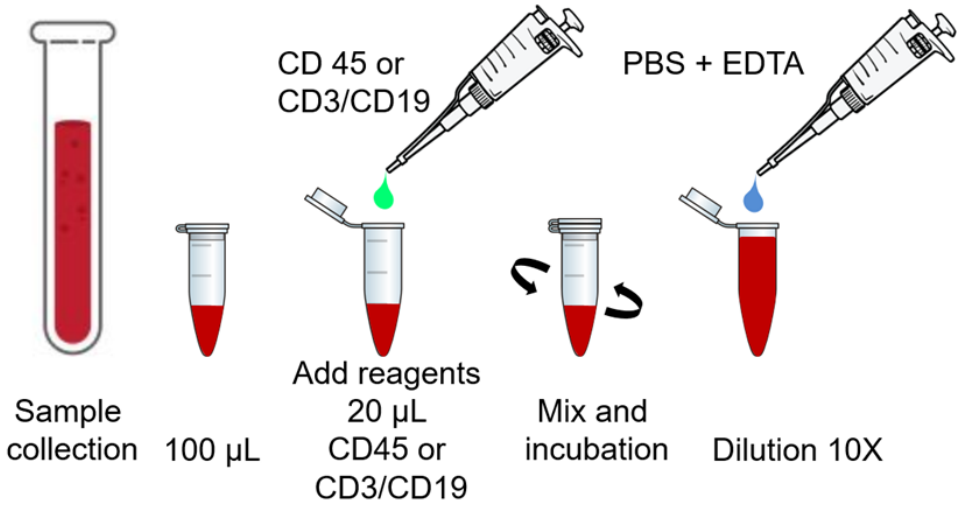

Figure 4.1 Sample immunofluorescence labelling process.

4.2.2 Experiment Setup and Analysis

A prepared blood sample (10 μL) was placed in a tube connected to a syringe pump. The sample flow speeds (i.e., sample flow rates) were set to 1.5, 3, and 6 μL/min, with a total experiment time of 6.7, 3.4, and 1.6 min, respectively. From the preliminary experiments, the sample flow speed of 1 μL/min indicated that the majority of the blood cells stagnated near the inlet port and were not properly filtered through the microfilters (data is not shown). The stagnated cells at the inlet port connecting to the sample tube was caused by the low pressure in the microfluidic device, preventing the blood cells from moving towards the microfilters. Therefore, the minimum sample flow speed suitable for this device have decided on 1.5 μL/min.

The prepared sample is flowed according to the set sample flow speed and stopped after the entire sample had finished (10 μL of sample). The sheath supply, which moved at a similar speed as the sample, flowed for approximately 10 seconds longer than the sample supply to prevent inappropriate sample flow to the microfilters. If the sheath supply was not included, dumping of cells near the inlet would occur after the sample has been stopped. After the sheath flow process is completed, the system begins imaging the capture area and determining the count of the captured and uncaptured cells.

The WBCs count was determined from the sum of the captured and uncaptured WBCs in the separation and waste areas of the microfluidic device, respectively. The WBCs were determined using a custom-made imaging system for automatic cell detection and counting as previously described in chapter 3. The leukocyte capture rate in the microfluidic device was defined as:

$$\text{Cell capture rate (\%)} = \left(\frac{\text{Total number of captured cells}}{\text{Total number of captured cells} + \text{Total number of uncaptured cells}}\right) \times 100 \quad (1)$$

where the number of captured cells was determined from the separation area and the number of uncaptured cells determined from the waste area.

The captured cell distribution on a specific microfilter gap size could be determined from the total number of captured cells (according to the gap size) over the total number of cells captured at the separation area, is defined as:

$$\text{Cell distribution (at specified gap size) (\%)} = \left(\frac{\text{Total number of captured cells at specified gap size}}{\text{Total number of captured cells at separation area}}\right) \times 100 \quad (2)$$

Another important analysis which provides understanding of results variation on each experiment using the purposed device. Thus a repeatability in repeated measurements on the same sample over the microfluidic device is carried out. Therefore, we determine an analysis of variation i.e. coefficient of variation (CV) to demonstrate that the developed microfluidic device result is reliable and accurate.

The WBCs were identified using the CD45 antibodies and blue fluorescence by light-emitting diode excitation (M490L4, Thorlabs, USA) and ultraviolet light (M365L2, Thorlabs Inc., NJ, USA), respectively, on a custom inverted fluorescence microscopy and optical system (IDEX Health & Science, LLC, Semrock, NY, USA). Images of WBCs (CD45+ cells) and T and B lymphocytes (CD3+ and CD19+ cells) were captured and recorded using a high-sensitivity and low-noise CMOS (Complementary metal–oxide–

semiconductor) camera (ASI178MC Zhen Wang Optical Company, China, 3096 x 2080, pixel size 2.4 μm) (Figure 4.2).

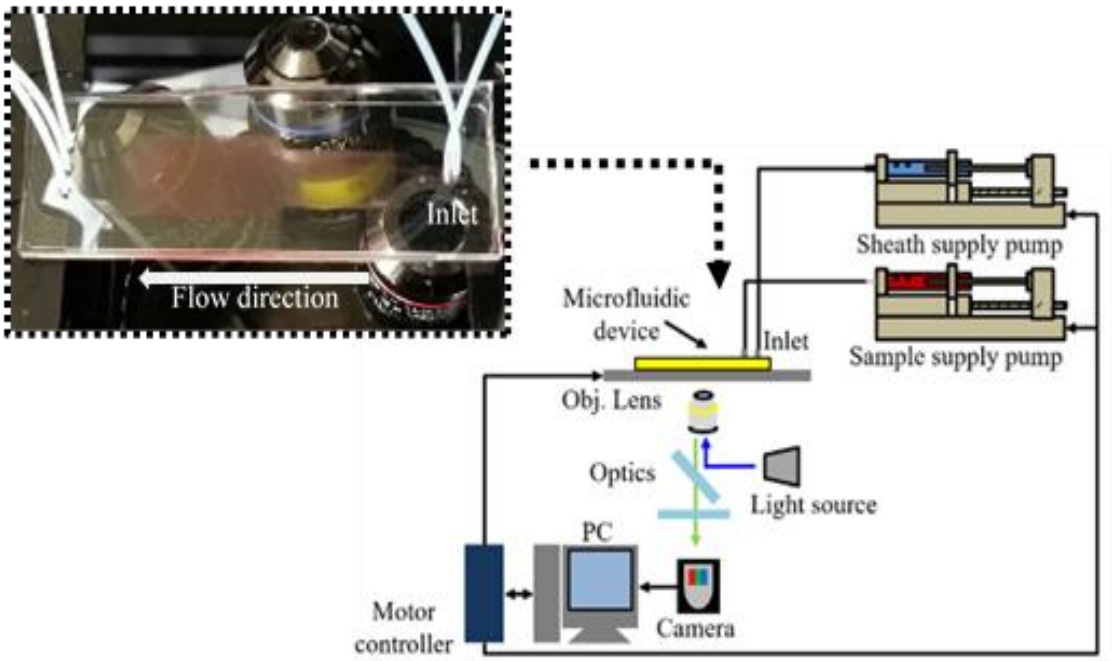

Figure 4.2 Schematic of microfluidic experiment setup.

4.3 Results and Discussion

Images of cells captured by the microfluidic device are shown in Figure 4.3. Clogging and fouling were not observed when using 10 μL of each prepared blood sample for all applied flow speeds. We observed and confirmed that there was no unprocessed (e.g., cell sedimentation) sample at the sample inlet area, which is critical to ensuring that the sample was appropriately processed. The required processing times (i.e., the total time to complete cell separation) were approximately 6.6, 2.8, and 1.6 min at sample speeds of 1.5, 3, and 6 μL/min, respectively. Using the developed system, the CD45+ cells were detected clearly under florescence imaging (Figure 4.3), and the captured cells were accurately counted using a simple system.

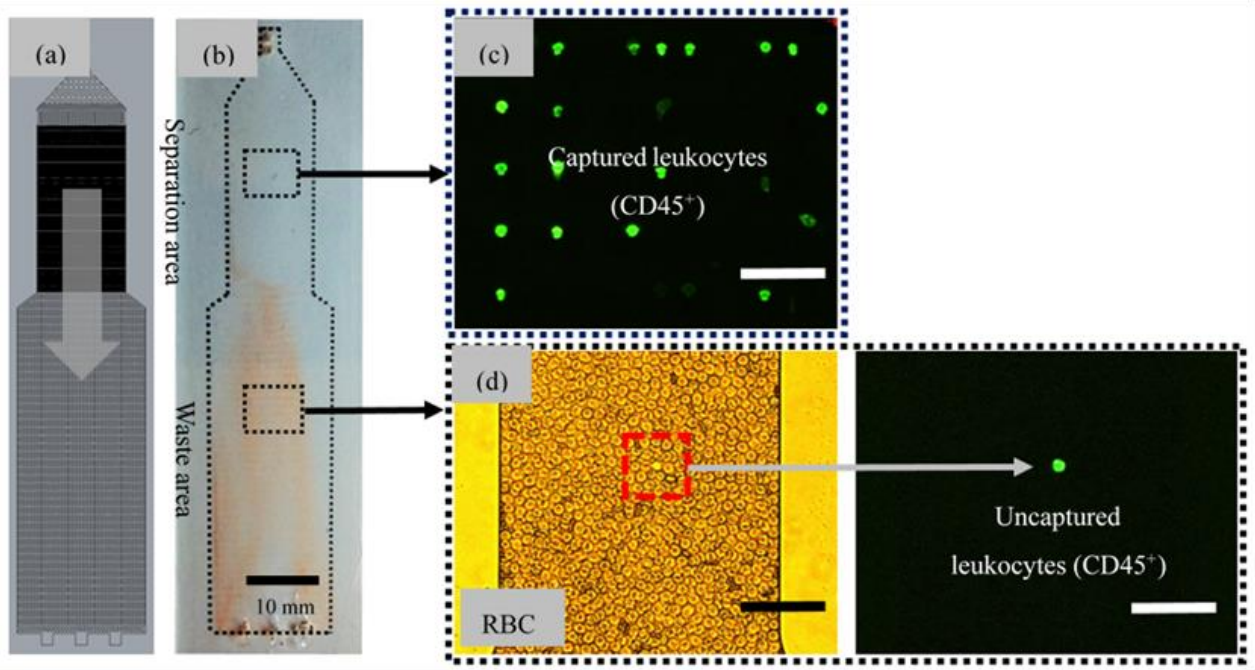

Figure 4.3 The Separated Cells on the Microfluidic Device. (a) Schematic diagram of the microfluidic device. (b) The fabricated PDMS microfluidic device used for the experiments in this study. The processed blood sample is dumped in the waste area. (c) Captured CD45+ cells (green) in the separation area. No cell clogging was observed in the device. (d) Bright field (left) and fluorescence (right) images of the processed sample in the waste area. Example of an uncaptured CD45+ cell in the waste area identified by fluorescence. The cell size is approximately 7 μm. The lightly shaded area in red in (b) denotes the RBCs that were not captured by the filter and found their way to the waste area instead. Scale bar: 100 μm.

The CD45+ cells were captured and distributed across the microfilters (Figure 4.4). All of the images were taken at the same position in the microfluidic device. The results obtained from the experiments are summarized in Table 4.1. Table 4.1 shows the average calculations using the proposed method described in Eq. (2). The distribution and positions of the captured cells in the microfilters demonstrate significant variations depending on the flow speed. Using the highest flow speed of 6 μL/min as an example, most of the cells were captured at the smaller microfilter gap sizes of 3, 4, and 5 μm; however, for the slowest flow speed of 1.5 μL/min, the majority of the

cells were captured at gap sizes of 6 μm and greater. The cell counts were averaged for the larger gap sizes of 10 –15 μm, as no significant differences in the distribution of the cells were observed by the flow speeds. The distribution of the cells increased at gap sizes of 3, 4, and 5 μm for the speed of 6 μL/min compared with that at the other speeds. For instance, at a speed of 1.5 μL/min, the device could capture only 2%, 7%, and 13% of the cells at gap sizes of 3, 4, and 5 μm, respectively. In comparison, at 6 μL/min, the corresponding percentages increased significantly to 12%, 23%, and 13%. The most cells were captured at gap sizes of 9, 6, and 4 μm at speeds of 1.5, 3, and 6 μL/min, respectively.

The cell distribution data clearly indicate that the sample speed influenced the positions of the captured cells. These conditions are related to the ability of the cells to deform when pressure (fluid flow) is exerted, which is then used to develop an imaging profile (namely, the sample speed changes the cell capture distribution).

Table 4.1 Distribution of cells captured at the microfilter gaps at three different flow speeds. The average cell distribution (%) is shown.

	Sample flow speed (μL/min)		
Gap size (μm)	1.5 μL/min	3 μL/min	6 μL/min
10–15	25.5	12.7	8.4
9	26.7	15.8	10.5
8	21.1	19.1	13.0
6	20.0	31.1	17.8
5	3.8	12.8	15.2
4	1.8	7.0	23.4
3	1.1	1.5	11.7

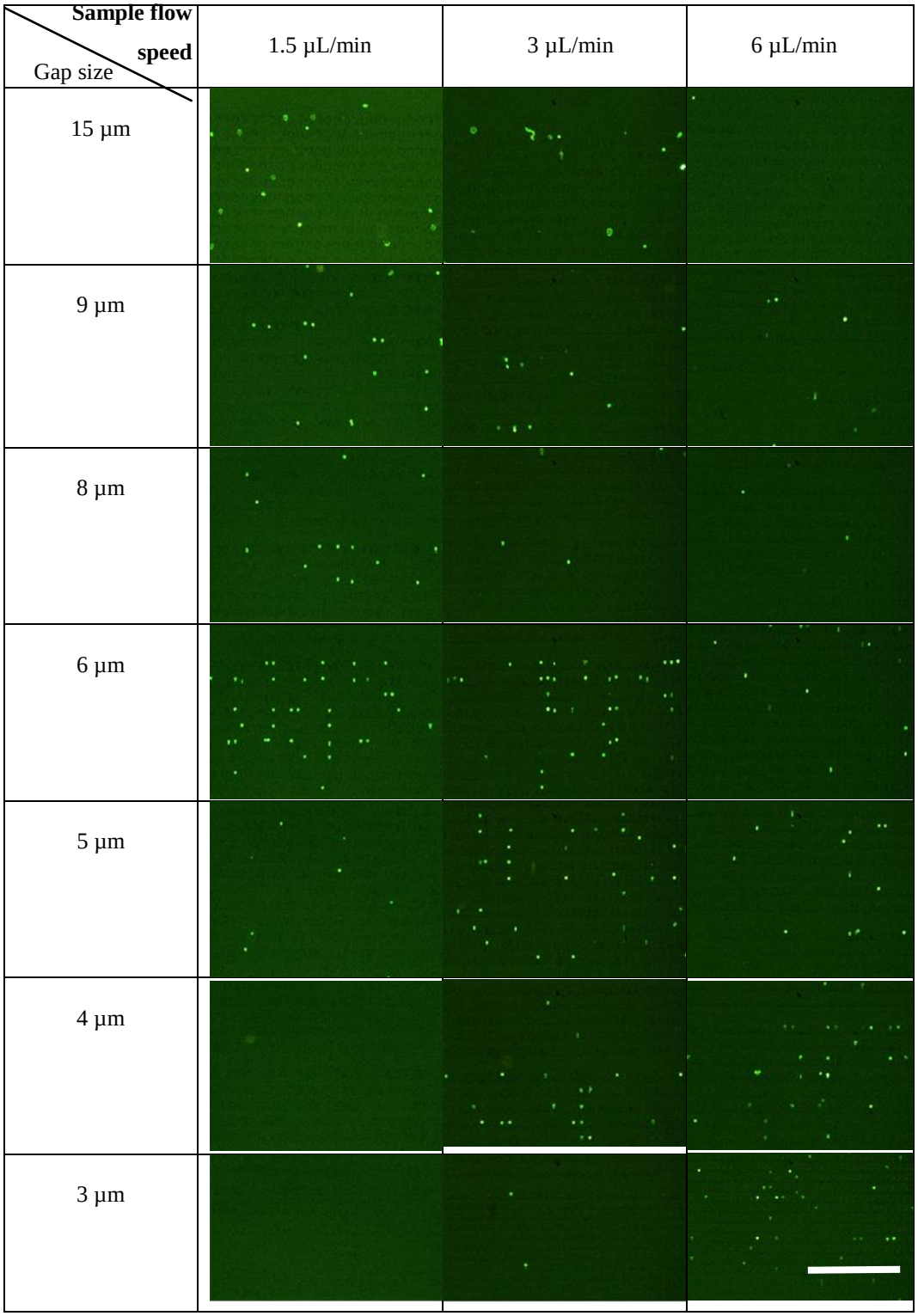

Figure 4.4 The distribution of captured cells on the microfilters by sample flow speed and gap size. Images of CD45+ cells (green) are captured at the same position (at the center of the

separation area in the microfluidic device). The distribution of the captured cell images can be used as a sample deformability profile. Scale bar is 300 μm.

The average counts of cells using the microfluidic device are shown in Figure 4.5. Using Eq. (1), the performance of the cell capture by the microfluidic device was 100%, 99.7%, and 96% at respective sample flow speeds of 1.5, 3, and 6 μL/min. For the uncaptured cell count, a significant cell loss was observed for the sample flow speed of 6 μL/min compared with the other speeds. Thus, the most efficient speed of this device was 3 μL/min among the three conditions, which required a sample processing time of less than 4 min for 10 μL of prepared sample.

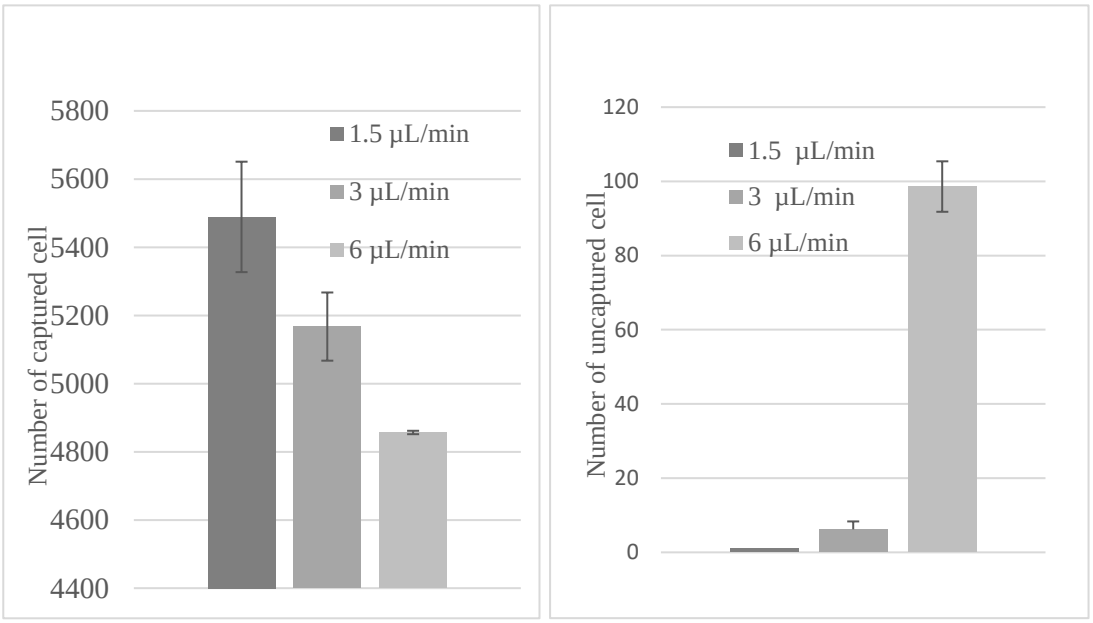

Figure 4.5 The average cell count using the microfluidic device. (a) Average captured cell count in the separation area using 1 μL of the whole blood sample. (b) Average uncaptured cell count in the waste area. The error bars denote the standard deviations.

Furthermore, for sample speed of 1.5, 3 and 6 μL/min, the coefficient of variation (CV) was 0.18%, 2.77% and 7% respectively over seven experiments (n = 7). The relative variability demonstrating that the microfluidic device

provides high repeatability and reliable result especially sample flow speed of 1.5 and 3 μL/min. % respectively over seven experiments (n = 7). The relative variability demonstrated that the microfluidic device provides high repeatability and reliable result especially sample flow speed of 1.5 and 3 μL/min. However, the variability becomes larger (greater dispersion) during sample flow speed of 6 μL/min. This result was expected as many of cells larger during sample flow speed of 6 μL/min. This was expected as many of cells were determined uncaptured (Figure 4.5 (b)).

At the highest sample flow speed of 6 μL/min, the hydrodynamic force in the device is large, and, thus, some WBCs escaped through the smallest micropillar gap size of 3 μm (Figure 4.6), which reduced the efficiency of the cell capture rate. This phenomenon could be attributed to the lower stiffness (high deformability) of cells pass through the filter due to the increase in sample flow speed. In addition, the escaped cells, which measure approximately 7 μm, are considered to be small lymphocytes (Figure 4.7). Lymphocytes usually range from 7–12 μm in size and have been identified as the smallest types of all WBCs. Moreover, Downey et al. [128] demonstrated that the average size of small lymphocytes is approximately 6 μm, which is smaller than typical RBCs. Thus, some small WBCs, such as lymphocytes, have a high possibility of escaping the microfilters compared with other cells. However, we did not analyse the phenotypes of the escaped cells, namely, whether they were polymorphonuclear (e.g., neutrophils, eosinophils, and basophils) or morphonuclear (e.g., lymphocytes and monocytes).

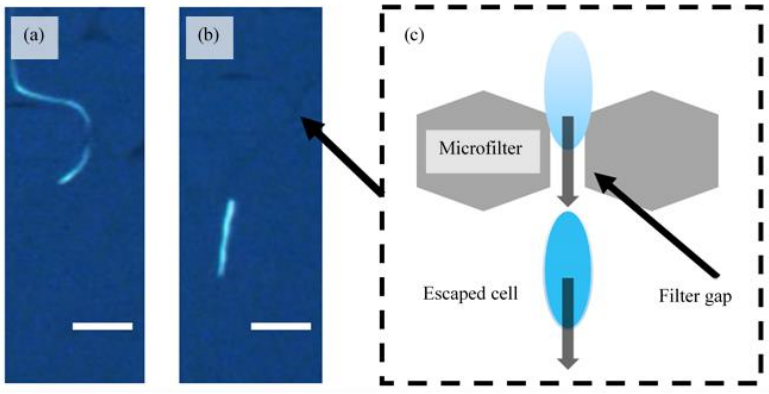

Figure 4.6 Images of leukocyte pass through the filter gap. (a) and (b): Images captured during a sample flow speed of 6 μL/min. WBCs were stained with Hoechst 33342 (blue). In case of an uncaptured cell, WBCs enter the microfilters, pass through the filter gap without being captured, and finally reached to the waste area. Scale bar: 20 μm. (c) Illustration of a leukocyte pass through the filter gap.

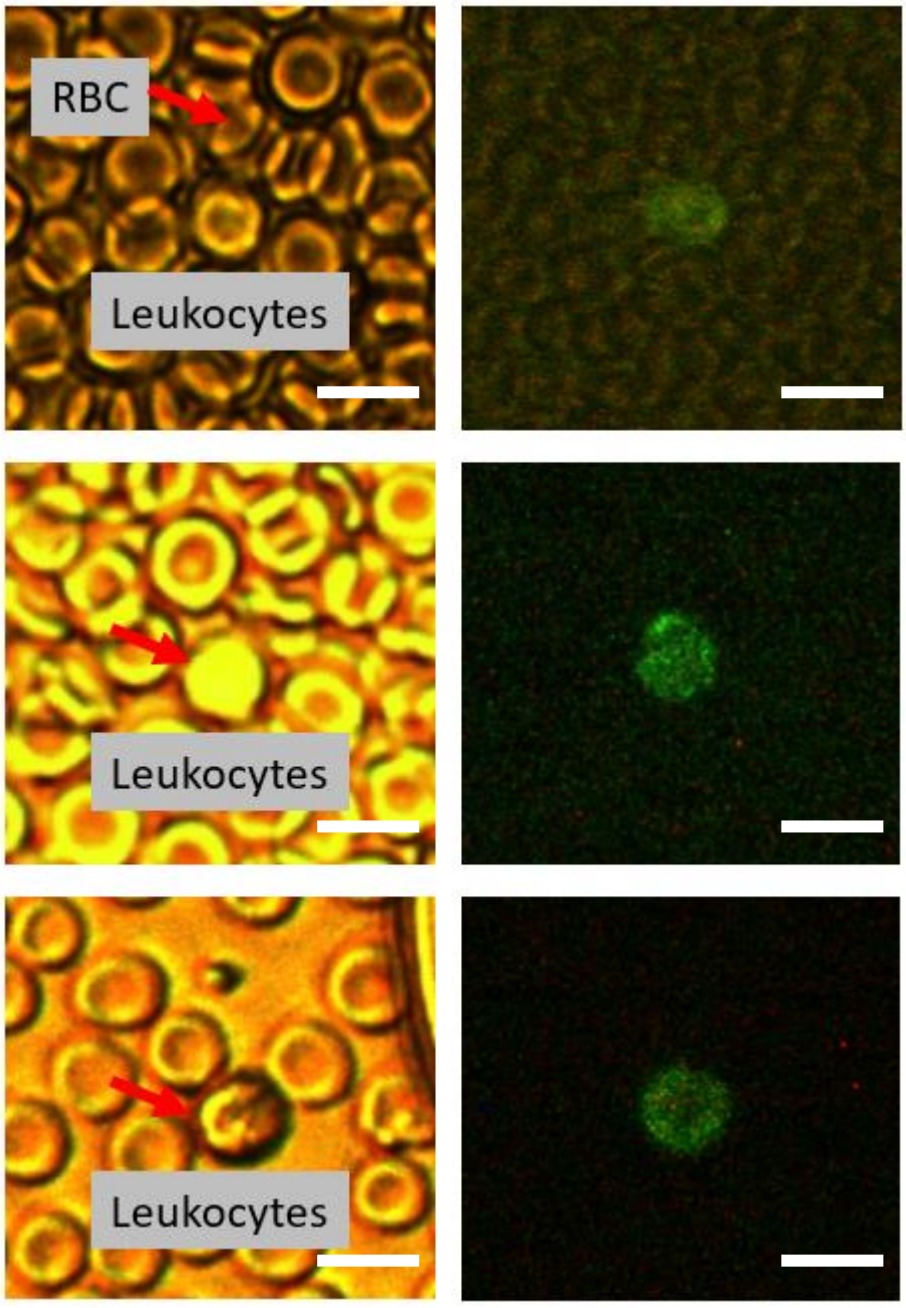

Figure 4.7 Examples of escaped cells image at the waster area of the microfluidic device under a bright field and fluorescence Images. The escaped cells are nearly similar to RBCs in terms of size. The size of an RBC is estimated as 7–8 μm. Scale bars: 10 μm

Cells that are captured by the microfilters depend on their size, the sample flow speed used, and the gap size of the filters. WBCs, including neutrophils, are the most abundant cells (68%), followed by lymphocytes (~20%), and then other cells (e.g., monocyte (< 7%), eosinophil (< 4%), basophil (< 1%) [129]. Therefore, we investigated the distribution of the majority of the lymphocytes (T and B lymphocytes) using a typical sample flow speed (i.e., 3 μL/min) and compared the results (lymphocytes captured distribution) to the majority of WBCs (neutrophils). As a result, the distribution of these lymphocytes suggested that larger gap size microfilters (e.g., 10–15 μm) had a lymphocyte capture rate 2% lower than the total captured lymphocytes on the microfluidic device. Thus, this suggests that the results in Table 4.1, for gap sizes ranging from 10–15 μm, contain less than 2% of the lymphocytes. Therefore, these larger gap sizes (e.g., 10–15 μm) captured cells other than the lymphocytes, where the majority of the cells are neutrophils.

As shown in Figure 4.8, the highest capture of the T and B lymphocytes are at the 6 μm gap size, where the average of the captured cells is about 42% for all test samples. Overall, these results indicate that the higher captured lymphocytes will be mostly at the 4–8 μm gap sizes, where the total captured cell average is about 89%. These results on T and B lymphocytes are similar to those of previous researchers, where lymphocytes were mostly filtered at 6 μm filter sizes [130]. This demonstrates that the deformability profile of healthy lymphocytes is fractionated to a specific value. As shown in Figure 4.4, if the deformability is different as in disease and drug treatment, the fractionation position of lymphocytes shifts to either. In the future, we will investigate the clinical potential to detect the deformability profile of in vitro samples of lymphocytes or other WBCs using this mechanism. The clinical potential applications such as comparison of deformability profile of tumour progress

investigation, drugs treatment assessment, normal and abnormal (diseases) patient etc. Hence, the cells physicals (stiffness) properties as potential diseases biomarkers.

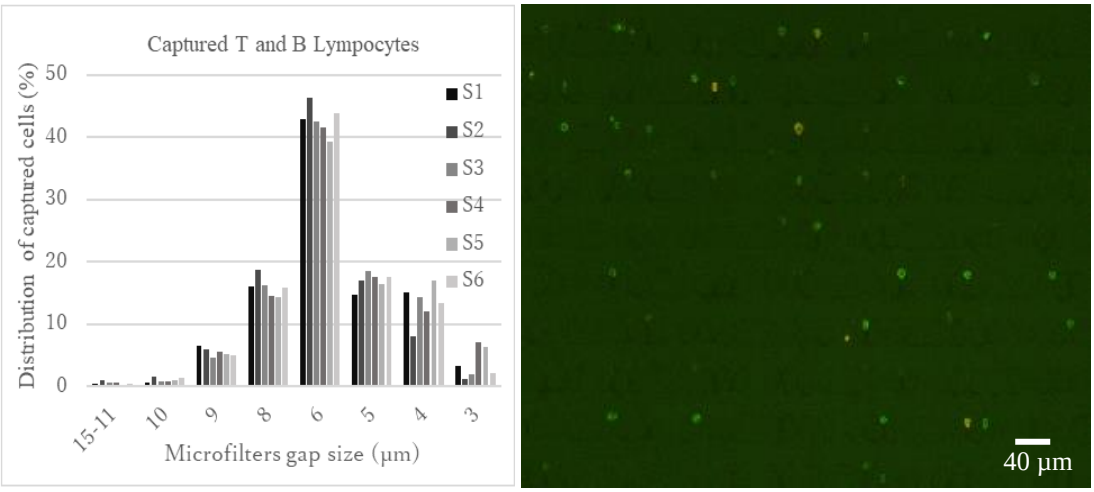

Figure 4.8 Distributions of captured T and B lymphocytes. Samples (S) from individual donors flowing at speed of 3 μL/min. (a) T and B lymphocytes show higher distribution percentages at a 6 μm gap size and lower distribution percentages at 10–15 μm and 3 μm gap sizes. (b) Example fluorescence image of captured T (green) and B (yellow) lymphocytes at a 6 μm gap size on the microfluidic device.

4.4 Conclusion

The proposed microfluidic device successfully recovered all of the CD45+ cells in 10 μL of prepared sample depending on the sample flow speed (e.g., 1.5 and 3 μL/min), without requiring sample pre-processing such as the density gradient centrifugation or RBC lysis. We conclude that, if the sample flow speed exceeds 6 μL/min, there is a high possibility that certain WBCs, such as small lymphocytes, have escaped through the filtration. Moreover, the distribution of the captured cells also depends on the microfiltration gap sizes in which cells are deformed when flowing through the gap. In our experiments, the gap sizes of 9, 6, and 4 μm exhibited the highest percentage of cell captures

at sample flow speeds of 1.5, 3, and 6 μL/min, respectively. Furthermore, T and B lymphocytes predominantly captured distributions at gap sizes of 4–8 μm gap, where the 6 μm size showed the highest captured percentages using a typical sample flow speed (3 μL/min). Thus, larger gap sizes (e.g., 9–15 μm) are suitable for capturing other cells such as neutrophils, monocytes, and eosinophils, which are greater than 12 μm in size. Additionally, the images of the captured cells in the device (i.e., images of cell distribution) could be used as a deformability profile of the sample. The deformability profile is dependent on the sample flow speed and gap sizes of the microfiltration device. However, the results are only limited to healthy blood samples.

Chapter 5

Microfluidic Device for Separation and Counting T and B Lymphocytes. A Comparison to Flow Cytometer.

5.1 Introduction

In this chapter, the application of T and B lymphocytes counting using the proposed microfluidic device is described. Cells counting such as T and B cells lymphocytes is important because human immunodeficiency virus (HIV) directly infects and damages T-cells, causing the number of T-cells in an HIV-infected person to decrease over time. When HIV disease progresses, and the T-cell count drops, the immune system is less able to fight off invading microorganism which causes disease. Therefore, a cell counting device is essential to monitor health or therapy conditions. This chapter have seven sections including introduction on important of cell counting in health monitoring, cell counting by state-of-the-art flow cytometry and its limitation, our approach of cell counting using microfluidic device. Also the sample preparation for microfluidic device and flow cytometry, experiment setup and analysis, results and discussion of cell counting using proposed device compared to flow cytometer, and conclusion.

5.2 White Blood Cells Count

Blood is one of the most common biological samples whose constituents are used for diagnosis of a large number of diseases. Blood consists of three types of cells; red blood cells (RBCs), white blood cells (WBCs) and platelets contained in a fluid known as plasma [130]. The function of RBCs is to carry oxygen from the lungs to body tissues and carbon dioxide is exhale out as a waste product, away from the tissues and back to the lungs. WBCs on the other hand, help to protect against bacteria, viruses, parasites, infections of all types, toxins, and even the development of cancer cells. The platelets or thrombocytes uses to form clumps, or a plug, in the hole of a vessel to stop bleeding. All blood cells are produced in the bone marrow.

Cell counting, such as WBCs count, is important to indicate health status [131]. For instance, a too low or too high of number of WBCs could indicate conditions such as autoimmune disease, immune deficiencies and blood disorder. Furthermore, WBCs cell count could help doctors to monitor the effectiveness of medicine such as chemotherapy or radiation treatment in people with cancer, and antiretroviral therapy in people with HIV [132][133]. A group of specialized cells known as lymphocytes have a major role in the immune system. Their various functions allow them to properly respond to foreign invaders in the body. There are three types of lymphocytes, known as T cells, B cells, and natural killer cells. Therefore, quantifying the number of WBCs subpopulations, such as CD3, CD19, CD4, and CD8 cells, could provide

more information on the condition of the immune system compared to the total count of WBCs [134-138].

5.3 Flow Cytometer Cell Counting and our approach using Microfluidic Device.

A standard method used in clinical and biological studies to determine a cell population relies on flow cytometer measurements such as fluorescence-activated cell sorting (FACS) [139][140] (Figure 5.1). FACS provides high throughput, high accuracy, for the detection of multiple types of cells, and the ability to separate cells into sub-populations. However, this approach has high operation and maintenance costs, including the need for a skilled operator, periodic system maintenance, calibration, and instruments consumables. Hence, this approach is not suitable for a small-scale diagnostic applications. In contrast, alternative techniques using the microfluidic device are promising substitutes for conventional flow cytometry systems since they allow faster analysis, reduced sample volume, and are portable. Advances in microfluidics allow miniaturized devices with capabilities similar to conventional flow cytometry systems. Simplicity in a microfluidic device and its auxiliary system is essential for cell analysis to match with conventional cell counting systems. [73].

Our approach is for a cost-effective, portability and cell counting system using a microfluidic device. The proposed microfluidic device, as described in chapter 2 previously. The principle of the developed device is to get separation of WBCs from whole blood and to detect T (CD3+) and B (CD19+) lymphocytes based on immunofluorescence technique. The device provides clogging-free, simple sample preparation which does not require

haemolysis, cell fixation, or centrifugation for sample pre-treatment process, thereby reducing preparation time and cost. The purposed microfluidic device and cell detection system as described in the early chapter (chapter 2 and 3) could be an alternative promise technique for determining cell populations in many applications in the near future.

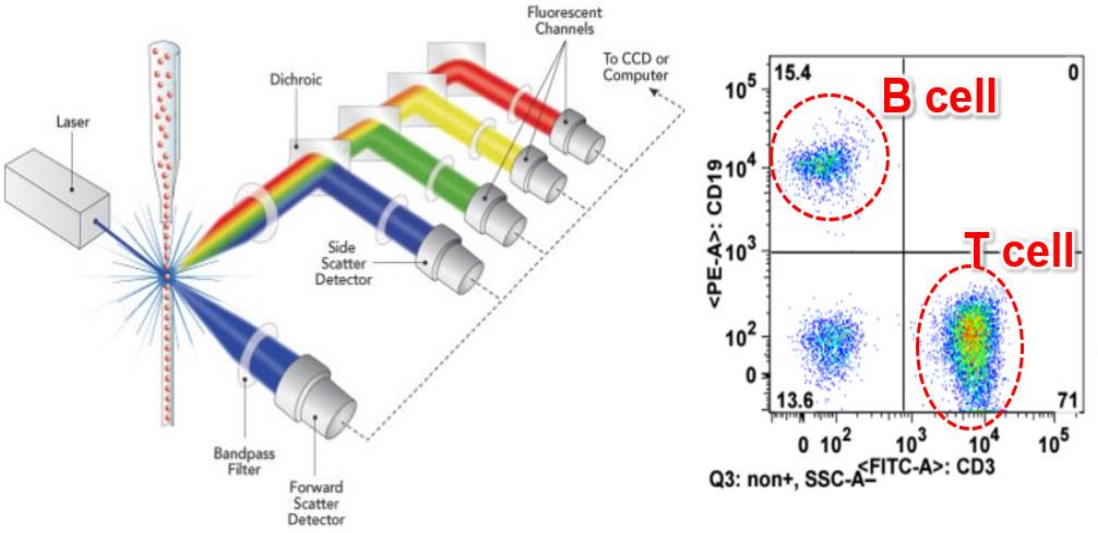

Figure 5.1 Standard conventional instrument using flow cytometry for determine subpopulations of WBCs such as T and B lymphocytes. (a) flow cytometer system. (b) example of flow cytometer cell count result. [image (flow cytometer) adapted from https://www.semrock.com/flow-cytometry.aspx]

5.4 Sample Preparation for Microfluidic Device

Blood samples were collected from 19 donors in BD vacutainer tubes containing Ethylenediaminetetraacetic acid (EDTA) anticoagulant to prevent it from clotting. Immunofluorescence labelling is used to identify T-cells and B-cells using the developed imaging system. This study was approved by the institutional review board of the National Hospital Organization Nagoya Medical Centre, and all participants provided written informed consent to participate in the study. The pre-treatment sample does not need to perform

haemolysis and washing cells by centrifuging process using our method. The haemolysis process is required by some standard procedure for sample pre-treatment using FACS to reduce error in analysis caused by clumped cells and excess monoclonal antibody (mAB) which caused non-target binding that could decreased the detection resolution in FACS. Therefore, our sample pre-treatment method provides an advantage of short process time. The samples were diluted with phosphate buffered saline (PBS) (Sigma-Aldrich Japan, Japan) containing 5 mM EDTA (Sigma-Aldrich). Samples were prepared by mixing 100 μL blood sample with 20 μL immunofluorescence reagent (BD SimultestTM CD3/CD19, BD Biosciences, CA, USA), then is incubated in the dark at room temperature (20 °C – 25 °C) for about 15 min. CD3 and CD19 antibody were labelled with fluorescein (FITC) and phycoerythrin (PE), respectively. The prepared sample was diluted 10 times with the dilution buffer (PBS + EDTA) and kept in the dark at room temperature until the experiments were performed. Total time sample preparation for microfluidic device is less than 20 minutes.

5.5 Sample Preparation for Flow Cytometer

Blood samples were collected from 19 donors in BD vacutainer tubes containing Ethylenediaminetetraacetic acid (EDTA) anticoagulant to prevent the blood from clotting. Placed a 100 μL sample to FACS tube. Add 20 μL each of FITC CD3 and PE CD19 fluorescence antibody reagent (BD SimultestTM CD3/CD19, BD Biosciences, CA, USA). Gently vortex protected from light, and incubate at room temperature (24 °C, 15 min). Next, add 2 mL of 10-fold diluted (red blood cell lysis buffer (Sigma-Aldrich, USA) diluted with distilled DI water (45 mL for 5 mL buffer)) at room temperature (24 °C) for haemolysis

& fixation process. Gently vortex (3 seconds) protected from light, incubate at room temperature (12 min). Then perform centrifugation (1200rpm, 5min, room temperature), discard supernatant (leave about 50μL at least as not to break the pellet). Next, suspend in 500 μL of FACS buffer, transfer to vortex tube and gently perform vortex. Sample ready for flow cytometer analysis. Set the number of events according to the setting of the laboratory (counting with lymphocyte set to 2500 events). Total time sample preparation for flow cytometer is less than 50 minutes.

5.6 Experiment Setup and Analysis

A suitable sample flow (3 μL/min) is applied to the microfluidic. This is the nominal condition of sample flow previously described in chapter 4 where the percentages of captured cells is about 99% and the sample introduction process to the microfluidic device is less than 4 minutes. Therefore, the condition was selected to ensure that results on cell counting (T and B cell counting) are accurate. On the other hand, the system setup including imaging system (Figure 3.6) and T and B cells detection algorithm (Figure 3.7) developed as describe previously in chapter 3.

A flow cytometer (BD FACSCanto II) (BD Biosciences, San Jose, CA, USA) is used as a standard reference device for evaluating the microfluidic device to determine the ratio of CD3+ and CD19+ cells in a whole blood sample. The analysis of correlation and agreement between the two methods (microfluidic and flow cytometer) results from by Passing-Bablok regression and a Bland-Altman plot using MedCalc version 18 (MedCalc Software, Ostend, Belgium). Passing and Bablok developed a regression method that allows comparing two measurement methods, which overcomes the

assumptions of the classical linear regression that are inappropriate to be used [141]. Furthermore, the analysis using Passing-Bablok is robust against data outliers. However, this analysis alone is insufficient since it only provides a confidence interval level (CI) (95% of CI) and an estimation of the relationships (regression) among variables. Thus, Bland-Altman analysis is used to provide further analysis from Passing-Bablok method. In contrast, Bland-Altman used in analysing the agreement between two different assays provides limits of agreement and a bias between the comparison methods using a graphical approach, which is more significant [125].

5.7 Results and Discussion

The CD3+ (T-cells) and CD19+ (B-cells) could be detected from the captured image using the microfluidic device (Figure 5.2). In Chapter 4, the higher captured percentage of T and B lymphocytes are at the gap size of 6 μm while lower percentage at others filter gap sizes (Figure 4.8). In this experiment, similar condition has been observed. An example result from flow cytometer for detection and counting of T and B lymphocytes as shown in Figure 5.4. The Passing-Bablok regression (Figure 5.4 (a)) and Bland-Altman plot (Figure 5.4 (b)) from the microfluidic device cells count and flow cytometer cells count is obtained. Details of compartmental results are shown in Table 5.1.

Passing-bablok regression procedures fits the parameters A and B value of the linear equation ($y = A + Bx$) . The x variable contains corresponding measurements from the other measurement system (microfluidic device) while y. The analysis will test whether A = 0 and B = 1. If they do, then the y = x (linear correlation of two system comparison). While, the 95% confidence

interval (CI) of the mean difference show that the magnitude of the systematic difference. If the line of equality ($y = x$) is not in the interval (CI range), there is a significant systematic difference, i.e. the second method (microfluidic device) constantly under- or over- estimates compared to the first method (flow cytometer). As a result, the Passing-Bablok analysis (n=19) of the results obtained revealed an A intercept value of 0.25 and a B slope value of 0.90 (Figure 5.4 (a)). The confidence interval (CI) ranged from −0.34 to 0.74 for the A value and 0.79 to 1.02 for the B value. No systematic or proportional biases were observed (the line of equality shown in the CI range).

The Bland-Altman plot analysis (graphical analysis) calculated the statistical limits by using the mean (average) and the standard deviations between two methods. This could be determined by (microfluidic device – flow cytometer method) for Y-axis and average of these methods ((microfluididc device + flow cytometer)/2) for X-axis in the plot analysis (figure 5.4). 95% of the data points suggested should lie within ± 2 of the mean difference to get a good agreement between two methods comparison [142]. Table 5.1 shows a hypothetical series of paired data, from which it is used to construct the Bland-Altman plot and to evaluate the agreement.

In the Bland-Altman plot analysis showed a mean bias of −0.6 with a standard deviation (SD) of 1.40 (Figure 5.4 (b)). The limits of agreement ranged from −3.4 to 2.1. Thus, both the Passing-Bablok regression and Bland-Altman plot analyses showed that at higher ratio of CD3+/CD19+, the difference in the results obtained using the microfluidic device or flow cytometer tends to become large. The results show that the CD3+/CD19+ ratio from the microfluidic device tended to be slightly lower than those from the flow cytometer, as shown in the Bland-Altman plot (mean bias value). On the other hand, the Pearson coefficient correlation value, r = 0.9876, between the two

methods indicates a strong relationship between the datasets. The regression equation in Passing-Bablok analysis indicated a coefficient of 0.898. In summary, despite the different principles used for cell counting by the two methods, the purposed microfluidic device shows a good agreement to the flow cytometer.

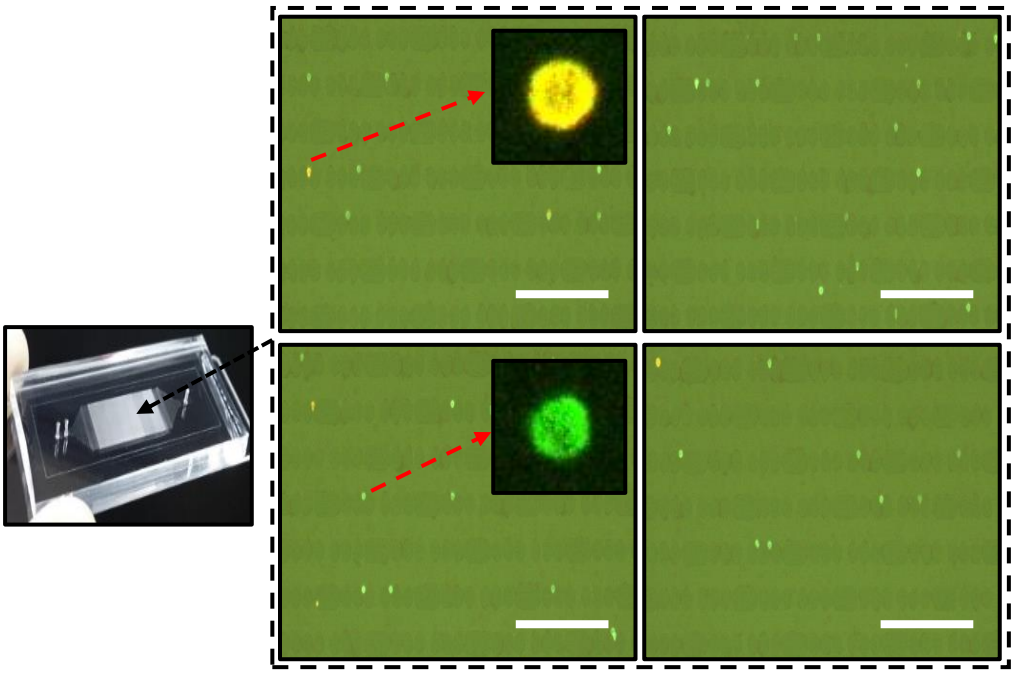

Figure 5.2 Example of T (green colour) and B (yellow colour) lymphocytes captured on the microfluidic device. The size of T and B lymphocytes is about 10 μm. Scale Bars: 200 μm

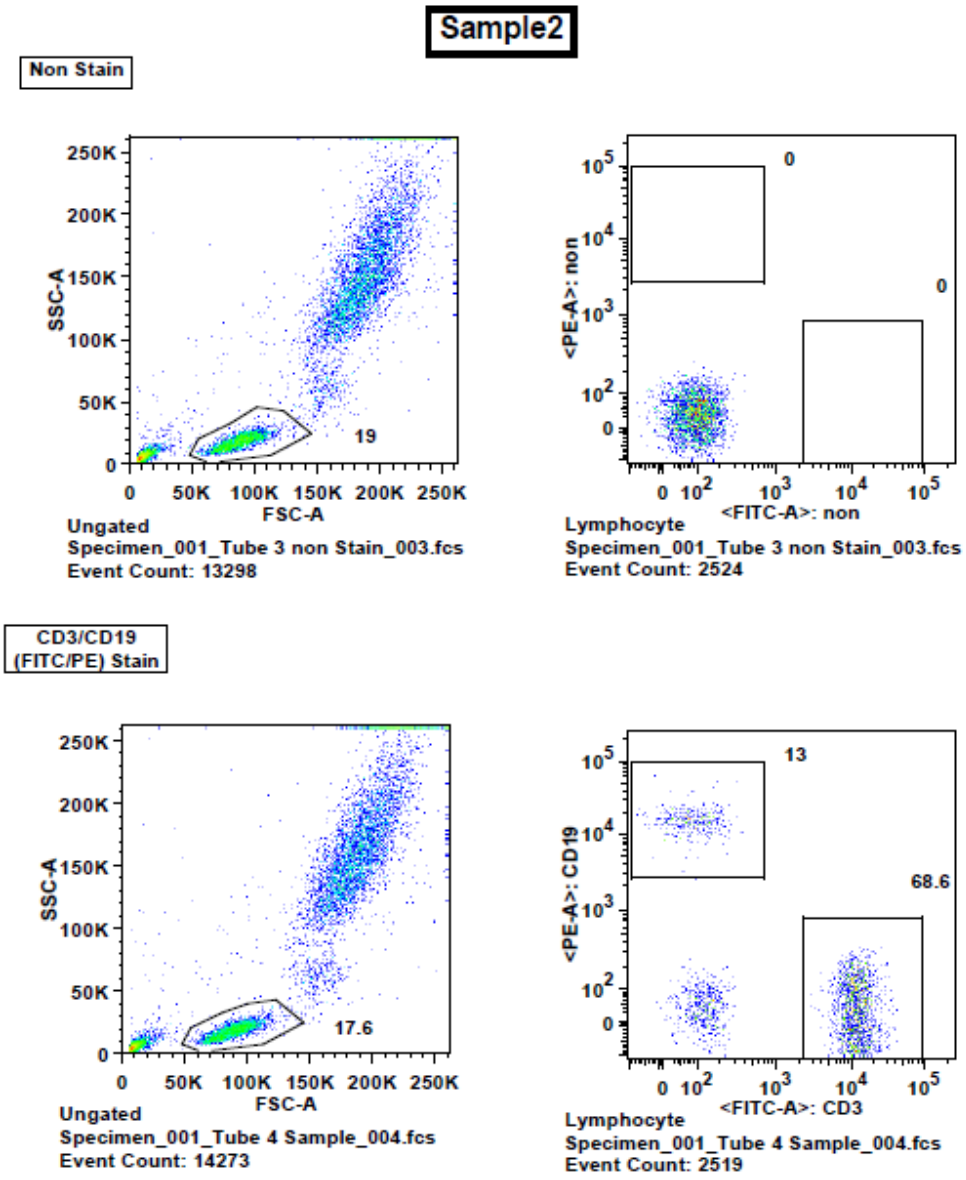

Sample2	Total Count	Lymphocyte		CD3+CD19-		CD19+CD3-		CD3/CD19
		Count	Sattistic	Count	Sattistic	Count	Statistic	
Non Stain	13298Cells	2524Cells (/13298Cells)	19.0%	0		0		
CD3/CD19 (FITC/PE)Stain	14273Cells	2519Cells (/14273Cells)	17.6%	1728Cells (/2519Cells)	68.6%	328Cells (/2519Cells)	13.0%	

Figure 5.3 Example of flow cytometer result. Detection of T and B lymphocytes.

Table 5.1 Hypothetical data of an agreement between microfluidic device and flow cytometer methods

Flow Cytometer (FC)	Microfluidic Device (MD)	Mean (MC+MD)/2	Difference MC-MD	(MC-MD) / Mean (%)
8.92	8.75	8.84	0.17	1.92
2.64	2.74	2.69	-0.10	-3.72
4.08	5.08	4.58	-1.00	-21.83
1.25	1.36	1.31	-0.11	-8.43
31.62	29.12	30.37	2.50	8.23
4.87	4.63	4.75	0.24	5.05
12.24	10.43	11.34	1.81	15.97
11.01	10.89	10.95	0.12	1.10
4.95	5.30	5.13	-0.35	-6.83
16.86	18.25	17.56	-1.39	-7.92
5.27	5.77	5.52	-0.50	-9.06
3.70	3.21	3.46	0.49	14.18
9.52	8.38	8.95	1.14	12.74
9.86	8.37	9.12	1.49	16.35
5.73	4.13	4.93	1.60	32.45
5.41	4.53	4.97	0.88	17.71
2.93	2.74	2.84	0.19	6.70
25.33	20.39	22.86	4.94	21.61
10.14	9.89	10.02	0.25	2.50

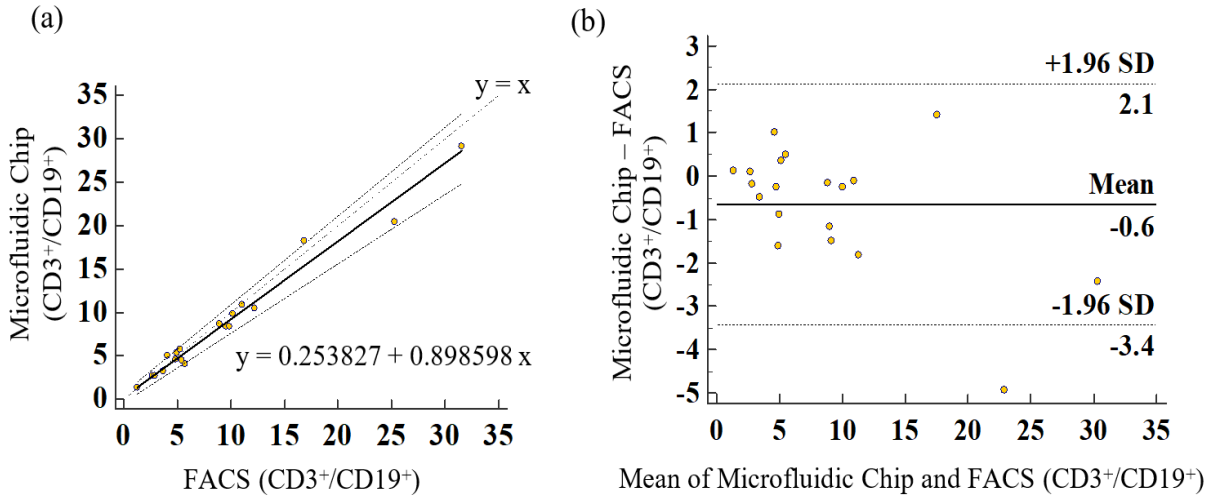

Figure 5.4 Comparison of the cell count obtained by the microfluidic chip with that obtained by the flow cytometer. (a) Correlation between the two methods (black line) of the total CD3+/CD19+ cell count obtained by the microfluidic chip versus the CD3+/ CD19+ count obtained by the flow cytometer, as determined by Passing-Bablok regression. The short dotted line indicates the line of identity (i.e., slope of the line is 1.). The long-dotted line indicates the 95% confidence limits between the methods. The calculated Pearson correlation, r, was 0.9876, and the significance level was $P < 0.0001$. (b) Microfluidic chip CD3+/CD19+ cell counts obtained using a Bland-Altman plot. The black line shows the mean difference of the methods, and the long upper and lower dotted lines represent the 95% limits (1.96 SD) of agreement

Table 5.2 The comparison experiment data between microfluidic device and flow cytometer cells.

	Microfluidic device			Flow cytometer (BD FACSCanto™ II)		
	$CD3^+$ cells (Trapped cell No.)	$CD19^+$ cells (Trapped cell No.)	T/B Ratio	$CD3^+$ cells (Event No.)	$CD19^+$ cells (Event No.)	T/B Ratio
1	1,111	127	8.75	2,051	230	8.92
2	989	361	2.74	1,667	632	2.64
3	1,604	316	5.08	1,590	390	4.08
4	879	645	1.36	1,002	802	1.25
5	495	17	29.12	1,486	47	31.62
6	1,346	291	4.63	1,890	388	4.87
7	1,804	173	10.43	1,616	132	12.24
8	719	66	10.89	1,928	175	11.01

9	1,044	197	5.30	1,471	297	4.95
10	803	44	18.25	1,871	111	16.86
11	1,200	208	5.77	1,728	328	5.27
12	912	284	3.21	1,731	467	3.70
13	1,618	193	8.38	2,029	213	9.52
14	1,431	171	8.37	1,973	200	9.86
15	1,141	276	4.13	1,794	313	5.73
16	1,223	270	4.53	1,514	280	5.41
17	699	255	2.74	1,301	443	2.93
18	1,468	72	20.39	2,128	84	25.33
19	1,454	147	9.89	1,795	177	10.14

5.8 Conclusion

The proposed microfluidic device for cell counting was demonstrated to have a high efficiency cells capture rate. The device uses a pillar-based cells separation technique and was used to count T-cells and B-cells on device in a small volume (1 μL) of whole blood. Moreover, the time taken for sample processing for a single sample for microfluidic device was less than 20 minutes compared to 50 minutes using flow cytometer. Our method is accurate, practical, inexpensive, and requires no additional reagents such as for haemolysis, and no fixation and centrifugation for sample pre-treatment. Furthermore, strong relationship between standard methods has been demonstrated. This method simplifies and speeds up sample preparation processes and reduces the cost of operation. Hence, this system could offer an alternative method to the current approach of cell cytometry.

Chapter 6

Summary and Future Work

6.1 Summary

In this thesis, we have presented some applications using the inhouse proposed microfluidic device for cell separation and counting. White blood cell (WBC) count remains one of the most frequently used clinical tests in hospitals. Furthermore, the subpopulation of WBCs counting such as lymphocytes, T and B cells count are very important to determine one health condition, specifically the immune system. Current trends of cell counting instrument are moving forward to have featured such as portability including miniaturized system, cost-effectively including sample processing, system management and maintenance. Moreover, the result produce is rapid, fast treatment, and provides superior monitoring system in a limited resources location.

In chapter 2, we presented high efficacy and easy technique to eliminates device clogging caused by cells captured at the microfilter. Compared to other clogging-free device techniques based on the mechanical separation, which required a precision flow control by an additional pump to generate oscillatory flow to released clog cells at the filtering mechanism. Another purposed technique such as tuneable micro filter which adjusts the opening area of the channel (with filter) to released clog cells requires a precision mechanism or actuator to tune the microfluidic device. Conventional cell separation and filtration such as dead-end, cross-flow and weir-type

filtering are suffering from clogging problems, not suitable for higher sample concentration which requires a tedious sampling pre-treatment process prior to separating the cells. The proposed technique, which uses an escape route in the filters shows significant improvement to device clogging without the need of any special tool or sophisticated pump and control system. In our preliminary observation as discussed, a 3 μL of whole blood caused the filters beginning to clog. This volume is estimated with at least 12K (thousand) WBCs (normal WBCs range, 4K – 10K cells), and at least 12M (million) of RBCs (normal RBCs range, 4M – 5 M cells). To handle such a concentrated sample, for a particular application such as capturing rare cells from a bulk sample is possible to be treated just by changing the dimensions (the filtration area) of the proposed microfluidic device. Furthermore, the gradually decreased filtration provides an advantage for size or deformability-based cell separation, which is useful to analyse biophysical properties such as cell stiffness. The gradual decreased filtration helps reduce cell clogging by separating larger size cells at the upper stream and smaller cells at the low stream of filtrations area. Thus, the combination of the gradual decrease in infiltration or permeation concept and escape route technique resulted in a clogging-free device.

In chapter 3, we presented the development of the imaging system. The imaging system is essential not only to captured cells images but be able to detect (fluorescence) at a very low intensity of some cells. The intensity is low due to the protein expression on the cell surface is varies on each cell. Direct immunofluorescence staining is faster, cheaper and less noise (reduced non-specific binding) than indirect immunolabelling methods. However, it suffers from low intensity (emission) problem. Thus, the selection of components including, optical filters, light source, and detector is very important.

Furthermore, the type of fluorescence labelling (immunofluorescence) use must be suitable for the developed system. Although the direct immunofluorescence labelling is used, the system is still able to detect and identify a low-intensity signal. On the other hand, the developed algorithm used to detect and count the cells based on colour thresholding, HSV colour space shows that cells could be successfully detected. Thresholding is the most straightforward methods for image segmented in the image processing technique compared to other complicated processes. Even though the technique is simple, a low noise image, including background, camera-noise, and foreground to background contrast, should be optimum. Which means a suitable imaging system setup will provide a good quality image for further analysed. Therefore, all the components and algorithm was selected and developed carefully to produces an accurate result.

In chapter 4, the application of WBC cells separation based on size and deformability using the purposed microfluidic device is performed. The mechanical properties of cells, such as their stiffness response to applied stress, is generally determined by their microstructure. Previous studies have reported that cells in a diseased state have different mechanical properties than healthy cells due to a change in their physical structures. They are two experiments involved in this topic. The CD45+ cells and lymphocytes (CD4+ and CD19+ cells) distribution on the purposed device is studied. The mechanical properties of these cells, particularly the deformability (stiffness) related to the hydrodynamic pressure (sample flow speed) applied was observed for the distribution of captured cells at the microfilters. WBCs including lymphocytes, neutrophils, monocytes, basophils, eosinophils sizes are ranging from 7 to 35 μm. However, the ability of these cells to deform is varied to each type of cells. For instance, during a low sample flow speed (1.5

μL/min) applied, most of the WBCs are captured at the upper stream of the microfluidic device. Compared to the fastest speed (6 μL/min), most of the cells are distributed at the lower stream of the microfilters. These show that, regardless of the size of WBCs, the ability to deform and passing through filters gap is depending on the microfilter gap sizes, applied flow speed, cell sizes, and the ability of the cells to deform. The results are useful for information of the health status, particularly, cells stiffness studies. However, our results only apply to a limited healthy subject. Furthermore, for a smallest microfilter gap size (3 μm), the results show a significant cell loss (passing through filters) under the highest speed (6 μL/min). It's also observed that the escaped cells are a small type of WBC cells with closer to RBCs size (7-8 μm). For further analysis of WBCs distribution, the lymphocytes, the subpopulations of WBCs, distribution shows that most of the cells (T and B lymphocytes) are captured or filtered at gap size 4-8 μm, where the total captured cell average is about 89% from total T and B lymphocytes. The highest captured of these cells was at 6 μm gap sizes. This indicated that, even though the size of the average lymphocytes is less than 10 μm, it still could be passing through a smaller filter gap size than its size. Thus, the information of cells distribution by the microfilter could be useful to the application of label free cell phenotype identification as well as deformability of cells. On the other hand, the distribution profile (from cells distribution image) and the deformability imaging profiles might be useful for preliminary screening (cell distribution to filters size) in the clinical applications. This work presents the development of a simple device for the study of cell deformability as the results provide a biophysical marker in high throughput and bulk sample analyses.

In chapter 5, the application of WBCs subpopulations T and B lymphocytes counting using the purposed microfluidic device was compared to a flow cytometer. Cells counting such as T and B cells lymphocytes is important because human immunodeficiency virus (HIV) directly infects and damages T-cells, causing the number of T-cells in an HIV-infected person to decrease over time. The detection of T and B lymphocytes are based on immunofluorescence principle. The identification of WBCs population could be clearly distinguished using the custom developed imaging system. On the other hand, the flow cytometry needs a long and tedious sample preparation setup as described earlier. Besides, our method of sample processing is rapid with less process steps, which gives advantage compare to conventional flow cytometry. Moreover, the reagents need in the pre-sample using this traditional instrument is costly. Microfluidic-based cell counting required a minimal sample volume, i.e. 1 μL (estimated from 10x dilutions) from the whole blood sample used. The Passing-Bablok analysis shows that confidence interval (CI) with a relationship (regression) while Bland-Altman provides the limits of agreement between two comparison methods (microfluidic and flow cytometer). Thus, these two comparison methods show a strong relationship ($r = 0.987$). A good agreement between the proposed method and flow cytometer shows that the microfluidic-based device provides advantages over the conventional method.

6.2 Future Work

The future works are briefly described in the following paragraph.

6.2.1 Clogging-free Microfluidic Device for Cell Counting

Microfluidic-based cell counting is a promising diagnostic tool for analysis in medicine, biology and clinical applications. Furthermore, a critical requirement for rapid diagnostic, cost-effectively, high throughput and portability, suitable as a point-of-care device is one of the advantages offers by this microfluidic technology. Integration of microfluidic system with such as LAB-on-Chip offers multiple processes and detection for numerous applications and fields.

However, limitations on an integrated system such Lab-on-Chip still requires an external system to work with, such as measurement device, precision flow control, additional to instrument support the system etc. Therefore, these require a complex system which technically increased the overall cost which was the major issue in the conventional device for example. Thus, our intentions are to develop a cell counting device as simple as possible without required any external system to operates and incorporated with available technologies such as mobile phone. Our developed system currently still required a custom imaging system which is bulky and required a high power to operates (e.g., source light, camera, computer, motorize system). These become a limitation where most of the application such example in monitoring health-related to disease and drug treatments, e.g., the point-of-care application is unsuitable. Therefore, future work will focus in utilize existing technology particularly, mobile sensing technology, for example, image sensing, incorporated to microfluidic device. Image sensing technology provides a large sensing area as well as able to detect very low signal (light).

Simple use of device such as finger-prick and sample drop on control area in microfluidic where the image of target cell could be detected using a mobile camera and provide the analysis (cell counting) using mobile apps. Furthermore, the application of internet-of-things (IoT) is possible to provide almost in real-time for further interpretation by experts or specialists anywhere without physically present. Even an intelligent device with advance apps would be able to sort the solution without an expert helps. The microfluidic device principle should be able to separate cells passively (no external force) in high concentration level (non-dilution condition), which is a challenge but possible. This future work will improve time, cost, energy and provides portability suitable to be used for rapid diagnostic device anywhere.

6.2.2 Deformability of Cell as a Disease Biomarker and Health Monitoring

Numbers of researchers have shown that pathological alterations (i.e., biomechanical properties) such as cell stiffness (deformability), especially RBCs and WBCs, have been associated with various diseases [94][143[144]. However, the limitations on methods of deformability measurement make the process of analysis tedious as an example require a carefully pre-treatment such as centrifuging, lysis, separating cells etc. On the other hand, current tools for measurement such as micropipette aspiration, optical, deformability flow cytometry and AFM (atomic force microscopy) suffers from throughput, introduced cell damage or alter cells' properties, tedious setup, bulky instruments, time-consuming and many more. Furthermore, preliminary screening and clinical applications or are not suitable to apply these conventional methods. Hence, a microfluidic-based device offers great potential to reduce cost, provides portability, suitable for pre-assessment

applications and clinical applications. Therefore, future work in this topic will focus on pre-assessment applications on healthy and diseases patient WBCs deformability measurements. Cells separation and its distributions provide information about bulk sample conditions. A mathematical model approach could estimate the deformability level for example, deformability index or force measurement. Even though estimation through the mathematical model is not accurate as physical measurement, it still provides useful fast information suitable for a preliminary assessment. This method would reduce the tedious process of sample preparation, and are suitable for numerous cell types applications. Deformability assessment also provides information about the health condition and suitable for monitoring a drug's effectiveness and early disease detection applications.

BIBLIOGRAPHY

[1] Manz A, Graber N, Widmer HM., 1990. Miniaturized total chemical analysis systems: a novel concept for chemical sensing. Sens Actuators. B1:244–8.

[2] Gervais, L.; Rooij, N.D.; Delamarche, E. Microfluidic chips for point-of-care immunodiagnostics. Adv. Mater. 2011, 23, H151–H176. [Google Scholar] [CrossRef] [PubMed]

[3] Beebe, D.J., Mensing, G.A. and Walker, G.M., 2002. Physics and applications of microfluidics in biology. Annual review of biomedical engineering, 4(1), pp.261-286.

[4] Luttge, R., 2011 Microfabrication for industrial applications, 1st edn. William Andrew, Boston, pp 91–146.

[5] Zhang, Q., and Austin, R. H., 2012. Applications of microfluidics in stem cell biology. BioNanoScience, 2(4), 277-286.

[6] Shields, C. W., Ohiri, K. A., Szott, L. M., and López, G. P., 2017. Translating microfluidics: Cell separation technologies and their barriers to commercialization. Cytometry Part B: Clinical Cytometry, 92(2), 115-125.

[7] Su, W., Gao, X., Jiang, L., and Qin, J., 2015. Microfluidic platform towards point-of-care diagnostics in infectious diseases. Journal of Chromatography A, 1377, 13-26.

[8] Ibrahim, S. F., and van den Engh, G., 2007. Flow cytometry and cell sorting. In Cell Separation (pp. 19-39). Springer, Berlin, Heidelberg.

[9] Miltenyi, S., Müller, W., Weichel, W., and Radbruch, A., 1990. High gradient magnetic cell separation with MACS. Cytometry: The Journal of the International Society for Analytical Cytology, 11(2), 231-238.

[10] Herzenberg, L. A., Parks, D., Sahaf, B., Perez, O., Roederer, M., and Herzenberg, L. A., 2002. The history and future of the fluorescence activated cell sorter and flow cytometry: a view from Stanford. Clinical chemistry, 48(10), 1819-1827.

[11] Chung, T. D., and Kim, H. C., 2007. Recent advances in miniaturized microfluidic flow cytometry for clinical use. Electrophoresis, 28(24), 4511-4520.

[12] Vembadi, A., Menachery, A., and Qasaimeh, M. A., 2019. Cell cytometry: review and perspective on biotechnological advances. Frontiers in bioengineering and biotechnology, 7.

[13] Shrirao, A. B., Fritz, Z., Novik, E. M., Yarmush, G. M., Schloss, R. S., Zahn, J. D., and Yarmush, M. L., 2018. Microfluidic flow cytometry: The role of microfabrication methodologies, performance and functional specification. Technology, 6(01), 1-23.

[14] Stavrakis, S., Holzner, G., Choo, J., and DeMello, A., 2019. High-throughput microfluidic imaging flow cytometry. Current opinion in biotechnology, 55, 36-43.

[15] Bain, B.J., 2014. Blood cells: a practical guide. John Wiley & Sons.

[16] Liotta, L. A., Ferrari, M., and Petricoin, E., 2003. Clinical proteomics: written in blood. Nature, 425(6961), 905.

[17] Stern, E., Vacic, A., Rajan, N.K., Criscione, J.M., Park, J., Ilic, B.R., Mooney, D.J., Reed, M.A. and Fahmy, T.M., 2010. Label-free biomarker detection from whole blood. Nature nanotechnology, 5(2), p.138

[18] Miale, J.B., 1962. Laboratory medicine-hematology. Academic Medicine, 37(10), p.1147.

[19] Williams, W.J., Hematology. 3rd ed. 1983, New York: McGraw-Hill. xxvi, 1728

[20] Zheng, S., On-chip blood count. Ph.D. thesis. 2007, Pasadena, California: California Institute of Technology.

[21] Zhang, X.Y., Simpson, J.L., Powell, H., Yang, I.A., Upham, J.W., Reynolds, P.N., Hodge, S., James, A.L., Jenkins, C., Peters, M.J. and Lin, J.T., 2014. Full blood count parameters for the detection of asthma inflammatory phenotypes. Clinical and experimental allergy, 44(9), pp.1137-1145.

[22] Tefferi, A., Hanson, C. A., and Inwards, D. J., 2005. How to interpret and pursue an abnormal complete blood cell count in adults. In Mayo Clinic Proceedings (Vol. 80, No. 7, pp. 923-936). Elsevier.

[23] Sullivan, E., 2006. Hematology analyzer: From workhorse to thoroughbred. Laboratory Medicine, 37(5), 273-278.

[24] Brown, M., and Wittwer, C., 2000. Flow cytometry: principles and clinical applications in hematology. Clinical chemistry, 46(8), 1221-1229.

[25] Shapiro, H. M., 2005. Practical flow cytometry. John Wiley and Sons.

[26] Matsuno, K., and Ishizuka, S., 1998. New technology of automated blood cell differential counting. Rinsho byori. The Japanese journal of clinical pathology, 46(4), 361-366.

[27] George, T.C., Basiji, D.A., Hall, B.E., Lynch, D.H., Ortyn, W.E., Perry, D.J., Seo, M.J., Zimmerman, C.A. and Morrissey, P.J., 2004. Distinguishing modes of cell death using the ImageStream® multispectral imaging flow cytometer. Cytometry Part A: The Journal of the International Society for Analytical Cytology, 59(2), pp.237-245.

[28] Ortyn, W.E., Hall, B.E., George, T.C., Frost, K., Basiji, D.A., Perry, D.J., Zimmerman, C.A., Coder, D. and Morrissey, P.J., 2006. Sensitivity measurement and compensation in spectral imaging. Cytometry Part A: The Journal of the International Society for Analytical Cytology, 69(8), pp.852-862.

[29] Vashist, S. K., Luppa, P. B., Yeo, L. Y., Ozcan, A., and Luong, J. H., 2015. Emerging technologies for next-generation point-of-care testing. Trends in biotechnology, 33(11), 692-705.

[30] World Health Organization, 2011. Manual for the laboratory diagnosis and virological surveillance of influenza.

[31] UNAIDS, G. H., and Statistics, A. I. D. S., 2019. 2018 Fact Sheet, 2019.

[32] Boyle, D. S., Hawkins, K. R., Steele, M. S., Singhal, M., and Cheng, X., 2012. Emerging technologies for point-of-care CD4 T-lymphocyte counting. Trends in biotechnology, 30(1), 45-54.

[33] Hosokawa, M., Hayata, T., Fukuda, Y., Arakaki, A., Yoshino, T., Tanaka, T., and Matsunaga, T., 2010. Size-selective microcavity array for rapid and efficient detection of circulating tumor cells. Analytical chemistry, 82(15), 6629-6635.

[34] Andersson, H., van der Wijngaart, W. and Stemme, G., 2001. Micromachined filter‐chamber array with passive valves for biochemical assays on beads. Electrophoresis, 22(2), pp.249-257.

[35] Ji, H.M., Samper, V., Chen, Y., Heng, C.K., Lim, T.M. and Yobas, L., 2008. Silicon-based microfilters for whole blood cell separation. Biomedical microdevices, 10(2), pp.251-257.

[36] Zheng, S., Lin, H., Liu, J.Q., Balic, M., Datar, R., Cote, R.J. and Tai, Y.C., 2007. Membrane microfilter device for selective capture, electrolysis and genomic analysis of human circulating tumor cells. Journal of chromatography A, 1162(2), pp.154-161.

[37] Hosokawa, M., Asami, M., Nakamura, S., Yoshino, T., Tsujimura, N., Takahashi, M., Nakasono, S., Tanaka, T. and Matsunaga, T., 2012. Leukocyte counting from a small amount of whole blood using a size - controlled microcavity array. Biotechnology and bioengineering, 109(8), pp.2017-2024.

[38] Ribeiro-Samy, S., Oliveira, M.I., Pereira-Veiga, T., Muinelo-Romay, L., Carvalho, S., Gaspar, J., Freitas, P.P., López-López, R., Costa, C. and Diéguez, L., 2019. Fast and efficient microfluidic cell filter for isolation of circulating tumor cells from unprocessed whole blood of colorectal cancer patients. Scientific reports, 9(1), p.8032.

[39] Lee, S.J., Sim, T.S., Shin, H.Y., Lee, J., Kim, M.Y., Sunoo, J., Lee, J.G., Yea, K., Kim, Y.Z., van Noort, D. and Park, S.K., 2019. Microslit on a chip: A simplified filter to capture circulating tumor cells enlarged with microbeads. PloS one, 14(10).

[40] Kang, Y.T., Doh, I., Byun, J., Chang, H.J. and Cho, Y.H., 2017. Label-free rapid viable enrichment of circulating tumor cell by photosensitive polymer-based microfilter device. Theranostics, 7(13), p.3179.

[41] Yusa, A., Toneri, M., Masuda, T., Ito, S., Yamamoto, S., Okochi, M., Kondo, N., Iwata, H., Yatabe, Y., Ichinosawa, Y. and Kinuta, S., 2014.

Development of a new rapid isolation device for circulating tumor cells (CTCs) using 3D palladium filter and its application for genetic analysis. PloS one, 9(2), p.e88821.

[42] VanDelinder, V. and Groisman, A., 2007. Perfusion in microfluidic cross-flow: separation of white blood cells from whole blood and exchange of medium in a continuous flow. Analytical Chemistry, 79(5), pp.2023-2030.

[43] Li, X., Chen, W., Liu, G., Lu, W. and Fu, J., 2014. Continuous-flow microfluidic blood cell sorting for unprocessed whole blood using surface-micromachined microfiltration membranes. Lab on a Chip, 14(14), pp.2565-2575.

[44] Faustino, V., Catarino, S., Pinho, D., Lima, R. and Minas, G., 2018. A Passive Microfluidic Device Based on Crossflow Filtration for Cell Separation Measurements: A Spectrophotometric Characterization. Biosensors, 8(4), p.125.

[45] Ji, H. M., Samper, V., Chen, Y., Heng, C. K., Lim, T. M., and Yobas, L., 2008. Silicon-based microfilters for whole blood cell separation. Biomedical microdevices, 10(2), 251-257.

[46] Chen, X., Liu, C. C., and Li, H., 2008. Microfluidic chip for blood cell separation and collection based on crossflow filtration. Sensors and Actuators B: Chemical, 130(1), 216-221.

[47] Chiu, Y. Y., Huang, C. K., and Lu, Y. W., 2016. Enhancement of microfluidic particle separation using cross-flow filters with hydrodynamic focusing. Biomicrofluidics, 10(1), 011906.

[48] Sethu, P., Sin, A., and Toner, M., 2006. Microfluidic diffusive filter for apheresis (leukapheresis). Lab on a Chip, 6(1), 83-89.

[49] Tan, S. J., Yobas, L., Lee, G. Y. H., Ong, C. N., and Lim, C. T., 2009. Microdevice for the isolation and enumeration of cancer cells from blood. Biomedical microdevices, 11(4), 883-892.

[50] Wei, H., Chueh, B.H., Wu, H., Hall, E.W., Li, C.W., Schirhagl, R., Lin, J.M. and Zare, R.N., 2011. Particle sorting using a porous membrane in a microfluidic device. Lab on a chip, 11(2), pp.238-245.

[51] Mohamed, H., Murray, M., Turner, J. N., and Caggana, M., 2009. Isolation of tumor cells using size and deformation. Journal of Chromatography A, 1216(47), 8289-8295.

[52] McFaul, S. M., Lin, B. K., and Ma, H., 2012. Cell separation based on size and deformability using microfluidic funnel ratchets. Lab on a chip, 12(13), 2369-2376.

[53] Yoon, Y., Kim, S., Lee, J., Choi, J., Kim, R.K., Lee, S.J., Sul, O. and Lee, S.B., 2016. Clogging-free microfluidics for continuous size-based separation of microparticles. Scientific reports, 6, p.26531.

[54] Cheng, Y., Ye, X., Ma, Z., Xie, S., and Wang, W. , 2016. High-throughput and clogging-free microfluidic filtration platform for on-chip cell separation from undiluted whole blood. Biomicrofluidics, 10(1), 014118.

[55] Pang, L., Shen, S., Ma, C., Ma, T., Zhang, R., Tian, C., Zhao, L., Liu, W. and Wang, J., 2015. Deformability and size-based cancer cell separation using an integrated microfluidic device. Analyst, 140(21), pp.7335-7346.

[56] Sarioglu, A. F., Aceto, N., Kojic, N., Donaldson, M. C., Zeinali, M., Hamza, B., ... and Luo, X., 2015. A microfluidic device for label-free, physical capture of circulating tumor cell clusters. Nature methods, 12(7), 685.

[57] Masuda, T., Song, W., Nakanishi, H., Lei, W., Noor, A. M., and Arai, F., 2017. Rare cell isolation and recovery on open-channel microfluidic chip. PloS one, 12(4), e0174937.

[58] Xu, B., Hu, W., Du, W., Hu, Y., Zhang, C., Lao, Z., Ni, J., Li, J., Wu, D., Chu, J. and Sugioka, K., 2017. Arch-like microsorters with multi-modal and clogging-improved filtering functions by using femtosecond laser multifocal parallel microfabrication. Optics express, 25(14), pp.16739-16753.

[59] Alvankarian, J., and Majlis, B. Y., 2015. Tunable microfluidic devices for hydrodynamic fractionation of cells and beads: a review. Sensors, 15(11), 29685-29701.

[60] Beattie, W., Qin, X., Wang, L., and Ma, H., 2014. Clog-free cell filtration using resettable cell traps. Lab on a Chip, 14(15), 2657-2665

[61] Alvankarian, J., and Majlis, B. Y., 2015. A technique of optimization of microfiltration using a tunable platform. Journal of Micromechanics and Microengineering, 25(8), 084011.

[62] Huang, S. B., Wu, M. H., and Lee, G. B., 2009. A tunable micro filter modulated by pneumatic pressure for cell separation. Sensors and Actuators B: Chemical, 142(1), 389-399.

[63] Lee, A., Park, J., Lim, M., Sunkara, V., Kim, S.Y., Kim, G.H., Kim, M.H. and Cho, Y.K., 2014. All-in-one centrifugal microfluidic device for size-selective circulating tumor cell isolation with high purity. Analytical chemistry, 86(22), pp.11349-11356.

[64] Kim, T.H., Lim, M., Park, J., Oh, J.M., Kim, H., Jeong, H., Lee, S.J., Park, H.C., Jung, S., Kim, B.C. and Lee, K., 2016. FAST: size-selective, clog-free isolation of rare cancer cells from whole blood at a liquid–liquid interface. Analytical chemistry, 89(2), pp.1155-1162.

[65] Peter, T., Badrichani, A., Wu, E., Freeman, R., Ncube, B., Ariki, F., Daily, J., Shimada, Y. and Murtagh, M., 2008. Challenges in implementing CD4 testing in resource - limited settings. Cytometry Part B: Clinical Cytometry: The Journal of the International Society for Analytical Cytology, 74(S1), pp.S123-S130.

[66] Lee, W.G., Kim, Y.G., Chung, B.G., Demirci, U. and Khademhosseini, A., 2010. Nano/Microfluidics for diagnosis of infectious diseases in developing countries. Advanced drug delivery reviews, 62(4-5), pp.449-457.

[67] Chen, H., Cao, B., Sun, B., Cao, Y., Yang, K., and Lin, Y. S., 2017. Highly-sensitive capture of circulating tumor cells using micro-ellipse filters. Scientific reports, 7(1), 610

[68] Wilding, P., Kricka, L.J., Cheng, J., Hvichia, G., Shoffner, M.A. and Fortina, P., 1998. Integrated cell isolation and polymerase chain reaction analysis using silicon microfilter chambers. Analytical biochemistry, 257(2), pp.95-100.

[69] VanDelinder, V. and Groisman, A., 2006. Separation of plasma from whole human blood in a continuous cross-flow in a molded microfluidic device. Analytical chemistry, 78(11), pp.3765-3771.

[70] Crowley, T. A., and Pizziconi, V., 2005. Isolation of plasma from whole blood using planar microfilters for lab-on-a-chip applications. Lab on a Chip, 5(9), 922-929.

[71] McNicol, G. P., 2012. Clinical aspects of blood viscosity and cell deformability. Springer Science and Business Media.

[72] Seal, S. H., 1964. A sieve for the isolation of cancer cells and other large cells from the blood. Cancer, 17(5), 637-642.

[73] Bhagat, A. A. S., Bow, H., Hou, H. W., Tan, S. J., Han, J., and Lim, C. T., 2010. Microfluidics for cell separation. Medical and biological engineering and computing, 48(10), 999-1014.

[74] Gossett, D.R., Weaver, W.M., Mach, A.J., Hur, S.C., Tse, H.T.K., Lee, W., Amini, H. and Di Carlo, D., 2010. Label-free cell separation and sorting in microfluidic systems. Analytical and bioanalytical chemistry, 397(8), pp.3249-3267.

[75] Mohamed, H., McCurdy, L.D., Szarowski, D.H., Duva, S., Turner, J.N. and Caggana, M., 2004. Development of a rare cell fractionation device: application for cancer detection. IEEE transactions on nanobioscience, 3(4), pp.251-256.

[76] Noor, A.M., Masuda, T., Lei, W., Horio, K., Miyata, Y., Namatame, M., Hayase, Y., Saito, T.I. and Arai, F., 2018. A microfluidic chip for capturing, imaging and counting CD3+ T-lymphocytes and CD19+ B-lymphocytes from whole blood. Sensors and Actuators B: Chemical, 276, pp.107-113.

[77] Sosa, J. M., Nielsen, N. D., Vignes, S. M., Chen, T. G., and Shevkoplyas, S. S., 2014. The relationship between red blood cell deformability metrics and perfusion of an artificial microvascular network. Clinical hemorheology and microcirculation, 57(3), 275-289.

[78] Sanderson, M. J., Smith, I., Parker, I., and Bootman, M. D., 2014. Fluorescence microscopy. Cold Spring Harbor Protocols, 2014(10), pdb-top071795.

[79] Tuchin, V.V. ed., 2010. Handbook of photonics for biomedical science. CRC Press.

[80] Park, K. S., Kim, D. U., Lee, J., Kim, G. H., and Chang, K. S., 2016. Simultaneous multicolor imaging of wide-field epi-fluorescence

microscopy with four-bucket detection. Biomedical optics express, 7(6), 2285-2294.

[81] Waters, J. C., 2009. Accuracy and precision in quantitative fluorescence microscopy. J. Cell Biol. 185, 1135-1148.

[82] Odell, I. D., and Cook, D., 2013. Immunofluorescence techniques. The Journal of investigative dermatology, 133(1), e4.CRC Press, 2010.

[83] Hendrickx, A. and Bossuyt, X., 2001. Quantification of the leukocyte common antigen (CD45) in mature B‐cell malignancies. Cytometry: The Journal of the International Society for Analytical Cytology, 46(6), pp.336-339.

[84] Baumgarth, N. and Roederer, M., 2000. A practical approach to multicolor flow cytometry for immunophenotyping. Journal of immunological methods, 243(1-2), pp.77-97.

[85] Magnan, P., 2003. Detection of visible photons in CCD and CMOS: A comparative view. Nuclear Instruments and Methods in Physics Research Section A: Accelerators, Spectrometers, Detectors and Associated Equipment, 504(1-3), 199-212.

[86] Chen, T.W., Chen, Y.L. and Chien, S.Y., 2008, October. Fast image segmentation based on K-Means clustering with histograms in HSV color space. In 2008 IEEE 10th Workshop on Multimedia Signal Processing (pp. 322-325). IEEE.

[87] Yabusaki, K., Faits, T., McMullen, E., Figueiredo, J.L., Aikawa, M. and Aikawa, E., 2014. A novel quantitative approach for eliminating sample-to-sample variation using a hue saturation value analysis program. PloS one, 9(3), p.e89627.

[88] Chebbout, S., and Merouani, H. F., 2012. Comparative study of clustering based colour image segmentation techniques. In 2012

Eighth International Conference on Signal Image Technology and Internet Based Systems (pp. 839-844). IEEE.

[89] Bora, D. J., Gupta, A. K., and Khan, F. A., 2015. Comparing the performance of L* A* B* and HSV color spaces with respect to color image segmentation. arXiv preprint arXiv:1506.01472.

[90] Schmid-Schönbein, G. W., Sung, K. L., Tözeren, H., Skalak, R., and Chien, S., 1981. Passive mechanical properties of human leukocytes. Biophysical Journal, 36(1), 243-256.

[91] Morikawa, M., Inoue, Y., Sumi, Y., Kuroda, Y., and Tanaka, H., 2015. Leukocyte deformability is a novel biomarker to reflect sepsis - induced disseminated intravascular coagulation. Acute medicine and surgery, 2(1), 13-20.

[92] Zheng, Y., Wen, J., Nguyen, J., Cachia, M. A., Wang, C., and Sun, Y., 2015. Decreased deformability of lymphocytes in chronic lymphocytic leukemia. Scientific reports, 5, 7613.

[93] Alexandrova, A., Antonova, N., Skorkina, M. Y., Shamray, E., and Cherkashina, O. V., 2017. Evaluation of the elastic properties and topography of leukocytes' surface in patients with type 2 diabetes mellitus using atomic force microscope.

[94] Toepfner, N., Herold, C., Otto, O., Rosendahl, P., Jacobi, A., Kräter, M., Stächele, J., Menschner, L., Herbig, M., Ciuffreda, L. and Ranford-Cartwright, L., 2018. Detection of human disease conditions by single-cell morpho-rheological phenotyping of blood. Elife, 7, p.e29213.

[95] Cross, S. E., Jin, Y. S., Rao, J., and Gimzewski, J. K., 2007. Nanomechanical analysis of cells from cancer patients. Nature nanotechnology, 2(12), 780.

[96] Plodinec, M., Loparic, M., Monnier, C. A., Obermann, E. C., Zanetti-Dallenbach, R., Oertle, P., Hyotyla JT, Aebi U, Bentires-Alj M, Lim RY. and Schoenenberger, C. A., 2012. The nanomechanical signature of breast cancer. Nature nanotechnology, 7(11), 757.

[97] Lam, W. A., Rosenbluth, M. J., and Fletcher, D. A., 2007. Chemotherapy exposure increases leukemia cell stiffness. Blood, 109(8), 3505-3508.

[98] Di Cerbo, A., Rubino, V., Morelli, F., Ruggiero, G., Landi, R., Guidetti, G., Canello, S., Terrazzano, G. and Alessandrini, A., 2018. Mechanical phenotyping of K562 cells by the Micropipette Aspiration Technique allows identifying mechanical changes induced by drugs. Scientific reports, 8(1), p.1219.

[99] Fregin, B., Czerwinski, F., Biedenweg, D., Girardo, S., Gross, S., Aurich, K., and Otto, O., 2019. High-throughput single-cell rheology in complex samples by dynamic real-time deformability cytometry. Nature communications, 10(1), 415.

[100] Zhang, X., Chu, H. K., Zhang, Y., Bai, G., Wang, K., Tan, Q., and Sun, D., 2015. Rapid characterization of the biomechanical properties of drug-treated cells in a microfluidic device. Journal of Micromechanics and Microengineering, 25(10), 105004.

[101] Rotsch, C., and Radmacher, M., 2000. Drug-induced changes of cytoskeletal structure and mechanics in fibroblasts: an atomic force microscopy study. Biophysical journal, 78(1), 520-535.

[102] Haase, K., and Pelling, A. E., 2015. Investigating cell mechanics with atomic force microscopy. Journal of The Royal Society Interface, 12(104), 20140970.

[103] Ding, Y., Xu, G. K., and Wang, G. F., 2017. On the determination of elastic moduli of cells by AFM based indentation. Scientific reports, 7, 45575.

[104] Guo, Q., Park, S., and Ma, H., 2012. Microfluidic micropipette aspiration for measuring the deformability of single cells. Lab on a Chip, 12(15), 2687-2695.

[105] Esteban-Manzanares, G., González-Bermúdez, B., Cruces, J., De la Fuente, M., Li, Q., Guinea, G.V., Pérez-Rigueiro, J., Elices, M. and Plaza, G.R., 2017. Improved measurement of elastic properties of cells by micropipette aspiration and its application to lymphocytes. Annals of biomedical engineering, 45(5), pp.1375-1385.

[106] Dao, M., Lim, C. T., and Suresh, S., 2003. Mechanics of the human red blood cell deformed by optical tweezers. Journal of the Mechanics and Physics of Solids, 51(11-12), 2259-2280.

[107] Fraczkowska, K., Bacia, M., Przybyło, M., Drabik, D., Kaczorowska, A., Rybka, J., Stefanko, E., Drobczynski, S., Masajada, J., Podbielska, H. and Wrobel, T., 2018. Alterations of biomechanics in cancer and normal cells induced by doxorubicin. Biomedicine and Pharmacotherapy, 97, pp.1195-1203.

[108] Gossett, D.R., Henry, T.K., Lee, S.A., Ying, Y., Lindgren, A.G., Yang, O.O., Rao, J., Clark, A.T. and Di Carlo, D., 2012. Hydrodynamic stretching of single cells for large population mechanical phenotyping. Proceedings of the National Academy of Sciences, 109(20), pp.7630-7635.

[109] Nyberg, K.D., Hu, K.H., Kleinman, S.H., Khismatullin, D.B., Butte, M.J. and Rowat, A.C., 2017. Quantitative deformability cytometry:

rapid, calibrated measurements of cell mechanical properties. Biophysical journal, 113(7), pp.1574-1584.

[110] Urbanska, M., Rosendahl, P., Kraeter, M., and Guck, J., 2018. High-throughput single-cell mechanical phenotyping with real-time deformability cytometry. In Methods in cell biology (Vol. 147, pp. 175-198). Academic Press.

[111] Hirose, Y., Tadakuma, K., Higashimori, M., Arai, T., Kaneko, M., Iitsuka, R., Yamanishi, Y. and Arai, F., 2010, May. A new stiffness evaluation toward high speed cell sorter. In 2010 IEEE International Conference on Robotics and Automation (pp. 4113-4118). IEEE.

[112] Sakuma, S., Kuroda, K., Tsai, C. H. D., Fukui, W., Arai, F., and Kaneko, M., 2014. Red blood cell fatigue evaluation based on the close-encountering point between extensibility and recoverability. Lab on a Chip, 14(6), 1135-1141.

[113] Adamo, A., Sharei, A., Adamo, L., Lee, B., Mao, S., and Jensen, K. F., 2012. Microfluidics-based assessment of cell deformability. Analytical chemistry, 84(15), 6438-6443.

[114] Guo, Q., Duffy, S. P., Matthews, K., Islamzada, E., and Ma, H., 2017. Deformability based cell sorting using microfluidic ratchets enabling phenotypic separation of leukocytes directly from whole blood. Scientific reports, 7(1), 6627.

[115] Rosenbluth, M. J., Lam, W. A., and Fletcher, D. A., 2006. Force microscopy of nonadherent cells: a comparison of leukemia cell deformability. Biophysical journal, 90(8), 2994-3003.

[116] Giessibl, F. J., 2003. Advances in atomic force microscopy. Reviews of modern physics, 75(3), 949.

[117] Zhang, H., and Liu, K. K., 2008. Optical tweezers for single cells. Journal of the Royal Society interface, 5(24), 671-690.

[118] Yu, H., Tay, C.Y., Leong, W.S., Tan, S.C.W., Liao, K. and Tan, L.P., 2010. Mechanical behavior of human mesenchymal stem cells during adipogenic and osteogenic differentiation. Biochemical and biophysical research communications, 393(1), pp.150-155.

[119] Sato, M., Ohshima, N. and Nerem, R.M., 1996. Viscoelastic properties of cultured porcine aortic endothelial cells exposed to shear stress. Journal of biomechanics, 29(4), pp.461-467.

[120] Lee, L. M., and Liu, A. P., 2014. The application of micropipette aspiration in molecular mechanics of single cells. Journal of nanotechnology in engineering and medicine, 5(4), 040902.

[121] Ren, X., Ghassemi, P., Babahosseini, H., Strobl, J. S., and Agah, M., 2017. Single-cell mechanical characteristics analyzed by multiconstriction microfluidic channels. ACS sensors, 2(2), 290-299.

[122] Otto, O., Rosendahl, P., Mietke, A., Golfier, S., Herold, C., Klaue, D., Girardo, S., Pagliara, S., Ekpenyong, A., Jacobi, A. and Wobus, M., 2015. Real-time deformability cytometry: on-the-fly cell mechanical phenotyping. Nature methods, 12(3), p.199.

[123] Xue, C., Wang, J., Zhao, Y., Chen, D., Yue, W., and Chen, J., 2015. Constriction channel based single-cell mechanical property characterization. Micromachines, 6(11), 1794-1804.

[124] Shukla, V. C., Kuang, T. R., Senthilvelan, A., Higuita-Castro, N., Duarte-Sanmiguel, S., Ghadiali, S. N., and Gallego-Perez, D., 2018. Lab-on-a-Chip platforms for biophysical studies of cancer with single-cell resolution. Trends in biotechnology, 36(5), 549-561.

[125] Raj, A., and Sen, A. K., 2018. Microfluidic Sensors for Mechanophenotyping of Biological Cells. In Environmental, Chemical and Medical Sensors (pp. 389-408). Springer, Singapore.

[126] Li, Y. J., Yang, Y. N., Zhang, H. J., Xue, C. D., Zeng, D. P., Cao, T., and Qin, K. R., 2019. A Microfluidic Micropipette Aspiration Device to Study Single-Cell Mechanics Inspired by the Principle of Wheatstone Bridge. Micromachines, 10(2), 131.

[127] Myrand-Lapierre, M. E., Deng, X., Ang, R. R., Matthews, K., Santoso, A. T., and Ma, H., 2015. Multiplexed fluidic plunger mechanism for the measurement of red blood cell deformability. Lab on a Chip, 15(1), 159-167.

[128] Downey, G. P., Doherty, D. E., Schwab 3rd, B., Elson, E. L., Henson, P. M., and Worthen, G. S., 1990. Retention of leukocytes in capillaries: role of cell size and deformability. Journal of applied physiology, 69(5), 1767-1778.

[129] Waite, L., and Fine, J. M., 2007. Applied biofluid mechanics.

[130] K. Rogers, Blood: physiology and circulation. New York: Britannica Educational Publishing, 2011.

[131] George-Gay, B., and Parker, K., 2003. Understanding the complete blood count with differential. Journal of PeriAnesthesia Nursing, 18(2), 96-117.

[132] Ford, N., Meintjes, G., Pozniak, A., Bygrave, H., Hill, A., Peter, T., Davies, M.A., Grinsztejn, B., Calmy, A., Kumarasamy, N. and Phanuphak, P., 2015. The future role of CD4 cell count for monitoring antiretroviral therapy. The Lancet Infectious Diseases, 15(2), pp.241-247.

[133] Barnett, D., Walker, B., Landay, A. and Denny, T.N., 2008. CD4 immunophenotyping in HIV infection. Nature Reviews Microbiology, 6(11supp), p.S7.

[134] Watkins, N.N., Hassan, U., Damhorst, G., Ni, H., Vaid, A., Rodriguez, W. and Bashir, R., 2013. Microfluidic CD4+ and CD8+ T lymphocyte counters for point-of-care HIV diagnostics using whole blood. Science translational medicine, 5(214), pp.214ra170-214ra170.

[135] Serrano-Villar, S., Moreno, S., Fuentes-Ferrer, M., Sánchez-Marcos, C., Avila, M., Sainz, T., de Villar, N.G.P., Fernández-Cruz, A. and Estrada, V., 2014. The CD 4: CD 8 ratio is associated with markers of age-associated disease in virally suppressed HIV-infected patients with immunological recovery. *HIV medicine*, *15*(1), pp.40-49.

[136] Sweiss, N.J., Salloum, R., Ghandi, S., Alegre, M.L., Sawaqed, R., Badaracco, M., Pursell, K., Pitrak, D., Baughman, R.P., Moller, D.R. and Garcia, J.G., 2010. Significant CD4, CD8, and CD19 lymphopenia in peripheral blood of sarcoidosis patients correlates with severe disease manifestations. PLoS One, 5(2), p.e9088.

[137] Abraham, R.S. and Aubert, G., 2016. Flow cytometry, a versatile tool for diagnosis and monitoring of primary immunodeficiencies. Clin. Vaccine Immunol., 23(4), pp.254-271.

[138] Keeney, M., Hedley, B.D. and Chin-Yee, I.H., 2017. Flow cytometry—recognizing unusual populations in leukemia and lymphoma diagnosis. International journal of laboratory hematology, 39, pp.86-92.

[139] Schreibman, T., and Friedland, G., 2004. Use of total lymphocyte count for monitoring response to antiretroviral therapy. Clinical Infectious Diseases, 38(2), 257-262.

[140] Passing, H., and Bablok, W., 1983. A new biometrical procedure for testing the equality of measurements from two different analytical methods. Application of linear regression procedures for method comparison studies in clinical chemistry, Part I. Clinical Chemistry and Laboratory Medicine, 21(11), 709-720.

[141] Bland, J.M. and Altman, D., 1986. Statistical methods for assessing agreement between two methods of clinical measurement. The lancet, 327(8476), pp.307-310.

[142] Tomaiuolo, G., 2014. Biomechanical properties of red blood cells in health and disease towards microfluidics. Biomicrofluidics, 8(5), 051501.

[143] Skoutelis, A. T., Kaleridis, V., Athanassiou, G. M., Kokkinis, K. I., Missirlis, Y. F., and Bassaris, H. P., 2000. Neutrophil deformability in patients with sepsis, septic shock, and adult respiratory distress syndrome. Critical care medicine, 28(7), 2355-2359.

[144] Giavarina, D., 2015. Understanding bland altman analysis. Biochemia medica: Biochemia medica, 25(2), pp.141-151.

ACCOMPLISHMENTS

I. Journal Articles

Noor, A. M., Masuda, T., Arai, F. (2019) Microfluidic device for rapid investigation of the deformability of leukocytes in whole blood samples (2019)
ROBOMECH Journal. Accepted.

Noor, A. M., Masuda, T., Lei, W., Horio, K., Miyata, Y., Namatame, M., ... & Arai, F. (2018). A microfluidic chip for capturing, imaging and counting CD3+ T-lymphocytes and CD19+ B-lymphocytes from whole blood. Sensors and Actuators B: Chemical, 276, 107-113.

II. International Conferences

Noor, A. M., Lei, W., Masuda, T., Horio, K., Saito, T., Miyata, Y., & Arai, F. (2017, December). A high-efficiency and clogging-free microfluidic device for size-selective cell separation. In 2017 International Symposium on Micro-NanoMechatronics and Human Science (MHS) (pp. 1-2). IEEE.

III. Domestic Conferences

益田, **AMNoor**, WLei, 堀尾, 斎藤, 宮田, 新井, 1μL 末梢血からのリンパ球の分画および計測,36 回化学とマイクロ・ナノシステム学

IV. Awards

"1 μL Whole Blood Separation and Measurement". Lecture on Chemistry and Micro / Nano Systems Society (Cheminas 37) 2018.

Best Research Award in the 37 Cheminas.

Taisuke Masuda, **Anas Mohd Noor**, Wu Lei, Koji Horio, Toshiki I Saito, Yasuhiko Miyata and Fumihito Arai